U.S. Department of the Interior
U.S. Geological Survey

Prepared in cooperation with the
PUERTO RICO DEPARTMENT OF NATURAL AND ENVIRONMENTAL RESOURCES AND
THE JOBOS BAY NATIONAL ESTUARINE RESEARCH RESERVE

Effects of Changes in Irrigation Practices and Aquifer Development on Groundwater Discharge to the Jobos Bay National Estuarine Research Reserve near Salinas, Puerto Rico

Scientific Investigations Report 2010-5022

USGS
science for a changing world

Effects of Changes in Irrigation Practices and Aquifer Development on Groundwater Discharge to the Jobos Bay National Estuarine Research Reserve near Salinas, Puerto Rico

By Eve L. Kuniansky and José M. Rodríguez

Prepared in cooperation with the
Puerto Rico Department of Natural and Environmental Resources and
the Jobos Bay National Estuarine Research Reserve

Scientific Investigations Report 2010–5022

U.S. Department of the Interior
U.S. Geological Survey

U.S. Department of the Interior
KEN SALAZAR, Secretary

U.S. Geological Survey
Marcia K. McNutt, Director

U.S. Geological Survey, Reston, Virginia: 2010

For product and ordering information:
World Wide Web: http://www.usgs.gov/pubprod
Telephone: 1-888-ASK-USGS

For more information on the USGS--the Federal source for science about the Earth, its natural and living resources, natural hazards, and the environment:
World Wide Web: http://www.usgs.gov
Telephone: 1-888-ASK-USGS

Suggested citation:
Kuniansky, E.L., and Rodríguez, J.M., 2010, Effects of Changes in Irrigation Practices and Aquifer Development on Groundwater Discharge to the Jobos Bay National Estuarine Research Reserve near Salinas, Puerto Rico: U.S. Geological Survey Scientific Investigations Report 2010-5022, 106 p.

Acknowledgments

The authors thank Angel Dieppa, Puerto Rico Department of Natural and Environmental Resources-Jobos Bay National Estuarine Research Reserve and others at the Reserve who assisted with data collection at the site.

The authors also wish to thank the following USGS employees who contributed substantially to this study and report. Jesús Rodríguez-Martínez developed the geologic information provided on illustrations, plates, and appendixes, and prepared all of the geologic setting and part of the hydrogeologic setting sections. Carole Johnson and Eric White of the USGS, Branch of Geophysics collected and processed the continuous resistivity profiling (CRP) data. Francisco Maldonado assisted with illustrations and Marilyn Santiago provided assistance with geographic information system datasets. Internal reviews of this manuscript were provided by Fernando Gómez-Gómez, Claudia Faunt, and Alyssa Dausman.

Contents

Acknowledgments....iii
Abstract....1
Introduction....2
Purpose and Scope....2
Description of the Study Area....5
Hydrologic Setting....5
Rainfall, Evapotranspiration, and Net Recharge....7
Streamflow Estimates....7
Infiltration Estimates....9
History of Water Resources Development and Changes in Irrigation Practices....11
Land Use....11
Surface-Water Use....11
Groundwater Use....15
Geologic Setting....15
Hydrogeologic Setting....16
Hydraulic Properties....17
Groundwater Flow Patterns....23
Simulation of Groundwater Flow....23
Model Conceptualization and Construction....23
Boundary Conditions....27
Model Calibration Strategy....30
Sensitivity Testing and Analysis....44
Effects of Water-Resources Development....50
Alternative Strategies for Groundwater Management....51
Limitations of the Model....55
Summary....62
Selected References....63
Appendix....67
Plates....92

Figure

1. Map showing the location of the study area and the Jobos Bay National Estuarine Research Reserve and extent of deposits of the South Coast aquifer, Puerto Rico. 3
2. Graph showing comparison of (A) annual and (B) monthly rainfall at the Aguirre Central National Weather Service Station, and (C) groundwater level at the USGS Piezometer C observation well. 4
3. Map showing locations of geographic features, hydrologic features, and streamflow measurements sites in the study area. 6

4a. Spatial extent of sugar-cane cultivation in the study area during 1986 as inferred from the distribution of flood-irrigation areas. 12

4b. Distribution of active agricultural areas with microdrip and center-pivot irrigation in the study area during 2002. 13

4c. Graph showing irrigation water deliveries from Canal de Patillas and rainfall from 1985 to 2005 14

5. Map showing sand and gravel percentage and interpretative structure in the South Coast aquifer in the vicinity of Salinas and Bahía de Jobos 21
6. Map showing generalized distribution of hydraulic conductivity in the South Coast aquifer in the vicinity of Salinas and Bahía de Jobos between the Río Jueyes and Río Guamaní. 22
7. Map showing the potentiometric surface in the Río Jueyes to Río Guamaní part of the South Coast aquifer during March 1986. 24
8. Map showing the potentiometric surface in the South Coast aquifer in the vicinity of Salinas during July 2002. 25
9. Map showing the potentiometric surface in the South Coast aquifer in the vicinity of Salinas during July 2004. 26
10. Map showing finite difference grid and boundary conditions for model layers 1 through 5. 29
11. Map showing specified altitudes for top of model layers 1 and 2. 31
12. Map showing specified altitudes for bottom of model layers 1 through 5. 33
13. Map showing simulated potentiometric surface for model-calibrated conditions during March 1986. 36
14. Observed and simulated water levels between 1986 and 2004 at selected wells within the study area. 39
15. Map showing simulated potentiometric surface for model-calibrated conditions during 2002. 40
16. Map showing simulated potentiometric surface for model-calibrated conditions during 2004 and posted residuals. 41
17. Map showing final calibrated horizontal hydraulic conductivity values assigned to each of the five model layers for the South Coast aquifer between the Río Jueyes and Río Guamaní, southern Puerto Rico. 43
18. Map showing final storage values assigned to each of the five model layers for the South Coast aquifer between the Río Jueyes and the Río Guamaní, southern Puerto Rico. 47
19. Map showing recharge rates assigned to uppermost active layer (layer 1 or 2) for the 1986 steady state simulation. 48

20. Sensitivity analysis based on transient simulation using the residual standard deviation from water-level hydrographs....49
21. Calibrated transient model simulated water budget for annual stress periods 1986 through 2004....52
22. Graph showing model simulated flow to the mangroves (part of the general-head boundary cells in model layer 2) in the Jobos Bay National Estuarine Research Reserve near Salinas, Puerto Rico (A) as obtained in calibrated transient model and (B) flux to mangroves with a 10-year stress period added while maintaining 2004 pumping rates with average precipitation and with 75 percent of average precipitation....53
23. Graph showing model simulated groundwater flux to the mangrove area in the Jobos Bay National Estuarine Research Reserve and required water from sources for each of the groundwater management strategies tested....56
24. Map showing model-simulated potentiometric surface in the South Coast aquifer after 10-years of average rainfall recharge and 2004 pumpage with artificial recharge by use of injection wells located north of Jobos Bay National Estuarine Research Reserve boundary, Salinas , Puerto Rico (alternative 1)....57
25. Map showing model-simulated potentiometric surface in the South Coast aquifer for 2014 following 10 years of average recharge and 2004 pumpage rates, and incorporating artificial recharge applied over agricultural areas north of Jobos Bay National Estuarine Research Reserve, Salinas, Puerto Rico. (alternative 2). 58
26. Map showing the model-simulated potentiometric surface in the South Coast aquifer for 2014 following 10 years of average recharge and 2004 pumpage rates, except at wells located in the area bounded by Canal de Patillas, Jobos Bay National Estuarine Research Reserve, Hacienda Magdalena, and Cerro Aguirre (alternative 3). 59
27. Map showing model-simulated potentiometric surface in the South Coast aquifer for 2014 following 10 years of average recharge and a 50 percent reduction in 2004 pumpage rates from agricultural use wells (alternative 4)....60
28. Map showing model-simulated potentiometric surface in the South Coast aquifer for 2014 following 10 years of average recharge incorporating artificial recharge applied over an area of about 587 acres north of the Jobos Bay National Estuarine Research Reserve and a 50 percent reduction in 2004 pumpage rates from agricultural use wells (alternative 5)....61

Table

1. Drainage area of principal streams in the study area. 5
2. Miscellaneous streamflow measurements or observations along Canal de Patillas and Río Nigua. 8
3. Estimated streamflow infiltration into the alluvial aquifer, 1986 to 2004. 10
4. Estimates of agricultural areas and water requirements for 1986, 1991, and 2002, in the vicinity of Salinas and Jobos areas, Puerto Rico. 14
5. Estimated horizontal hydraulic conductivity from specific-capacity data. 18
6. Composite scaled sensitivity for selected parameters, steady-state simulation for existing conditions in 1986. 45
7. Model derived water budget for the steady-state simulation for 1986. 50
8. Summary of years where irrigation return flow occurs, precipitation conditions are less than average, and model simulated water budget indicates estuary water enters the South Coast aquifer. 54

Appendix

1. Estimated average annual rates of groundwater withdrawals in the Río Jueyes to Río Guamaní part of the South Coast aquifer from 1986 to 2004 68

2a. Lithologic description for test boring SC-2 at Salinas, Puerto Rico, March 16-17, 1987 70

2b. Lithologic description for test boring SC-3 at Guayama, Puerto Rico, March 19-20, 1987 71

3. General information for wells in the South Coast aquifer between the Río Jueyes and Río Guamaní used in this study 72

4. Lithologic and construction data for the JBNERR East 1 and 2 and JBNERR West 1 and 2 piezometer nests installed near the northern boundary of the Jobos Bay National Estuarine Research Reserve. JBNERR 1 and JBNERR 2 reference nos. are 184 and 185, respectively, in appendix 3 81

5. Zoned recharge values used for transient calibration 82

6a. Observed water levels, simulated water levels, and calculated residuals for March, 1986, July 2002, and May 2004 85

6b. Observed water levels, simulated water levels, and calculated residuals for March, 1986, July 2002, and May 2004 88

6c. Observed water levels, simulated water levels, and calculated residuals for March, 1986, July 2002, and May 2004 90

Plate

1. Transects along the study area used in constructing fence diagrams. 93
2. Part of the South Coast aquifer between the Río Jueyes and Río Guamaní in south central Puerto Rico for which a digital groundwater flow model was developed. 94
3. Generalized surficial geology in the south coastal plain from Río Jueyes to Río Guamaní area, Puerto Rico. 95
4. Fence diagrams showing the spatial variation in thickness of undifferentiated gravel and sand units of the fan-delta deposits in the study area. 96
5. The altitude of the top of the permeable aquifer deposits (equivalent to the base of semi-confining clay and silt deposits). 97

6a. Transects of Continuous Resistivity Profiles and corresponding Interpretation of the distribution of resistivity with depth along survey lines 1A through 1B. 98

6b. Transects of Continuous Resistivity Profiles and corresponding Interpretation of the distribution of resistivity with depth along survey lines 2A through 2E. 99

6c. Transects of Continuous Resistivity Profiles and corresponding Interpretation of the distribution of resistivity with depth along survey lines 2F through 2J. 100

6d. Transects of Continuous Resistivity Profiles and corresponding Interpretation of the distribution of resistivity with depth along survey lines 3A through 3F. 101

6e. Transects of Continuous Resistivity Profiles and corresponding Interpretation of the distribution of resistivity with depth along survey lines 3G through 3K. 102

6f. Transects of Continuous Resistivity Profiles and corresponding Interpretation of the distribution of resistivity with depth along survey lines 4A through 4E. 103

6g. Transects of Continuous Resistivity Profiles and corresponding Interpretation of the distribution of resistivity with depth along survey lines 5A through 5E´. 104

6h. Transects of Continuous Resistivity Profiles and corresponding Interpretation of the distribution of resistivity with depth along survey lines 6A through 6D. 105

7. Estimated spatial distribution of the base of the South Coast aquifer within the study area. 106

Conversion Factors, Datum, and Acronyms

Multiply	By	To obtain
	Length	
inch (in.)	2.54	centimeter (cm)
foot (ft)	0.3048	meter (m)
mile (mi)	1.609	kilometer (km)
	Area	
acre	4,047	square meter (m^2)
acre	0.4047	hectare (ha)
square mile (mi^2)	2.590	square kilometer (km^2)
	Volume	
acre-foot (acre-ft)	1,233	cubic meter (m^3)
acre-foot (acre-ft)	0.001233	cubic hectometer (hm^3)
	Flow rate	
gallon per minute (gal/min)	0.06309	liter per second (L/s)
acre-foot per year (acre-ft/yr)	1,233	cubic meter per year (m^3/yr)
foot per day (ft/d)	0.3048	meter per day (m/d)
foot per year (ft/yr)	0.3048	meter per year (m/yr)
cubic foot per second (ft^3/s)	0.02832	cubic meter per second (m^3/s)
million gallons per day (Mgal/d)	0.04381	cubic meter per second (m^3/s)
inch per year (in/yr)	25.4	millimeter per year (mm/yr)
	Specific capacity	
gallon per minute per foot [(gal/min)/ft)]	0.2070	liter per second per meter [(L/s)/m]
	Transmissivity and Conductance*	
foot squared per day (ft^2/d)	0.09290	meter squared per day (m^2/d)
	Concentration	
parts per million (ppm)	1	milligrams per liter (mg/L)
	Specific Conductance	
µS/cm (microsiemens per centimeter at 25 °C)	0.55 to 0.75 **	milligrams per liter (mg/L) of total dissolved solids

*Transmissivity and Conductance: The standard unit for transmissivity is cubic foot per day per square foot times foot of aquifer thickness [(ft^3/d)/ft^2]ft. In this report, the mathematically reduced form, foot squared per day (ft^2/d), is used for convenience.

**Range in multiplier is typical for natural waters (Hem, 1985).

Altitude, as used in this report, refers to distance above the vertical datum.

Temperature in degrees Fahrenheit (°F) may be converted to degrees Celsius (°C) as follows:

$$°C=(°F-32)/1.8$$

Vertical coordinate information is refered to local mean sea level.
Horizontal information is referenced to the Puerto Rico Datum, 1940 Adjustment.

Acronyms

CRP	Continuous resistivity profiling
GPS	Global positioning system
JBNERR	Jobos Bay National Estuarine Research Reserve
NOAA	National Oceanographic and Atmospheric Administration
NWS	National Weather Service
PRDNER	Puerto Rico Department of Natural and Environmental Resources
USGS	U.S. Geological Survey

Effects of Changes in Irrigation Practices and Aquifer Development on Groundwater Discharge to the Jobos Bay National Estuarine Research Reserve near Salinas, Puerto Rico

By Eve L. Kuniansky and José M. Rodríguez

Abstract

Since 1990, about 75 acres of black mangroves have died in the Jobos Bay National Estuarine Research Reserve near Salinas, Puerto Rico. Although many factors can contribute to the mortality of mangroves, changes in irrigation practices, rainfall, and water use resulted in as much as 25 feet of drawdown in the potentiometric surface of the aquifer in the vicinity of the reserve between 1986 and 2002. To clarify the issue, the U.S. Geological Survey, in cooperation with the Puerto Rico Department of Natural and Environmental Resources, conducted a study to ascertain how aquifer development and changes in irrigation practices have affected groundwater levels and groundwater flow to the Mar Negro area of the reserve.

Changes in groundwater flow to the mangrove swamp and bay from 1986 to 2004 were estimated in this study by developing and calibrating a numerical groundwater flow model. The transient simulations indicate that prior to 1994, high irrigation return flows more than offset the effect of reduced groundwater withdrawals. In this case, the simulated discharge to the coast in the modeled area was 19 million gallons per day. From 1994 through 2004, furrow irrigation was completely replaced by micro-drip irrigation, thus eliminating return flows and the simulated average coastal discharge was 7 million gallons per day, a reduction of 63 percent. The simulated average groundwater discharge to the coastal mangrove swamps in the reserve from 1986 to 1993 was 2 million gallons per day, compared to an average simulated discharge of 0.2 million gallons per day from 1994 to 2004. The average annual rainfall for each of these periods was 38 inches. The groundwater discharge to the coastal mangrove swamps in the Jobos Bay National Estuarine Research Reserve was estimated at about 0.5 million gallons per day for 2003-2004 because of higher than average annual rainfall during these 2 years.

The groundwater flow model was used to test five alternatives for increasing groundwater discharge to the coastal mangrove swamps to approximately 1.4 million gallons per day: (1) artificially recharging the aquifer with injection wells or (2) by increasing irrigation return flow by going back to furrow irrigation; (3) termination of groundwater withdrawals near the mangroves; (4) reduction of groundwater withdrawals at irrigation wells by 50 percent; and (5) a combination of alternatives 2 and 4 increasing irrigation return flows and decreasing irrigation withdrawals. Each alternative assumed average climatic conditions and groundwater withdrawals at 2004 rates. Alternative 1 required 1.5 million gallons per day of injected water. Alternative 2 required flooding 958 acres with a rate of 1.84 million gallons per day if no crops are grown. Alternative 3 required the termination of 2.44 million gallons per day of withdrawals to achieve 1.34 million gallons per day of discharge to the mangroves. Alternative 4 did not achieve the objective with only 0.80 million gallons per day simulated discharge to the mangroves, while requiring a 1.26 million gallon per day reduction in groundwater withdrawals. Alternative 5 required flooding fields with additional 1.13 million gallons of day and the same reduction in groundwater withdrawals, but did achieve the objective of about 1.4 million gallons per day discharge to the mangroves. Alternative 1, incorporating injection wells near the reserve required the least amount of water to raise groundwater levels and maintain discharge of 1.4 million gallons per day through the mangroves.

Introduction

The Jobos Bay National Estuarine Research Reserve (JBNERR), commonly known as Jobos Bay Estuary, is one of 26 estuarine areas under the National Estuarine Research System designated by the National Oceanographic and Atmospheric Administration (NOAA) in 1981. The JBNERR is located near Salinas on the north side of Jobos Bay (labeled in Spanish as Bahía de Jobos on figures and plates herein) on the south coast of Puerto Rico (fig. 1. and plate 1). The reserve was established under the Coastal Zone Management Act of 1972, and is managed by the Puerto Rico Department of Natural and Environmental Resources (PRDNER) in cooperation with the NOAA Office of Ocean and Coastal Resource Management. The JBNERR covers 2,833 ac (acres) of mangrove forest and diverse habitats from the landward transition zone of coastal fan-delta and alluvial deposits to offshore cays in the Caribbean Sea. The habitats represented at the JBNERR include salt flats and mudflats, shallow lagoons, fringing reefs, several offshore cays, and a diverse mangrove forest lying mostly within 15 islets.

Since about 1990, about 75 ac of mature black mangroves have died in the part of the JBNERR near Mar Negro (plate1). In the affected area, not only have mature mangroves died, but the density of new seedlings has been reduced and their growth seriously inhibited (Angel Dieppa, Puerto Rico Department of Natural and Environmental Resources Jobos Bay National Estuarine Research Reserve, oral commun., 2005). The area with the affected mangroves lies immediately south of intensively cultivated agricultural land within the Salinas fan delta (fig. 1). Mangrove mortality can be caused by many factors, including hurricanes, storms, tsunamis, droughts, hydrologic changes, erosion and subsidence, hypersalinity, and pollution (Jimenez and others 1985). Additionally, naturally occurring events such as hurricanes can lead to the expansion and contraction of the areas of red versus black mangroves (Cintrón and others, 1978; Pool and others, 1977). However, the affected mangrove stand is over 30 years old and its proximity to farms bordering the JBNERR may indicate that the hydrology within the stand has changed as a result of changes in irrigation practices, water use, and rainfall. The most important change in agriculture in the Salinas fan-delta area has been the abandonment of sugarcane mono-culture, practiced from the early 1900s to the 1990s, and its replacement by the cultivation of diversified crops such as corn, sorghum, and truck farm crops. In addition, furrow irrigation was replaced by more efficient watering techniques such as micro-drip irrigation in truck farm crops and irrigation by center-pivot overhead sprinklers in corn and sorghum crops. As a result of these changes, surface-water-derived irrigation deliveries within the Salinas fan delta decreased from a maximum of 9,400 ac-ft/yr (acre-feet per year) in 1950 to 6,000 ac-ft/yr in 1986, and decreased further to about 1,700 ac-ft in 2004 after sugarcane cultivation had ceased in the area. Micro-drip irrigation systems apply water more efficiently to the root zone of the plants than furrow irrigation; however, only a small percentage of the water applied through micro-drip irrigation recharges the aquifer. This is in contrast to the furrow irrigation method in which as much as an estimated 30 percent of the water applied at land surface recharges the aquifer (Bennett, 1976; Kuniansky and others, 2004).

As indicated by data from the U.S. Geological Survey (USGS) piezometer C observation well, the potentiometric surface in the Salinas fan aquifer generally declined from 1993 to 1997, primarily because of (1) reduced recharge to the local aquifer with the cessation of sugarcane cultivation; (2) below-average rainfall during 1993 to 1995; and (3) relatively constant groundwater withdrawals for public supply, agricultural, and industrial use (fig. 2). By 1995, groundwater levels in the Salinas fan were below those of 1986 by as much as 25 ft (feet) (Torres-González and Gómez-Gómez, 1987; Rodríguez, 2005). Groundwater levels recovered in 1999 from above normal rainfall and then continued to decline and did not recover to conditions similar to 1986 until an extreme rainfall event occurred in November 2003 (fig. 2). Thus, it is reasonable to assume that the aquifer head within the affected mangrove area was also lowered, from 3 to 5 ft above mean sea level in 1986 to below mean sea level by 1995 until about November 2003. The relative effect that these changes in land/agricultural use, irrigation practices, and resultant lowering of the potentiometric surface may have had on the ecological health of the black mangrove forest is unknown. As part of the mission of the USGS in regards to management of water and biological resources, the USGS, in cooperation with the PRDNER, conducted a study to ascertain how aquifer development and changes in irrigation practices have impacted groundwater levels and groundwater flow to the Mar Negro area of JBNERR (plate 1).

Purpose and Scope

The purpose of this report is to document changes in irrigation practices and aquifer development in the vicinity of the JBNEER and to quantify changes in groundwater discharge into the JBNERR. These objectives were accomplished by collecting, synthesizing, and analyzing data, and developing a numerical groundwater flow model calibrated to transient conditions from 1986 through 2004. The period chosen covers a range of hydrologic conditions, such as flooding and droughts, and the switch

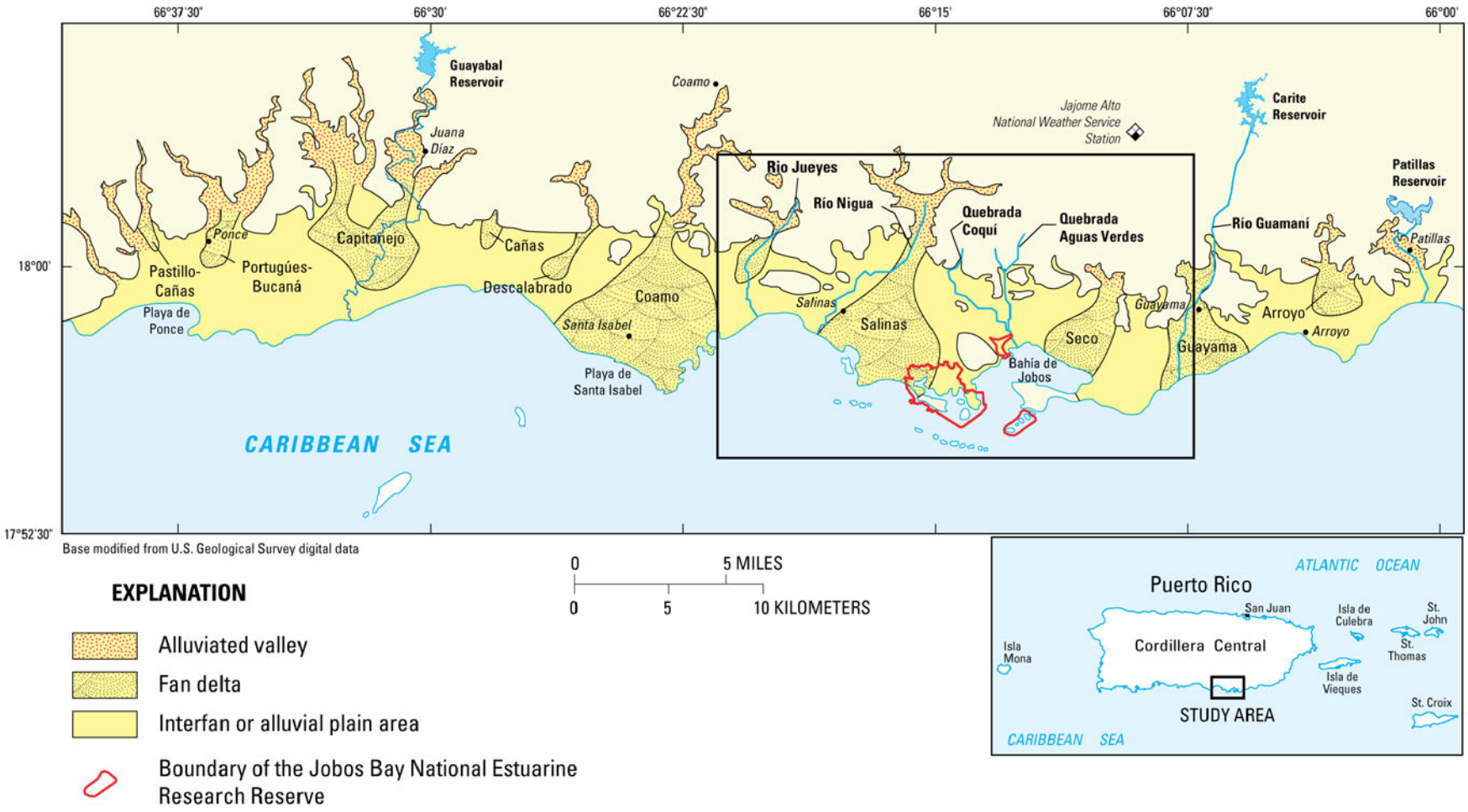

Figure 1. Location of the study area and the Jobos Bay National Estuarine Research Reserve and extent of deposits of the South Coast aquifer, Puerto Rico (modified from Renken and others, 2002).

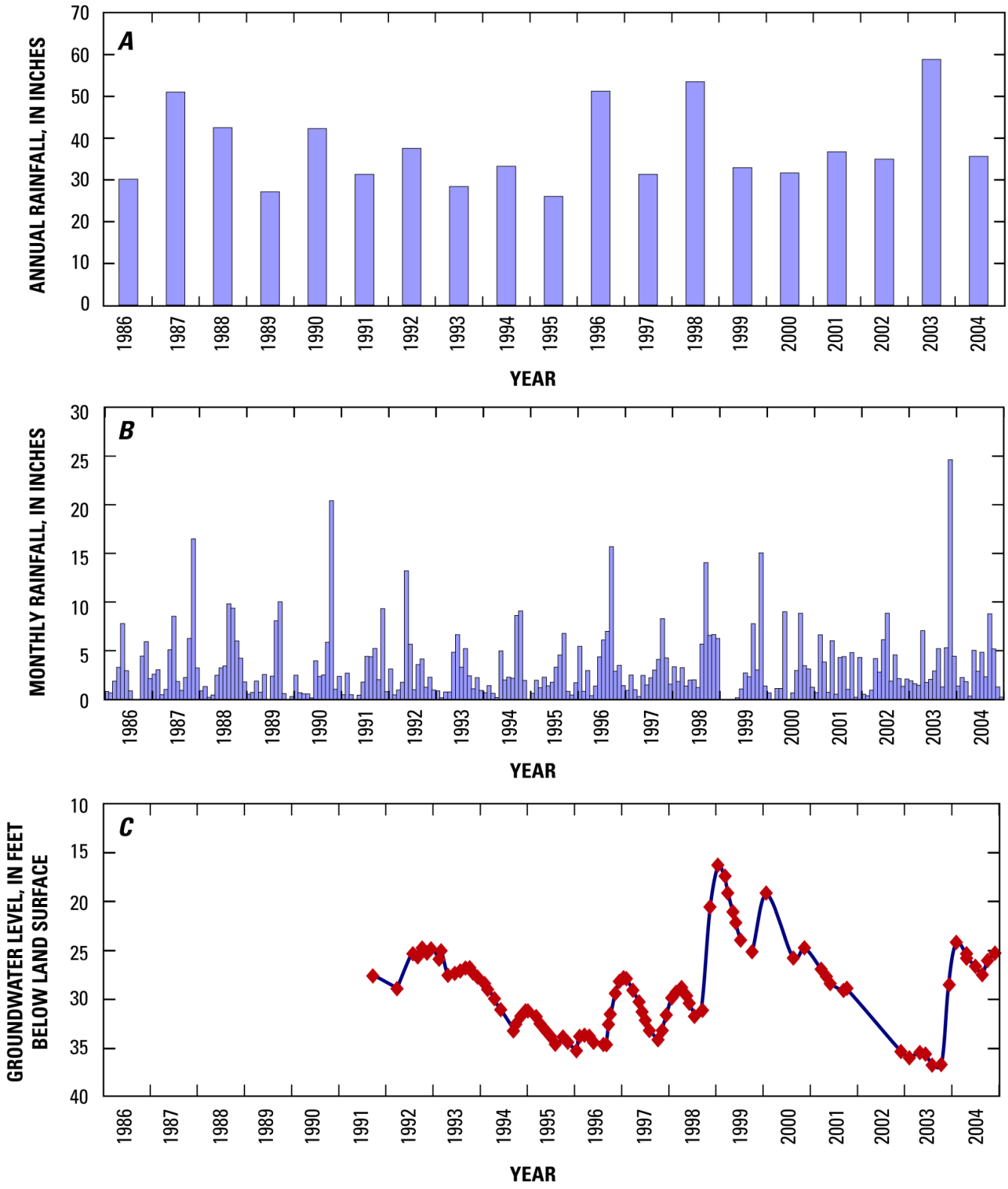

Figure 2. Comparison of (*A*) annual and (*B*) monthly rainfall at the Aguirre Central National Weather Service Station, and (*C*) groundwater level at the USGS Piezometer *C* observation well.

from furrow to micro-drip irrigation practices. Most of the study was concentrated on the Salinas fan delta along the Río Nigua, north of the JBNERR.

This report documents the hydrologic setting and geologic setting; freshwater discharge in the estuary and freshwater/seawater interface locations, determined with continuous resistivity profiling (CRP); historical changes in land use, surface-water use, and groundwater use; digital model development and calibration; and alternative water-management strategies. Three alternative water-management strategies were tested with the calibrated model: (1) artificially recharging the aquifer, (2) reducing groundwater withdrawals, and (3) a combination of both alternatives 1 and 2. These strategies were designed to maintain drawdown within the wetlands to at or above mean sea level throughout the mangrove forest, including periods of below average rainfall and increased discharge through the mangrove swamp to near predevelopment average rates.

Data in this report are presented in English customary units excluding the CRP data. The CRP data were collected during the surveys and presented in this report in International System (SI) units.

Description of the Study Area

The study area, which includes the Salinas fan delta and alluvial deposits, is in the eastern part of the South Coastal Plain of Puerto Rico, about 20 mi (miles) east of Ponce within the municipios of Salinas and Guayama (fig. 1). The principal aquifer in the study area is part of the South Coast aquifer (Gómez-Gómez, 1987 and 1991; Renken and others, 2002), which is composed of fan-delta, interfan, and alluvial valley deposits (called the aquifer for the remainder of this report (fig. 1)). Near the coastline, the study area is characterized by the presence of a series of interconnected environments: mangrove swamps, coastal lagoons, and salt and tidal flats (fig. 3). The study area (fig. 1) has an area of 36 square miles (mi^2) and is bordered to the north by foothills of the Cordillera Central mountain range, to the south by the Caribbean Sea, the Río Jueyes to the west, and the Río Guamaní to the east. The altitude of the alluvial valley and fan deltas ranges from sea level to approximately 130 ft above sea level along the northern edge of the foothills.

The study area is on the leeward side of the island and is characterized by a parched vegetative cover except in agricultural areas. All major streams in the study area flow only during major rainfall events. The Canal de Patillas and Canal de Guamaní are the major surface-water irrigation canals in the Río Jueyes to Río Guamaní area (fig. 3). These canals are part of a more extensive irrigation infrastructure that includes the Guayabal reservoir (fig. 1) and Canal de Juana Díaz, both west of the study area; the Patillas (fig. 1) and Melanía reservoirs, which supply the Canal de Patillas and Canal Guamaní, respectively; and the Carite reservoir (fig.1), which also supplies the Canal de Guamaní.

Hydrologic Setting

The South Coast Plain is warmer and drier than the rest of the island and lies within the rain shadow of the east-west trending Cordillera Central mountain range to the north. Annual average rainfall increases from the southern coast northward toward the Cordillera Central mountain range. As in the rest of the South Coast Plain, rainfall distribution is seasonal, with distinct wet and dry seasons. However, large storm systems can move toward Puerto Rico from the south and create higher than average rainfall and flooding over the south coast, as occurred in 1985 and 2003 (fig. 2*A*). Evapotranspiration from the aquifer is restricted to less than 1 mi (mile) from the coast, where the water table is at or near the ground surface.

The principal streams in the study area from west to east are the Río Jueyes, Río Nigua (also referred as Río Nigua de Salinas), Río Seco, and Río Guamaní; the minor streams include the Quebrada Honda, Quebrada Coquí, and Quebrada Cimarrona (fig. 3). The Río Nigua and Río Guamaní intermittently flow southward from the mountains across the coastal plain toward the sea. The Río Jueyes and Río Seco along with Quebrada Honda, Quebrada Coquí, and Quebrada Cimarrona flow only during extreme rainfall events. The drainage areas of these streams are presented in table 1.

Table 1. Drainage area of principal streams in the study area.

Description	Drainage area (mi^2)
Rio Jueyes	7.82
Rio Seco	7.85
Quebrada Honda	3.51
Quebrada Coqui	4.73
Quebrada Cimarrona	2.93
Río Lapa	9.92
Río Majada	16.7

In the study area and along the rest of the South Coast Plain, streams lose water to the aquifer. As a result, most streams lose their base flow and part of their stormflow to the aquifer in their middle and upper reaches, and do not flow across the entire coastal plain except shortly after rainfall-runoff events. Near the coast, the water table occasionally rises above the altitude of

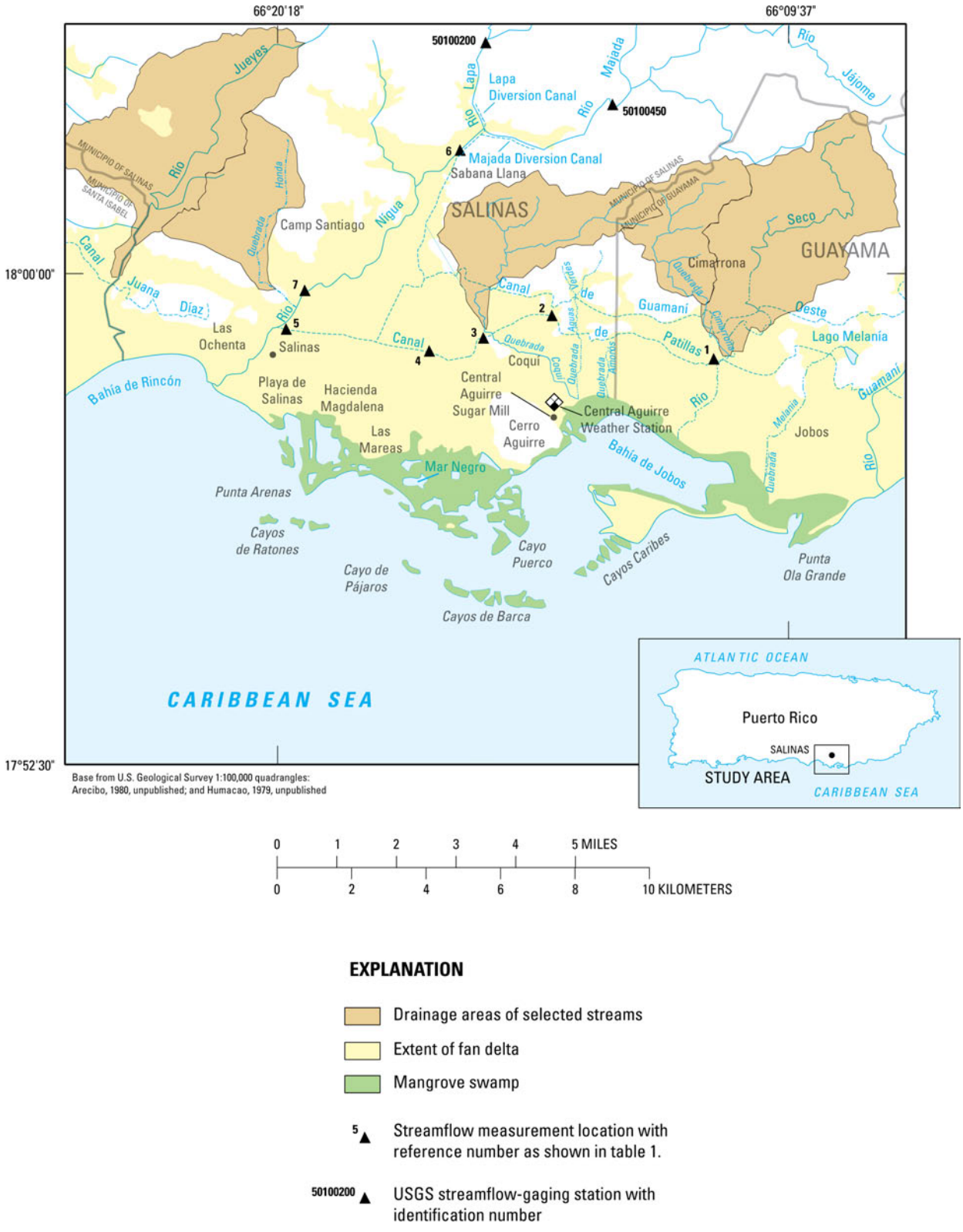

Figure 3. Locations of geographic features, hydrologic features, and streamflow measurements sites in the study area.

the stream channel beds and groundwater discharge to the streams occurs.

In addition to streams, a series of irrigation canals were constructed to convey surface water to the agricultural areas. The most important irrigation canals in the study area are the Patillas and Guamaní Canals. The Canal de Patillas conveys water from Lago Patillas (fig. 1), located north of the town of Patillas, east of the study area. Water for the Canal de Guamaní is diverted from Lago Carite (fig. 1)—located in the headwaters of the Río de la Plata on the northern side of the Cordillera Central—to the Río Guamaní in Guayama in the eastern part of the study area.

Rainfall, Evapotranspiration, and Net Recharge

The mean annual rainfall at a National Weather Service (NWS) station within the study area (Central Aguirre NWS station 660152) is about 40 in. (inches), compared to about 77 in. at 2,388 ft (feet) altitude in the Cordillera Central (Jájome Alto NWS station 664867) and about 53 in. at San Juan on the north coast (NWS station 668812). The mean monthly rainfall at the Central Aguirre National Weather Service (NWS) station ranges from 1.17 to 6.89 in. (National Oceanic and Atmospheric Administration, 2005). The dry season occurs from December to April, with March usually being the driest month (fig. 2*B*). The wet season occurs from May to November, with October being the wettest month. Monthly rainfall during 2002-2003 was below average during the first 10 months, followed in November 2003 by an extremely wet storm event (Rodríguez, 2006). The mean monthly temperature from 1955 to 2004 at the Central Aguirre NWS station ranged from 30 °C in January to 32 °C in August.

Evapotranspiration data were not collected as part of this study. However, Bennett (1976) obtained a maximum evapotranspiration rate of about 65 in/yr (inches per year) from a regional electric analog model of the South Coast aquifer when the water table is at or near the land surface. According to Bennett (1976), evapotranspiration decreases linearly to 0 in/yr once the depth to water table exceeds 6 ft below land surface. The depth to the water table throughout most of the study area exceeds 6 ft below land surface, except near the coast. Thus, substantial evapotranspiration rates from the aquifer may be restricted to areas along the coast where the water table is near or at the land surface—mangrove swamps, tidal flats, and salt flats.

Net areal recharge ("net recharge" herein) is the amount of precipitation that recharges an aquifer and equals precipitation minus surface runoff and evapotranspiration. Infiltration of surface-runoff is an intermittent process associated with rainfall; most runoff drains into streams and a small percentage infiltrates the soil zone. In contrast, evapotranspiration is a more continuous process that occurs from the soil zone through the plant root zone. Evapotranspiration from the soil zone greatly reduces net recharge. Giusti (1971) and Ramos-Ginés (1994) estimated that, on average, 10 percent of rainfall in the adjacent Coamo and the Santa Isabel-Juana Díaz areas is net recharge to the aquifer. However, McClymonds and Díaz (1972) speculated that greater than 10 percent of the rainfall may recharge the water table during wet years, and that less than 10 percent of the rainfall may recharge the water table during dry years. Kuniansky and others (2004) refined the estimate of net recharge through transient calibration of a digital groundwater flow model of the contiguous Santa Isabel area directly west of the current study area (fig. 1). The net recharge estimates from Kuniansky and others (2004) are 4 percent (30 in.) of the annual rainfall for dry years, 12 percent (40 in.) of the annual rainfall for wet years, and 8 percent (30-40 in.) of annual rainfall for average years.

Streamflow Estimates

Miscellaneous and instantaneous streamflow measurements were made at various sites and dates along the Canal de Patillas during this and earlier studies (table 2, fig.3). The measured streamflow ranged from 0 to 5.39 ft^3/s (cubic feet per second). The variation in streamflow may be ascribed to several causes: (1) non-uniform deliveries from Lago Patillas, (2) diversions by farmers for irrigation along the canal trajectory, and (3) losses by evapotranspiration and infiltration into the aquifer.

The only streams with long-term continuous streamflow data in the study area are the Río Lapa near Rabo del Buey (fig. 3; station 50100200) and the Río Majada at La Plena (station 50100450). Both streamgaging stations are near the foothills of the Cordillera Central mountain range, north of the coastal plain, where the streams are perennial; no reservoirs are present within these stream courses. Analysis of the flow record was made by hydrograph separation using the computer code PART (Rutledge, 1993) and mean daily discharge data; the data files were retrieved from the USGS National Water Information System web server on August 30, 2005. The average base flows estimated for 1989 to 2002 at the Río Lapa and Río Majada stations are 2.55 ft^3/s and 3.69 ft^3/s, respectively. At the Río Lapa station, the mean daily flow was higher than the mean daily base flow during 51 percent of the days, with a maximum mean daily flow of 1,900 ft^3/s. At the Río Majada station, the mean daily flow was higher than the mean daily base flow during 59 percent of the days with a maximum mean daily flow of 2,270 ft^3/s. Because the period of record is only of 14 years, another frequency

Table 2. Miscellaneous streamflow measurements or observations along Canal de Patillas and Río Nigua.

[All values are in cubic foot per second (ft^3/s) and a blank in a column indicates no measurement or observation made that date. Locations are shown on figure 3]

Reference number	Station description	Date of measurement or observation									
		3/19/1986	10/31/2001	7/9/2002	2/23/2005	3/23/2005	4/28/2005	6/21/2005	7/12/2005	8/25/2005	9/13/2005
1	Canal de Patillas at Hwy 713	5.03	8.60								
2	Canal de Patillas at Hwy 706	4.05		3.75	2.03	4.1	5.39				
3	Canal de Patillas at Sabater	3.89	5.62	3.36	2.05	3.53	4.64		3.64	2.94	2.15
4	Canal de Patillas at Fortuna	<3		2.22	1.67	2.85	4.32		3.58	2.98	0.85
5	Canal de Patillas at Salinas	0		0.51	0.61	1.21	2		2.88	1.9	0.32
6	R. Nigua at Sabana Llana				3.19	1.14	0.61	3.45	27.4	8.17	3.75
7	R. Nigua at Camp Santiago[1]				Dry	Dry	Dry	Dry	Flowing	Dry	Dry

[1]Observation at R. Nigua at Camp Santiago on 10/03/05 (1600 hours): no flow

statistic to consider is the percent of time daily base flow equaled or exceeded the 1989-2002 estimated average base flow, which was 61 and 21 percent of the days at the Río Lapa and Río Majada stations, respectively.

The estimated annual base flow for Río Majada and Río Lapa for 1986-1988 and 2003-2004, shown in table 3, are based on linear regressions of annual rainfall data from the NWS Jájome Alto station (664867). The regression equation for calculating base flow in inches over the Río Majada basin is:

$$BF_M = -5.62 + 0.1299 R_J \quad (1)$$

Where BF_M is the estimated or predicted value of base flow over the Río Majada drainage area in inches and R_J is the annual rainfall in inches at Jájome Alto. This regression had an R^2 value of 0.62 and an F-significance of 0.00126. Thus, this regression explains 62 percent of the variation in base flow and should not be rejected because the F-significance is small. The regression equation for calculating base flow in inches over the Río Lapa basin is:

$$BF_L = -8.21 + 0.1751 R_J \quad (2)$$

Where BF_L is the estimated or predicted value of base flow over the Río Lapa drainage area in inches and R_J is the annual rainfall in inches at Jájome Alto. This regression has an R^2 value of 0.69 and an F-significance of 0.00039. Thus, this regression explains 69 percent of the variation in base flow and should not be rejected because the F-significance is small. The regression equation for the Río Lapa basin is statistically better than the regression equation for the Río Majada basin. The base flow in inches in table 2 for 1989 to 2002 was also determined using the PART program and daily discharge data retrieved on August 30, 2005.

Infiltration Estimates

Estimates of streamflow infiltration rates for the study area contain a large degree of uncertainty because the Río Lapa and Río Majada stations are the only continuous discharge measurement sites within the study area boundaries and are tributaries of the Río Nígua. Infiltration rates have not been determined during stormflow for Río Seco and Río Jueyes when these ephemeral streams flow across the coastal plain and discharge into the ocean. It is reasonable to assume, however, that infiltration rates (in cubic feet per second per mile of stream) for these streams are similar to those for Río Nigua, based on similarities in channel gradient and streambed deposits.

The first estimates of infiltration from the streams in the study area to the aquifer were made by McClymonds and Díaz (1972), who estimated an infiltration rate during February 1962 from the Río Nígua, mainly from base flow, of at least 5 ft^3/s. The Río Seco and two minor creeks, Quebrada Cimarrona and Quebrada Coquí, flow throughout the year in the hills north of the coastal plain with a combined average flow ranging from about 4 to 6 ft^3/s (McClymonds and Díaz,1972). According to McClymonds and Díaz (1972), all of this flow is absorbed into the groundwater flow system along the southern margin of these hills where the alluvium thickens. McClymonds and Díaz (1972) estimated an average infiltration rate from Río Guamaní to the South Coast aquifer for June of 1962 of about 1 ft^3/s, mainly from base flow. Based on seepage run data collected during November 1961 and March 1962 in the streams that discharge into Jobos Bay, the groundwater discharge to the surface water and then to the bay was estimated as 13.8 ft^3/s (McClymonds and Díaz, 1972). During those years, however, sugarcane was intensively cultivated and surface-water deliveries for irrigation may have contributed additional infiltration from irrigation return flow.

The long-term continuous streamflow data in combination with miscellaneous discharge measurements indicate that base flow infiltrates into the aquifer between streamgaging stations 6 and 7 on the Río Nigua (fig. 3 and table 2). On August 25, 2005, intense rainfall events generated flow exceeding 8 ft^3/s at station 6 while station 7 remained dry, indicating that the infiltration rate was at least 8 ft^3/s between the streamgaging stations. On July 12, 2005, flow at station 6 was 27.4 ft^3/s and (unmeasured) flow was observed at station 7, indicating that the infiltration rate was less than 27 ft^3/s. Most of the infiltration from the Río Nigua into the aquifer occurs upstream from the bridge on Highway 1 at the entrance to Camp Santiago (or generally north of latitude 18°00'54", plate 1). A pool of standing or slowly moving water is usually present in the channel of the Río Nigua downstream from the bridge on Highway 1 near the coast where the river intersects the water table.

A conservative estimate of the infiltration to the aquifer along the course of the Río Nigua is equal to the sum of the base flows at USGS stations 50100200 and 50100450 (table 3). The sum of the average base flows for both of these tributaries is 8 ft^3/s.

The estimates for the infiltration to the aquifer from the other streams in the study area for 1986 to 2004 are based on the assumption that the base flow, expressed in inches per year, is half the average base flow over the Río Lapa and Río Majada drainage basins. Because the altitudes of the drainage areas of the other streams in the study generally are lower than those of the Río Lapa and the Río Majada, these lower drainage areas

Table 3. Estimated streamflow infiltration into the alluvial aquifer, 1986 to 2004.

[in., inches; ft^3/s, cubic foot per second]

Calendar Year	Baseflow (in/area)	Annual infiltration to aquifer (ft^3/s)							
	Río Lapa	Río Majada	Along Río Nigua	Quebrada Coquí	Río Seco	Río Jueyes	Quebrada Cimarrona	Quebrada Honda	Total
1986	[1]6.37	[2]5.20	11.05	1.01	1.67	1.67	0.62	0.75	16.77
1987	[1]8.49	[2]6.77	14.53	1.33	2.21	2.20	0.82	0.99	22.08
1988	[1]5.94	[2]4.88	10.34	0.94	1.56	1.56	0.58	0.70	15.68
1989	2.16	1.44	3.35	0.31	0.52	0.52	0.19	0.23	5.12
1990	10.71	4.66	13.56	1.34	2.22	2.21	0.83	0.99	21.15
1991	1.77	1.77	3.47	0.31	0.51	0.51	0.19	0.23	5.22
1992	3.84	3.76	7.43	0.66	1.10	1.09	0.41	0.49	11.18
1993	2.04	1.90	3.83	0.34	0.57	0.57	0.21	0.25	5.77
1994	0.43	0.36	0.76	0.07	0.11	0.11	0.04	0.05	1.14
1995	1.80	0.92	2.45	0.24	0.39	0.39	0.15	0.18	3.80
1996	2.64	3.15	5.80	0.50	0.84	0.83	0.31	0.37	8.65
1997	1.65	2.53	4.32	0.36	0.60	0.60	0.23	0.27	6.38
1998	7.34	7.03	14.01	1.25	2.08	2.07	0.78	0.93	21.12
1999	6.62	8.25	14.99	1.30	2.15	2.14	0.80	0.96	22.34
2000	5.40	4.00	8.87	0.82	1.36	1.35	0.51	0.61	13.52
2001	1.27	1.41	2.66	0.23	0.39	0.39	0.14	0.17	3.98
2002	1.24	0.79	1.88	0.18	0.29	0.29	0.11	0.13	2.88
2003	[1]9.26	[2]7.34	15.80	1.45	2.40	2.39	0.90	1.07	24.01
2004	[1]8.13	[2]6.5	13.94	1.27	2.11	2.11	0.79	0.95	21.17
Average	4.58	3.82	8.05	0.73	1.22	1.21	0.45	0.54	12.21

[1]These years were estimated by linear regression (base flow in inches at Río Lapa) = -8.21+0.1751 multiplied by (the annual rainfall at Jajome Alto in inches).

[2]These years were estimated by linear regression (base flow in inches at Río Majada) = -5.62 + 0.1299 multiplied by (the annual rainfall at Jajome Alto in inches)

may only receive half as much rainfall as the mountains, as indicated on areal precipitation maps (*http://www.climatesource.com/pr/fact_sheets/fact_precip_pr.html*, accessed July 2, 2009). The annual estimated infiltration rates are shown in table 3 for Río Jueyes and Río Seco, along with Quebrada Honda, Quebrada Coquí, and Quebrada Cimarrona. The total estimated annual infiltration of the streams ranges from 1.15 to 24.0 ft^3/s from 1986 to 2004 and averages 12.2 ft^3/s. These estimates may be conservative because they are derived from base flow data, and daily base flow is exceeded on the monitored streams over 20 percent of the time. The average estimated infiltration, however, is similar to the previous estimates of McClymonds and Díaz (1972).

History of Water Resources Development and Changes in Irrigation Practices

The historical changes in water resources development and agricultural practices near Salinas are representative of the entire South Coastal Plain. The hydrology of the South Coast aquifer, including the study area, has been progressively modified from its predeveloped state since the early 1800s, when the first diversion canals were constructed to capture base flow from the principal streams for irrigation of sugarcane fields (Gómez-Gómez, 1991). The most important changes, however, occurred between 1910 and 1935 as sugarcane cultivation expanded. A substantial investment was made to provide the South Coastal Plain with a network of irrigation canals and reservoirs to supply water to thousands of previously uncultivated acres. As part of the overall effort, two tunnels were constructed to allow inter-basin transfer of surface water across the insular hydrologic divide. Although ground was first used as a complementary source for irrigation in the early 1900s, the aquifer was not developed on a large scale until electricity and deep turbine pumps became available in the 1930s. Increasing sugarcane irrigation during these years caused groundwater withdrawals to peak at 95 million gallons per day (Mgal/d) or 106,500 ac-ft/yr in 1947 along the South Coastal Plain (Gómez-Gómez, 1991). After 1947, surface-water diversions began to decline as sugarcane, the principal surface-water-irrigated crop, decreased in acreage. This decline was followed by an increase in groundwater use for drip irrigation of truck-farm crops in the 1970s.

The history of water-resource development in the study area discussed herein was reconstructed by Quiñones-Aponte and others (1996) using mostly unpublished documents from the Engineering Department of the Central Aguirre sugar mill at Salinas (formerly known as Luce and Co.), the Puerto Rico Electric Power Authority at Guayama, and the Puerto Rico Aqueduct and Sewer Authority. Complementary information about the history of the water-resources development in the study area was also obtained from McClymonds and Díaz (1972).

Land Use

Sugar cane cultivation along the coastal plain and processing at the Central Aguirre sugar mill were the main land use and economic activity in the study area until the mid 1970s (Quiñones-Aponte and others, 1996). Beginning in the 1970s, petrochemical and pharmaceutical industries were established in Guayama and became the main source of economic activity. In the 1980s, sugarcane production decreased, although it was still an important economic activity as evidenced by the substantial portion of the study area under furrow irrigation during 1986 (fig. 4*A*). Beginning in the 1990s, agricultural activity started diversifying in the study area. Sugar cane cultivation ceased by about 1993 and the commercial production of vegetables and fruits had become commonplace by the early 2000s. This type of land use was incompatible with substantial surface-water deliveries from Canal de Patillas (fig. 4*B*; Quiñones-Aponte and others, 1996; Rodríguez, 2006). Additionally, large tracts of agricultural land were subdivided into smaller farms, some of which have since been used for suburban development or left fallow.

Land use in the Salinas Fan area during 2002 (the last year data are available) was distributed as follows: agricultural land use, which includes cropland, confined poultry feeding operations, and pasture land, approximately 35 percent; uncultivated land, 51 percent; urbanized land, 13 percent, of which only half was serviced by municipal sewer systems; and industrial land, 1 percent. About 35 percent of the active agricultural land is solely used to cultivate plantains and bananas.

Estimates of water use (both surface and ground water) required for irrigated crop acreages for 1986, 1991-92 and 2002 are provided in table 4. The estimates in table 4 for 1986 and 2002 apply to the areas shown on figures 4*A*-*B*. The estimates for 1991-92 are from crop area estimates provided by O.M. Ramos, (U.S. Forest Service, written commun., 2003). The demands estimated in table 3 were fulfilled, in part, by surface water imported to the area through irrigation canals.

Surface-Water Use

In 1861, the Lapa and Majada diversion canals (fig. 3), with maximum capacity of 13 ft^3/s, began conveying water from the Río Lapa and the Río Majada to farms northeast of Salinas. Large-scale use of surface water for irrigation in the study area began in 1914 with water deliveries from the Patillas and Carite reservoirs east of the study area. Initially, the Patillas and Guamaní Canals (the main irrigation canal systems) delivered about 65,000 ac-ft/yr of water to the agricultural areas. Surface-water deliveries remained fairly constant at approximately 65,000 ac-ft/yr from 1914 to the mid 1930s, decreased to 51,000 ac-ft/yr by late 1940s and later increased to an average delivery of 61,000 ac-ft/yr by late 1950s. Water deliveries remained fairly constant from the late 1950s until the mid 1960s, and declined substantially to 32,000 ac-ft/yr by 1986. Of the two diversion canals (Lapa and Majada), only the Majada diversion canal was in operation as of 1986, with an estimated average flow of 1 ft^3/s. Deliveries solely

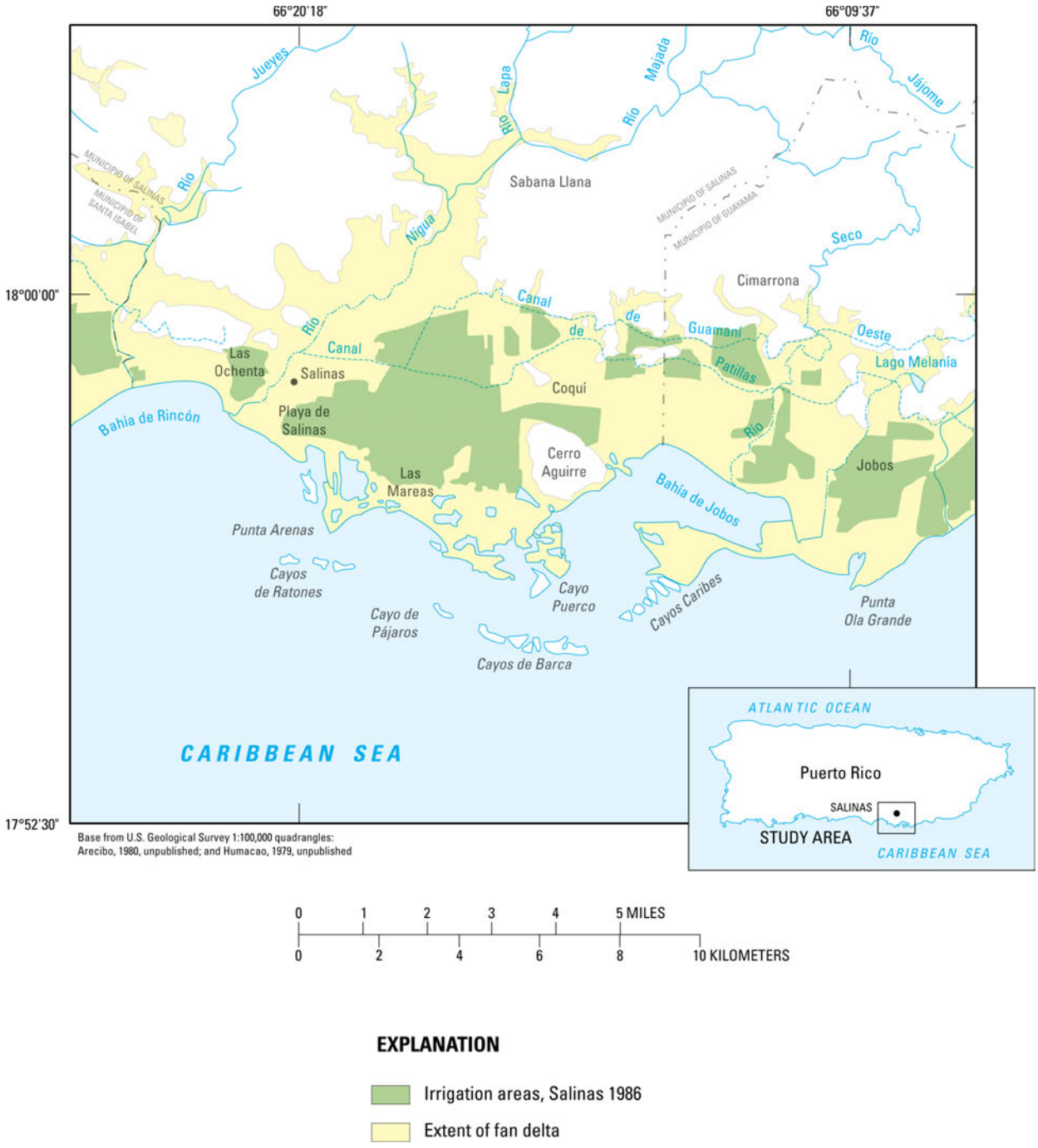

Figure 4*a*. Spatial extent of sugar-cane cultivation in the study area during 1986 as inferred from the distribution of flood-irrigation areas.

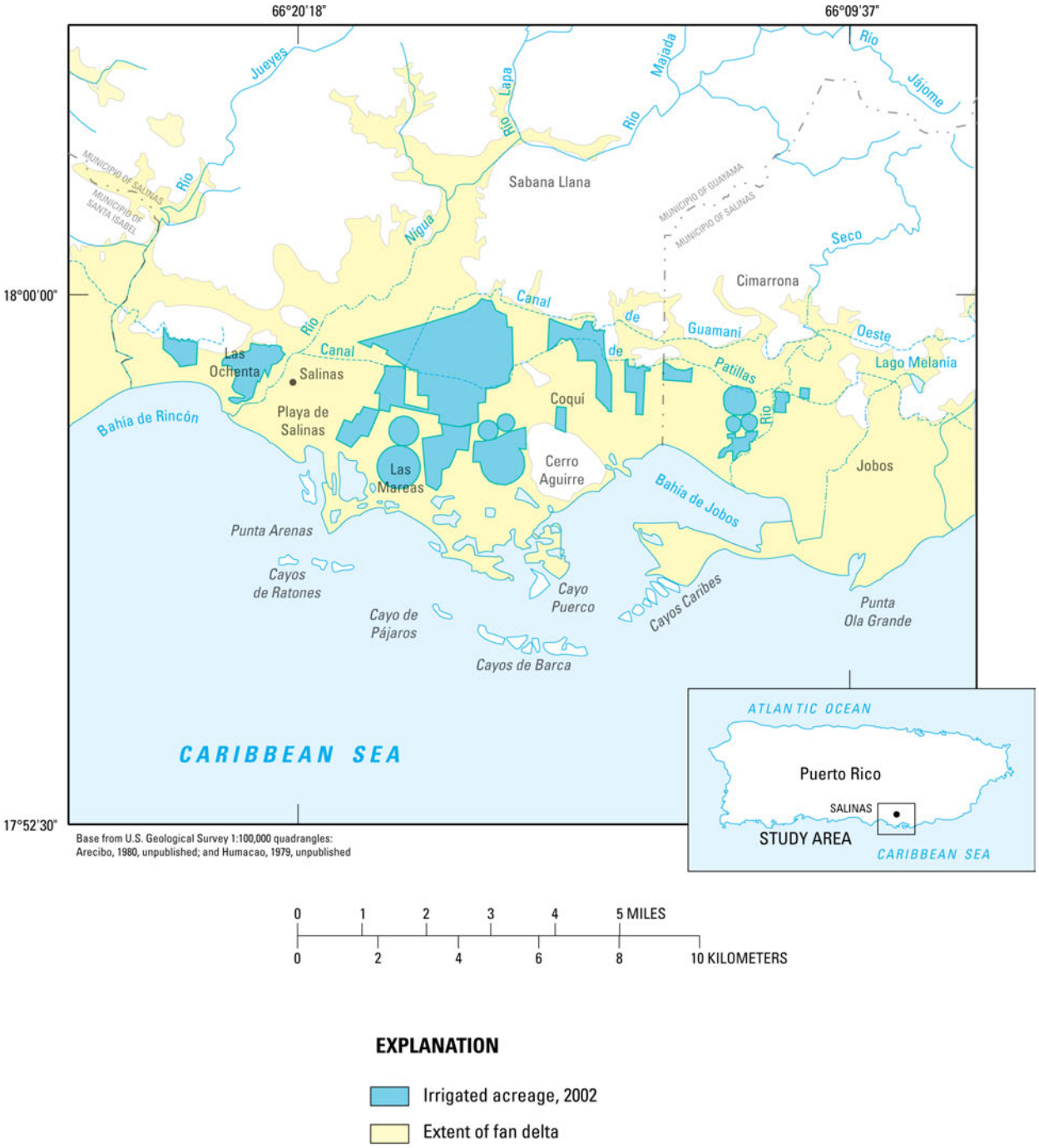

Figure 4*b*. Distribution of active agricultural areas with microdrip and center-pivot irrigation in the study area during 2002.

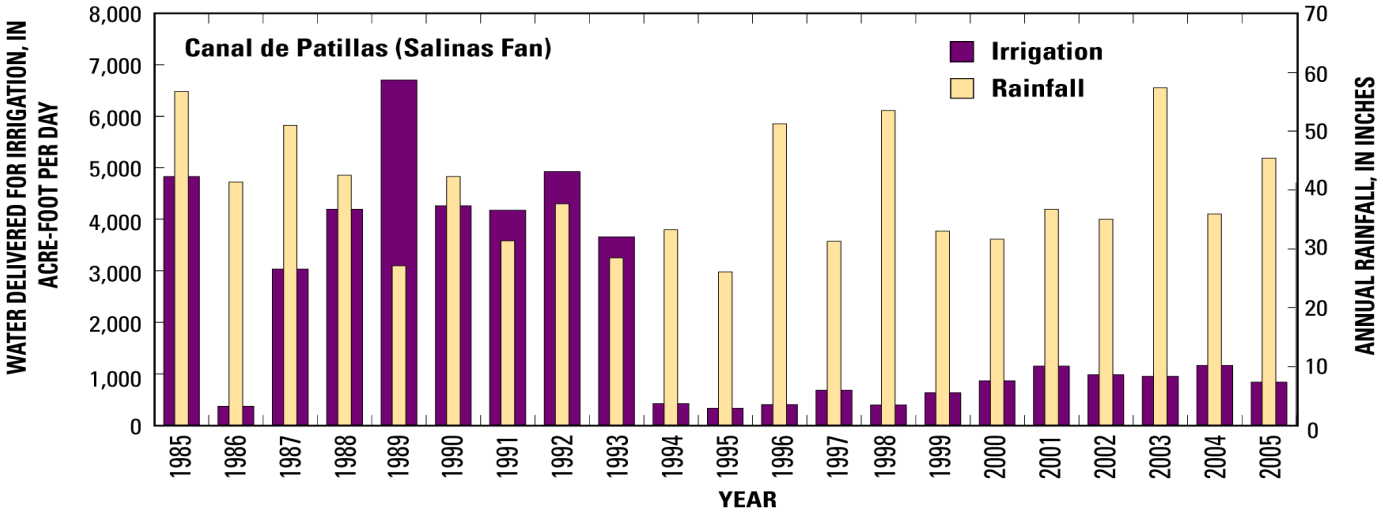

Figure 4*c*. Irrigation water deliveries from Canal de Patillas and rainfall from 1985 to 2005

Table 4. Estimates of agricultural areas and water requirements for 1986, 1991, and 2002, in the vicinity of Salinas and Jobos areas, Puerto Rico.

Description	Year(s)	Total area cultivated		Crop water application rate			Source of estimates
		Acres	Square miles	Feet per year	Million gallons per day	Acre-feet per year	
Sugarcane	1986	9,290	14.5	4	33.2	37,160	Field survey (Torres-González and Gómez-Gómez,1987; Quiñones-Aponte and Gómez-Gómez,1987)
Sugarcane (active/ abandoned)	1991	5,214	8.1	4	18.6	20,856	Estimates of 1991-92 Landsat Thematic Mapper (Helmer and others, 2002; reclassification of Landsat Thematic Mapper Imagery by O.M. Ramos, U.S. Forest Service, written commun., 2003)
Row crops		1,176	1.8	2	2.1	2,352	
Pasture/hay		4,747	7.4	1	4.2	4,747	
Row crops	2002	4,000	6.3	2	7.1	8,000	Field survey (Rodríguez, 2006)
Pasture/hay		542	0.8	1	0.5	542	

from Canal de Patillas to farms within the Salinas fan averaged about 4,000 ac-ft/yr from 1985 to 1993, and dropped sharply to an average of 645 ac-ft/yr from 1993 to 2002 (fig. 4*C*).

Groundwater Use

In the early 1900s, the feasibility of using groundwater was directly related to the availability of steam-driven centrifugal pumps and total withdrawals were about 8 Mgal/d between 1905 and 1910 (Quiñones-Aponte and others, 1996). The groundwater withdrawal capacity of these pumps, however, was limited to shallow depths, generally less than 40 ft below land surface. In the mid-1920s, groundwater withdrawals increased to about 28 Mgal/d when these pumps were replaced by more efficient kerosene-driven pumps; by in the 1930s, the kerosene-driven pumps were replaced by electrically driven deep turbine pumps. Total estimated groundwater withdrawals were about 33 Mgal/d in the early 1970s. After 1970, groundwater withdrawal by different use types became more readily available. Groundwater withdrawals for public supply have been mostly constant from 1986 to 2002, 3.98 and 4.5 Mgal/d, respectively. By 2002, agricultural groundwater withdrawals in the study area declined to about 6 Mgal/d as a result of the switch to more efficient irrigation practices in the 1990s. In 2002, total groundwater withdrawals in the study area were estimated at 11.4 Mgal/d. The construction of shallow domestic wells, which is a widespread practice, contributed to the constant groundwater withdrawals for public supply from 1986 to 2002.

The construction of drainage canals was necessary to lower the water table in water-logged areas and reclaim land for cultivation, particularly along the coastal wetlands. The water-logged areas result from poorly drained soils, combined with a high water table in areas of surplus irrigation water. In the 1940s, additional coastal dewatering structures were built primarily as part of malaria control programs.

The replacement of sugarcane cultivation with truck-farm crops, sorghum, and corn, and the concurrent change from furrow to micro irrigation not only modified groundwater withdrawal patterns but also substantially reduced recharge to the aquifer from irrigation return flow provided by furrow application of surface waters. Nearly all of the water applied by micro irrigation is transpired by the crops, resulting in zero irrigation return flow (Yamauchi, 1984; Kuniansky and others 2004).

Although groundwater withdrawals for irrigation have decreased since the 1970s within the study area, the potentiometric surface in coastal portions of the aquifer has been lowered by reduced irrigation return flow to the aquifer and increasing groundwater withdrawals for public supply and industrial use, as indicated by the cones of depression delineated by Rodríguez (2006). Additionally, local groundwater withdrawals may have contributed to deteriorating water quality by causing deeper groundwater with high dissolved solids concentrations and saline waters near the coast to migrate toward pumping wells. Evidence of saline-water encroachment has been detected within the study area by Díaz (1974) and Rodríguez (2006). Annual pumpage data compiled for the current study is provided in appendix 1.

Geologic Setting

The study area is mostly underlain by 10- to 200-ft-thick fan delta and alluvial deposits predominantly Quaternary in age (plate 3). These deposits overlie highly faulted, undifferentiated volcanic breccias, lava, volcanogenic sandstone and siltstone (volcaniclastic), minor limestone, local minor igneous intrusive and hydrothermally altered rocks of Cretaceous to early Tertiary age (Krushensky and Schellekens, 2001; Renken and others, 2002). These older rocks extend southward to the coast beneath the fan-delta deposits. Generally, a weathered bedrock layer (regolith) of varying thickness is present between the older rocks and the overlying fan-delta deposits, particularly along the northern part of the study area, near the foothills, and at sites where horst and graben-type structures are present (plate 3). The bedrock locally protrudes above the fan-delta deposits near the foothills and in the vicinity of the Central Aguirre sugar mill near the coast due to normal faulting, differential erosion, or both. Fracturing in the bedrock is locally intense, as indicated by logs for boreholes drilled as part of the feasibility study for the proposed Aguirre Nuclear Power Plant (Puerto Rico Water Resources Authority, 1972).The fan-delta and alluvial deposits include thick to very thick, crudely stratified, clast-supported conglomerates; and horizontal and planar cross-stratified gravels (boulders, cobbles, and pebbles), sand, and thickly bedded to massive silt and clay (Renken and others, 2002). These lithologic facies may be present as thick horizontal beds, but also may be present as channel-fill deposits enclosed within thickly bedded and massive silt and clay deposits as defined in unpublished USGS lithologic logs and field reconnaissance notes, and defined by Renken and others (2002, plates 1 and 4). Generally, the coarsest-grained deposits (gravel and sand) are found in the proximal facies of the fan-delta deposits in the upper part of the coastal plain and in the vicinity of streams. In general, the fan-delta sequence thickens toward the coast and its thickness may range from about 10 ft at the northern edge of the coastal plain to as much as 200 ft at the seaward edge of the sequence. The fan-delta

deposits are represented by time-equivalent units that extend an undetermined distance offshore, as indicated by surface-resistivity data collected inland, continuous resistivity profiles (CRP, discussed in more detail in the Hydrogeology section) collected offshore near the coastline, and lithologic data available from the USGS files and collected as part of the geologic assessment for the proposed Aguirre Nuclear Power Plant (Puerto Rico Water Resources Authority, 1972). The sequence of fan-delta deposits thickens or thins at sites where horst and graben-type structures, caused by normal faulting, are present in the underlying Cretaceous and early Tertiary rocks, as described in litholigic logs for wells 46 (SC-2) and 89 (SC-3) (appendix 2 , locations shown on plate 3). The lithologic logs of wells SC-2 and SC-3 were drilled in the study area as part of a regional hydrogeologic study of the South Coast aquifer (Gómez-Gómez, 1987; Renken and others 2002). At SC-2, drilled in the downthrown (graben) side of a normal fault, the fan-delta deposits at the base of the sedimentary sequence may be of Miocene age with a thickness that exceeds 400 ft. At SC-3, drilled on the upthrown (horst) side of a normal fault, the Cretaceous and early Tertiary basement was encountered at a depth of about 200 ft below land surface (lithologic log SC-3, app. 2).

Along the coast, the surface of the fan-delta sequence is separated from the Caribbean Sea by a narrow land-marine transition zone of marsh and mangrove swamps, tidal and supratidal salt flats, and beach deposits. In the Jobos Bay area, mangroves, marshes, and tidal flats are mostly restricted to those areas protected by offshore, fringing reefs. Within the marsh and mangrove swamp area, the fan-delta deposits are mostly overlain by organically rich clay deposits. These deposits were defined near the coast during construction of two piezometers—JBNERR East and JBNERR West at wells 185 and 184, respectively (plate 2 and app. 3). At both piezometer sites, two separate main zones were identified, each having medium- to coarse-grained gravel with a coarse sand matrix, and both bounded by a predominantly clay and silt sequence (app. 4).

The inland (northward) extent of the gravel zones present in the vicinity of piezometers JBNERR East and West is unknown. The offshore time-equivalent fan-delta deposits near these piezometers resulted from deposition during low sea level stands, the last occurring approximately 10,000 to 14,000 years ago, when the subaerially exposed fan-delta plain extended further southward. The time-equivalent offshore fan-delta deposits are overlain by modern inner shelf deposits that may extend from the shoreline to water depths of 60 to 100 ft. These inner shelf deposits are separated into nearshore, shelf platform, and shelf basin areas (Renken and others, 2002). Nearshore, these inner shelf deposits consist primarily of terrigenous fine sand. The shelf-platform zone consists of a layer of gravel-to-silt size bioclastic detritus underlain by a cemented hardground surface. The shelf basin acts as a depocenter for terrigenous sediment and carbonate detritus from contiguous fringing reefs. All of these inner shelf deposits may be considered to be the modern, active part of the modern fan-delta depositional system that partially isolated the underlying older fan-delta deposits already described.

Hydrogeologic Setting

Fan-delta and alluvial deposits constitute the South Coast aquifer in the study area. The regolith zone in conjunction with fractures in the underlying Cretaceous and Early Tertiary basement can be considered an aquifer of secondary importance, although it may be the only groundwater source along the foothills and other areas where the alluvium is thin or absent. The less permeable regolith and underlying fractured bedrock may be hydraulically connected with the South Coast aquifer in areas not separated by silt and clay.

The fan-delta and alluvial deposits in the study area compose a highly heterogeneous aquifer characterized by multiple water-bearing, impermeable, and semi-permeable units with gravel and sand facies constituting the main water-bearing units. The thickness of the gravel and sand facies is highly variable and mainly controlled by the position of the horst and graben structures and high energy streams, particularly the Río Nigua. The fence diagram shown in plate 4 indicates that the combined thickness of gravel and sand facies may range from 10 ft in the northern part of the study area to as much as 110 ft along the southern border of the study area. In the vicinity of streams such as Río Nigua, the combined gravel and sand facies locally may range in thickness from 80 to 100 ft. Although clay and silt deposits have poor hydraulic properties, they function as leaky confining beds to contiguous gravel and sand deposits throughout the study area, particularly along the coastal area near Jobos Bay. For example, lithologic and water-level data collected at the two piezometer nests along the northern boundary of the JBNERR indicate confined groundwater conditions exist in the immediate vicinity of Mar Negro and the Bosque de Jagueyes areas. The thickness of surficial clay and silt in the study area, as determined from drillers' logs, ranges from less than 5 ft to a maximum of 70 ft. The base of this clay-silt unit was used to define the altitude of the top of the more permeable sediments that constitute the aquifer (plate 5). Throughout the northern part of the coastal plain and near major streams, the clay-silt unit is thin or absent and the aquifer is unconfined.

The lithologic logs of wells SC-2 and SC-3 (app. 2), indicate that the sediments become increasingly consolidated with depth; therefore, the permeability

may decrease with depth. The gravel and sand become increasingly cemented by silica, calcite, clay, and silt. The most permeable zone in these two wells is less than about 200 ft below land surface.

Fresh groundwater-bearing gravel and sand units extend offshore, as indicated by hydrogeologic data collected during the installation of piezometers along the coastal margin near Mar Negro and the Bosque de los Jagueyes, and by results obtained from CRP surveys conducted as part of this study offshore between Punta Arenas and the mouth of Río Seco, including Jobos Bay. Brackish and fresh-water-bearing gravels were encountered at JBNERR West and JBNERR East piezometer nest sites (wells 184 and 185, plate 2), as discussed earlier. The specific conductances measured in the permeable deposits of the shallow piezometers were 13,000 and 8,000 µS/cm (microsiemens per centimeter) at 25 °C at the JBNERR East and JBNERR West sites, respectively. The specific conductances measured in the permeable deposits of the deep piezometers were 5,600 and 817 µS/cm at 25 °C at the JBNERR East and JBNERR West sites, respectively. No apparent resistivity values equal to or less than 3.0 Ω·m (ohm-meters), representative of saline groundwater, were obtained from the direct current (DC) resistivity surveys conducted along the coastal margin near the Mar Negro and Bosque de los Jagueyes.

The CRP survey lines along the coast and the interpreted vertical resistivity distribution obtained along each transect are shown on plates 6*A*-*H*. In each section, resistivity values equal and greater than 1 Ω·m represent freshwater, a value of 0.4 represents sea water, and values between 0.4 and 1.0 Ω·m may represent a mixture of fresh groundwater and sea water. The vertical resistivity distributions shown on some of the plates indicate that the inland freshwater-bearing units extend offshore and that freshwater, sea water, and mixed (brackish) groundwater discharge may occur at some sites on the sea bed. The possibility exists, however, that seawater may be encroaching upon the aquifer.

The offshore extent of the freshwater-bearing units is unknown, but CRP surveys (plates 6*C*, section lines 2F and 2J, respectively) indicate that the freshwater-bearing zones detected beneath Jobos Bay may extend underneath Punta Pozuelo. Similarly, the freshwater-bearing zones may extend southward of the Mar Negro area as indicated by section lines 2A-E in plate 6*B*. The freshwater-bearing zones, in general, are overlain by a diffuse zone that results from the mixing of fresh groundwater and seawater. Brackish to fresh submarine groundwater discharge may be occurring at some sites in the Mar Negro area, according to the interpretation of the CRP data (plates 6*D*-*E*; section lines 3C-I). The freshwater zones beneath Jobos Bay are generally more continuous and extend from 20 to greater than 80 ft below sea level (about the maximum penetration depth of the CRP method). The freshwater-bearing zones in the Mar Negro area are generally fragmented and the CRP data indicate that most of these zones may be present below the penetration depth of the CRP method, although some are present locally from 30 to 50 ft below sea level. West of Mar Negro, the freshwater-bearing units are mostly continuous and extend 23 ft below sea level (plates 6*A* and 6*G*). The continuous and widespread character of the freshwater-bearing units east of the Mar Negro area, in Jobos Bay, is probably due to paleochannel deposits of the Río Seco, Quebrada Amorós, and Quebrada Aguas Verdes that were submerged during the last sea level rise at the end of the last ice age (between 10,000 and 12,000 years ago; Renken and others, 2002). The submerged parts of these streams might be rich in sand and gravel deposits that were enveloped by clay and silt deposits as a result of sea level rise. These submerged paleochannels might be hydraulically connected with the up dip sediments along the current streams. Thus, upward seepage from the aquifer is likely to occur beneath parts of Jobos Bay (plates 6*C*, 6*F*, and 6*H*).

The base altitude of the aquifer within the study area (plate 7) is considered to be the base of the permeable units in the study area. The altitude and lithologic data used to delineate the bottom of the aquifer was obtained from drillers' logs in the USGS files and published studies within the area by the USGS and Commonwealth agencies. The base of the aquifer is the top of underlying impermeable or low-permeability rocks, including volcanic and volcaniclastic rocks, lithified conglomeratic sandstone, claystone-shale, siltstone, and minor limestone. Although of lesser importance than the lithologic character of the rocks, most of the wells in the study area have completion depths that are less than 250 ft below land surface, indicating that most water-producing zones are at less than 250 ft below land surface. The general southward dip of this basal surface is locally interrupted by lows and highs that result mainly from the presence of the horst and graben-type structures discussed earlier in the geology discussion. The base altitude of the aquifer in the offshore areas was approximated from previous studies (Puerto Rico Water Resources Authority, 1972; Renken and others, 2002).

Hydraulic Properties

Multiwell aquifer test results in the study area are sparse and limited to a few sites (Quiñones-Aponte, 1989). Consequently, the hydraulic conductivity of the entire aquifer in the study area cannot be determined by extrapolating the few multiwell aquifer test results given the depositional heterogeneity of the fan-delta deposits.

Analytical solutions for flow to wells under water-table or confined conditions were used to obtain

estimates of transmissivity from specific-capacity data using the methods described by Theis and others (1963). The horizontal hydraulic conductivity (K_h) was then calculated at each well by dividing the estimated transmissivity by the total saturated thickness of the aquifer penetrated by a particular well as reported mostly by water-well drillers (table 5).

The calculated horizontal hydraulic conductivity estimates ranged from 2 to 500 ft/d (feet per day). The hydraulic conductivity values are greatest in those areas where coarse-grained deposits such as gravels and sands predominate (figs. 5 and 6). The percentage of sand and gravel is calculated as the reported total thickness of sand and gravel penetrated by water wells divided by total well depth. The largest percentages of sand and gravel are in areas along the graben structures, paleochannels, and in the vicinity of relatively high energy streams, such as the Río Nigua.

Quiñones-Aponte (1989) estimated a storage coefficient of 0.0003 from an aquifer test conducted in the southeastern section of the Salinas fan. This value is representative of semi-confined to confined beds present in the coastal portions of the study area. Specific yield values ranging from 0.1 to 0.2, representative of unconfined conditions, were assumed to prevail in the upper fan-delta areas where semi-confined and confined beds are not present.

The great heterogeneity of the aquifer in the study area results from the predominant fan-deltaic depositional environment. It is reasonable to assume that the aquifer in the study area must have some vertical anisotropy, in which the horizontal hydraulic conductivity (K_h) would be greater than the vertical hydraulic conductivity (K_v). Bennett and Giusti (1971) constructed a three-layer electric analog model of the South Coast aquifer using a K_v to K_h ratio of 1:1,000 between model layers representing an aquifer thickness of 30 to 100 ft. Ratios of K_v to K_h of 1:10 were used in a digital model study of the Santa Isabel fan delta immediately west of the study area between model

Table 5. Estimated horizontal hydraulic conductivity from specific-capacity data.

[Number within parenthesis as in appendix 3. Number in bold is the depth to the aquifer base. USGS ID, U.S. Geological Survey identification number; ft, foot; gal/min, gallon per minute; gal/min/ft; gallons per minute per foot; ft/d, foot per day; (u), unconfined; (c), confined]

Well name and reference number	USGS ID	Test duration, (days)	Well depth (ft)	Depth to water (static), (ft)	Discharge (Q), (gal/min)	Pumping water level, (ft)	Specific capacity, in (gal/min/ft)	Hydraulic conductivity (k)[1] (ft/d)
Benito 1 (1)	175854066114900	0.58	60	1	350	59	6.0	20 (u)
San Felipe (old) (2)	175816066125400	0.125	54	0	125	53	2.4	10(c)
PRASA Coqui #1 (3)	175826066134400	0.208	80	17	156	29	13.0	60(c)
Templo Glove (4)	175830066135400	1	80	18	150	28	15.0	70(c)
Aguirre Sugar 9 (6)	175810066145300	0.33	128	11	1200	20	133.3	200(u)
PRWRA 1 (7)	175824066142300	0.33	250	5	800	50	17.8	10(u)
Cautiño 3 (11)	175822066104300	0.125	130	12	550	20	68.8	80(u)
Josefa Norte (16)	175732066091900	0.17	100/**86**	8	420	30	19.1	40(u)
La Ana at Josefa (17)	175756066095700	0.17	195/**175**	15	500	50	14.3	20(u)
PRASA Pte Jobos (18)	175724066095600	0.54	150	4	125	70	1.9	2(u)
Merced Batt Well 2 (23)	175648066081600	1	110/**65**	2	222	13	20.2	60(u)
Melania (31)	175755066084800	0.33	105	11.5	1040	28	63.0	100(u)
Reunion 3 (32)	175735066085900	0.5	132/**48**	15	300	60	6.7	30(u)
Phillips #7 (33)	175718066083900	0.25	151/**100**	16	400	29	30.8	90(c)
Fibers 1 (34)	175754066084100	1.08	120/**114**	26	210	60	6.2	20(c)
Phillips Dom #2 (35)	175716066083400	0.25	150	21	225	96	3.0	6(c)

Table 5. Estimated horizontal hydraulic conductivity from specific-capacity data.—Continued

[Number within parenthesis as in appendix 3. Number in bold is the depth to the aquifer base. USGS ID, U.S. Geological Survey identification number; ft, foot; gal/min, gallon per minute; gal/min/ft; gallons per minute per foot; ft/d, foot per day; (u), unconfined; (c), confined]

Well name and reference number	USGS ID	Test duration, (days)	Well depth (ft)	Depth to water (static), (ft)	Discharge (Q), (gal/min)	Pumping water level, (ft)	Specific capacity, in (gal/min/ft)	Hydraulic conductivity (k)[1] (ft/d)
PRASA Fibers 3 (38)	175735066090500	0.25	150	11	450	84	6.2	10(c)
Aguirre 3 (41)	175804066150700	1	150	6	1900	28	86.4	200(c)
Caraballo (43)	175856066151000	0.25	140	21	1000	42	47.6	50(u)
Esperanza #1 (44)	175810066153500	0.25	150	4	225	15	20.5	40(c)
Magdalena #2 ((49)	175855066161400	0.25	150/**128**	45	920	54	102.2	300 (c)
Salinas Airfield (53)	175819066160600	1	90/**85**	25	60	25.8	75.0	400 (c)
Salinas 1(54)	175851066174600	1	120	16	550	20	137.5	200(u)
Salinas 2 (55)	175850066174500	1	120	18	670	22	167.5	300(u)
Antonneti #1 (56)	175821066182100	0.25	60/**23**	8	440	11.5	125.7	400(u)
Margarita #3 (57)	175839066180700	0.25	154/**95**	11	748	24	57.5	100(u)
U.S. Army #1 (59)	175928066171500	0.25	165/**151**	27	370	29.5	148.0	200(u)
Vélez #1 (61)	175928066174000	0.25	107/**70**	6	465	17	42.3	100(u)
Pueblito (62)	175905066172000	0.33	126	14	480	27	36.9	50(u)
Pozas Test #1 (66)	175848066190100	0.25	168	0.5	460	51.5	9.0	10(c)
Sabater Viejo (67)	175926066141100	0.17	200/**30**	20	180	72	3.5	50(u)
Godreau 6 (71)	175921066165500	0.33	150	35	1600	54	84.2	200(c)
Godreau 5 (72)	175931066160100	0.25	146/**144**	38	450	45	64.3	200(c)
U.S. Army #2 (73)	175952066162400	0.25	165/**85**	43	96	53	9.6	60(c)
Porrata (74)	17594366150600	0.25	272/**128**	53	380	106	7.2	20 (c)
Sostre #2 (80)	175959066201200	0.5	236/**123**	70	340	102	10.6	30(u)
Sostre #1 (81)	175956066205400	0.25	146/**102**	45	800	61.5	48.5	200(c)
Coco 1 (82)	180044066153500	0.75	120	25	120	91	1.8	5(c)
Theater 1 (86)	180023066175400	0.71	80	58	15	97	0.4	3(u)
Aguirre Sugar 1A (93)	175747066075800	0.125	107/**93**	4	153	9	30.6	50(u)
Godreau 7 (94)	175903066165000	1	140	11	1350	49	35.5	70(c)
Amadeo Gonzalez (95)	175933066161800	2	175	62	735	96	21.6	30(u)
Jauca 2b (98)	175820066215000	0.125	100/**78**	9.5	48	17	6.4	30(c)
U.S. Army #2 (C. Sant) (100)	175924066171500	0.17	175	28	720	47	37.9	40(u)
U.S. Army Test #1 (101)	175942066170100	2.17	57/**42**	25	14	39.5	1.0	10(u)
Bomba Pozas #2 (103)	175917066194300	0.4	160/**136**	3	450	44	11.0	10(u)
San José #1 (107)	175957066200800	0.33	117	63.8	330	93.8	11.0	30(u)
Santiago Batt #1 (108)	175954066210500	0.25	53/**39**	20	130	40	6.5	90(c)

Table 5. Estimated horizontal hydraulic conductivity from specific-capacity data.—Continued

[Number within parenthesis as in appendix 3. Number in bold is the depth to the aquifer base. USGS ID, U.S. Geological Survey identification number; ft, foot; gal/min, gallon per minute; gal/min/ft; gallons per minute per foot; ft/d, foot per day; (u), unconfined; (c), confined]

Well name and reference number	USGS ID	Test duration, (days)	Well depth (ft)	Depth to water (static), (ft)	Discharge (Q), (gal/min)	Pumping water level, (ft)	Specific capacity, in (gal/min/ft)	Hydraulic conductivity (k)[1] (ft/d)
Santiago #2 DW (109)	175959066210200	0.67	200	0	140	30	4.7	7(c)
PREPA #4 (113)	175835066145700	1	196	56.4	873	79.7	37.5	40(u)
PREPA #6 (114)	175825066142500	1	260/**195**	38	952	77	24.4	40(c)
PREPA #7 (115)	175845066142800	1	112	15.3	471	32	28.2	50(u)
PREPA #9 (116)	175810066151400	2	275	44	710	91	15.1	20(c)
Phillips 11 (117)	175715066084500	0.5	125/**48**	27	400	83	7.1	90 (c)
PRASA Fibers 2 (118)	175738066084500	0.25	100/**72**	30	325	72	7.7	30(c)
Reunión 2 (119)	175721066085500	0.25	125/**75**	30	325	72	7.7	50(c)
Fibers 2 (120)	175755066085200	1	100/**30**	22	205	50	7.3	20(c)
PRASA Pte Jobos (old) (121)	175735066095900	1	148	6	125	100	1.3	2(c)
Hormigonera Bruja (122)	175755066105000	0.25	100	16.5	180	33	10.9	40(u)
Central Guamani #2 (123)	175752066105300	0.25	153/**130**	8	1250	23	83.3	200(u)
Cora #1 (124)	175757066103900	0.25	155	27	150	32	30.0	60(c)
PRASA Villodas (126)	175841066104500	0.5	143/**31**	26	55	52	2.1	70(c)
PRASA Perpetuo (127)	175822066134900	1.5	118	0	635	22	28.9	70(c)
González #2 (132)	175959066141500	0.125	51	6	75	27	3.6	10(u)
PRWRA 5 (133)	175924066142300	1	305/**45**	25	500	41.5	30.3	300(c)
A-01 TW (134)	175721066090200	0.08	101	15.4	20	25	2.1	7(c)
Cautino 7 (135)	175908066081800	0.25	72	3	25	19.5	1.5	3(u)
Aguirre Sugar 10 (136)	175810066145100	0.33	55	4.5	920	14	96.8	500(c)
Coqui 5 (137)	1758160066133100	0.33	150	2.15	1450	44.15	34.5	60(c)
Juana #2 (138)	175823066101300	0.33	129	13	1045	21.3	125.9	200(u)
PRASA (139)	175823066084500	1	58	30	325	72	7.7	50(u)
PRASA (140)	175742066082900	0.5	67	27	400	83	7.1	30(u)
Reunión DW 1 (141)	175756066082900	0.33	118	12	1000	21.5	105.3	100(u)
Salinas 4 (142)	175922066171200	0.33	180	49	300	53	75.0	20(u)
PRASA Campamento (143)	175930066165600	1	140	72	200	88	12.5	30(u)
Godreau 3A (144)	175913066163500	0.33	102	39	520	61.5	23.1	60(u)

[1] Derived from T values estimated from Theis and others (1963)

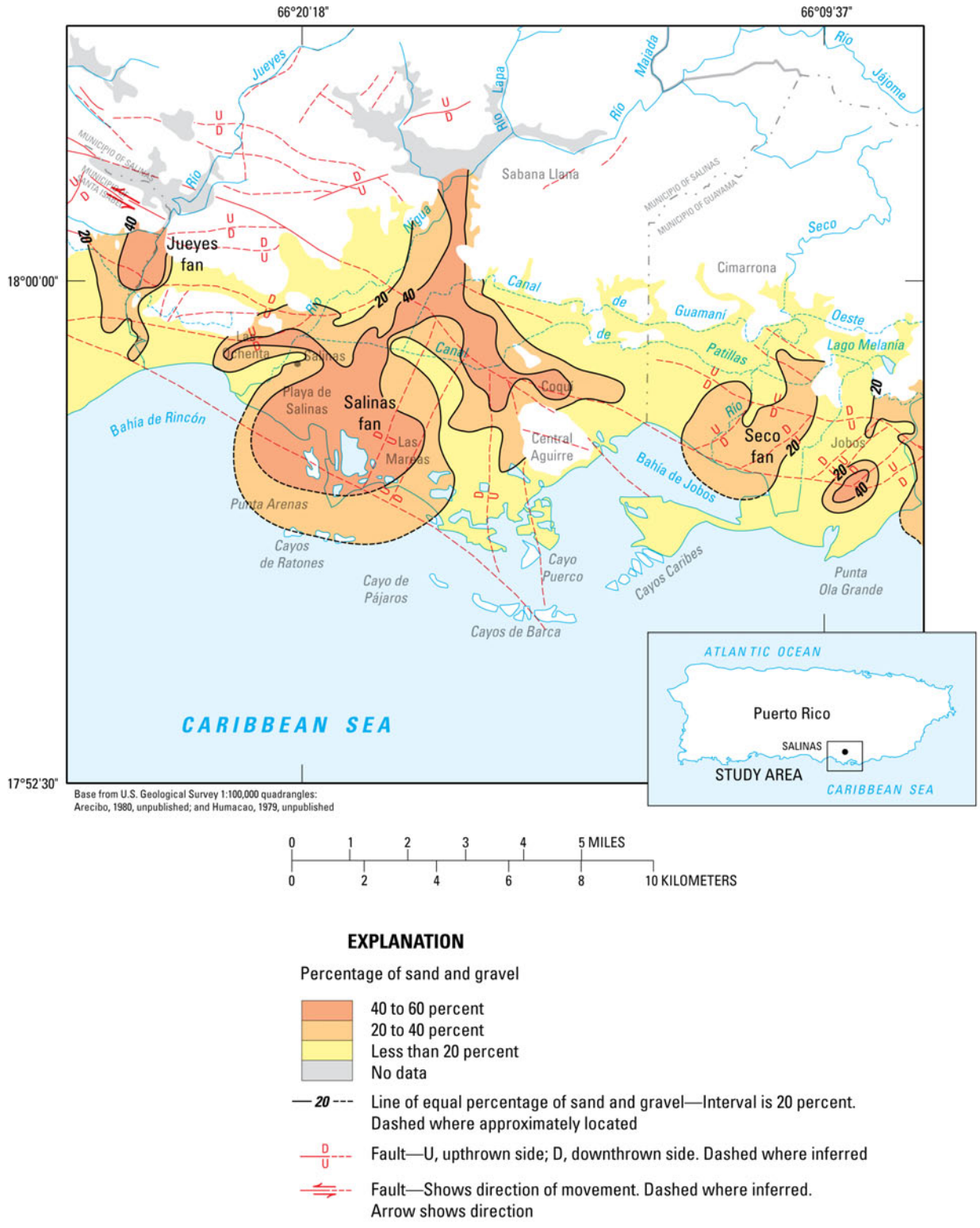

Figure 5. Sand and gravel percentage and interpretative structure in the South Coast aquifer in the vicinity of Salinas and Bahía de Jobos (modified from Renken and others, 2002).

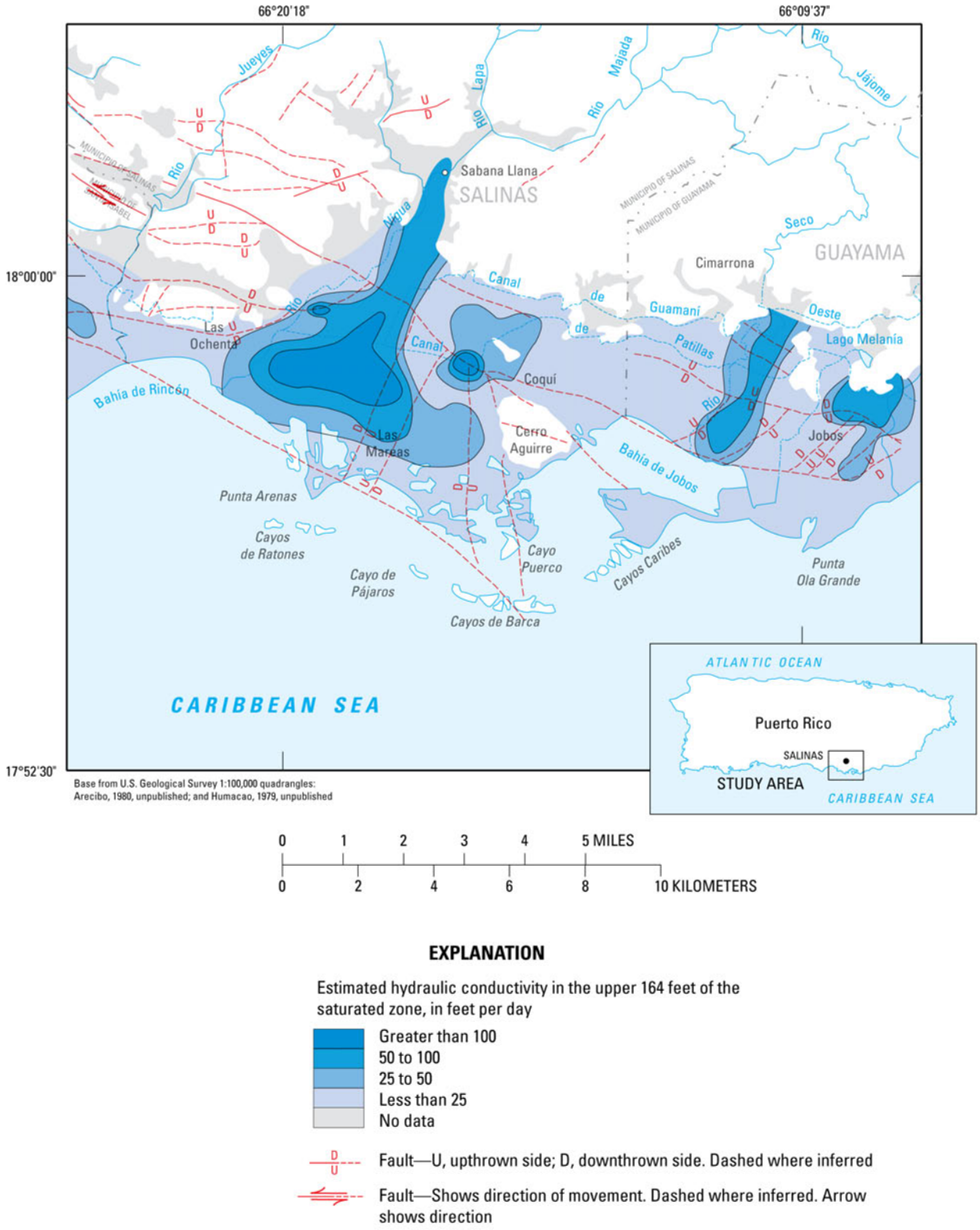

Figure 6. Generalized distribution of hydraulic conductivity in the South Coast aquifer in the vicinity of Salinas and Bahía de Jobos between the Río Jueyes and Río Guamaní (modified from Renken and others, 2002).

layers representing an aquifer thickness of 50 to 450 ft (Kuniansky and others, 2004). For this study, the ratio of K_v to K_h of 1:10 was initially used because these are more representative of the predominant unconsolidated to poorly consolidated deposits in the Río Nigua area (Bouwer, 1978; Fetter, 1994).

Groundwater Flow Patterns

The configuration of the potentiometric surface during March 1986 (Torres-González and Gómez-Gómez, 1987; Quiñones-Aponte and Gómez-Gómez, 1987) in the Salinas to Guayama area generally reflects topography (fig. 7) except for a single cone of depression north of Central Aguirre. The potentiometric surface indicates that inferred direction of groundwater flow was mainly toward the coast in the Salinas and Río Seco alluvial fan-deltas (fig. 1). Reductions in groundwater withdrawals combined with above-average precipitation conditions during the mid 1980s caused the water table to recover from previous levels.

Below-average rainfall during 12 years between 1986 and 2004 in conjunction with a general reduction in surface-water irrigation deliveries from Canal de Patillas and Canal Guamaní (fig. 2) have contributed to aquifer storage depletion and lowering of water levels in the aquifer. As a result, the potentiometric surface in July 2002 (Rodríguez, 2005) was about 15 ft lower than in 1986. Two cones of depression were inferred from the potentiometric-surface map during July 2002 (fig. 8), the largest of which extended over about 700 ac west of Central Aguirre. By May 2004, however, groundwater levels in the area had rebounded 6 to 13 ft (fig. 9) and both cones of depression were no longer present. The water-level recovery is most likely a result of infiltration from a severe storm and associated flooding during November 2003. Central Aguirre received 25 in. of rainfall that month, an event with a 25-year frequency of occurrence. The soils and deposits were permeable enough to allow the excess water to infiltrate.

Simulation of Groundwater Flow

The groundwater flow in part of the South Coast aquifer between the Río Jueyes and Río Guamaní area was simulated with a numerical groundwater flow model to evaluate how changing irrigation practices affected water levels, flow to the coast, and how future groundwater withdrawals may affect the aquifer. Specifically, the numerical simulations were used to determine: (1) how the change from furrow to drip irrigation systems have affected groundwater flow; (2) how future changes in groundwater withdrawals may affect groundwater levels in the study area; and (3) how changes in groundwater discharge to part of the JBNERR in the area of the affected black mangroves.

The groundwater flow system was simulated using the MODFLOW88/96 and MODFLOW-2000 computer codes for simulating groundwater flow of uniform density (McDonald and Harbaugh, 1988; Harbaugh and McDonald, 1996; Harbaugh and others, 2000; Hill and others, 2000). The model was initially constructed in MODFLOW88/96, using the hydrogeologic framework presented in previous sections. Model construction was followed by conducting a parameter sensitivity analysis. The model data files were then converted to MODFLOW-2000 for use of parameter estimation and calibrated in steady-state to groundwater levels from March-April 1986 and estimated water-balance conditions in 1986. Transient (time-varying) simulations were run for the 1986 to 2004 period using public supply and irrigation groundwater withdrawal rates and streamflow infiltration rate estimates previously discussed (table 3 and apps. 1 and 5). Hydraulic conductivity parameters and zones were adjusted based on parameter estimation until satisfactory matches to estimated ranges were achieved and were in general agreement with the hydrogeologic framework previously described.

Model Conceptualization and Construction

A previous digital groundwater flow model (Quiñones-Aponte and others, 1996) covered more of the South Coast aquifer than the current model and had three layers. The top layer simulated leakage in the coastal part of the aquifer including the clayey zone along the coast that partially confines the aquifer; the second layer represented the principal groundwater flow zone tapped by wells; and the third layer represented the fractured bedrock. The groundwater model used in the present study differs from the model just described in that the current model does not include the fractured rock (regolith) beneath the unconsolidated deposits and five layers are used to represent freshwater flow in the hydrogeologic units that constitute the South Coast aquifer between the Río Jueyes and the Río Guamaní. The top model layer represents the inland-most part of the aquifer, which is unconfined and where most of the streams and irrigation canal infiltration recharges the aquifer. The lower four model layers represent the unconsolidated fan-delta, interfan, and alluvial deposits, all of which are confined. The lateral extent of each model layer was estimated from the surface geology and the base (bottom) altitude of the more permeable alluvial materials of the South Coast aquifer (plates 3 and 7). The active areas and boundary conditions for each layer are shown on figure 10. The model

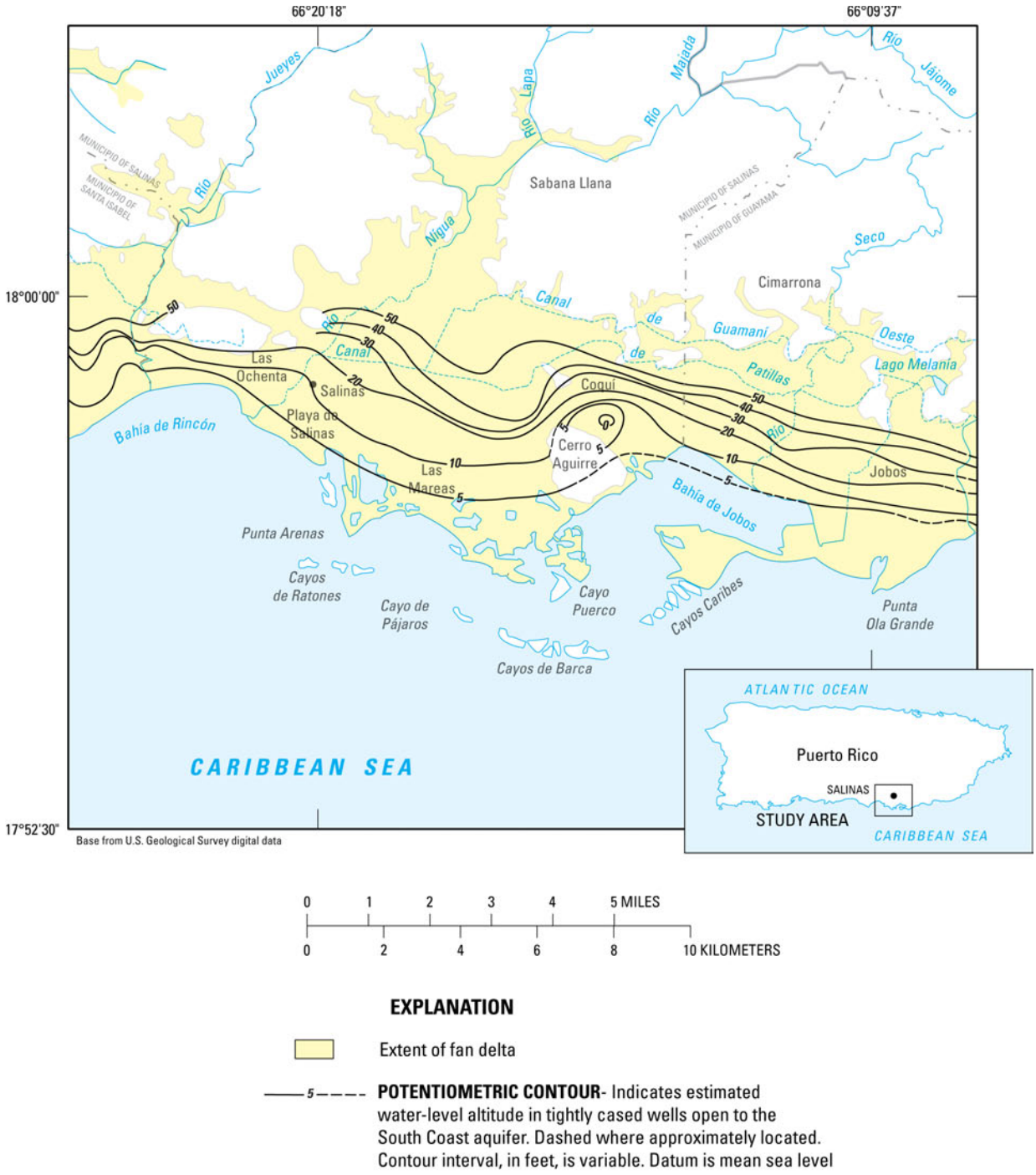

Figure 7. Potentiometric surface in the Río Jueyes to Río Guamaní part of the South Coast aquifer during March 1986 (modified from Torres and Gomez, 1987).

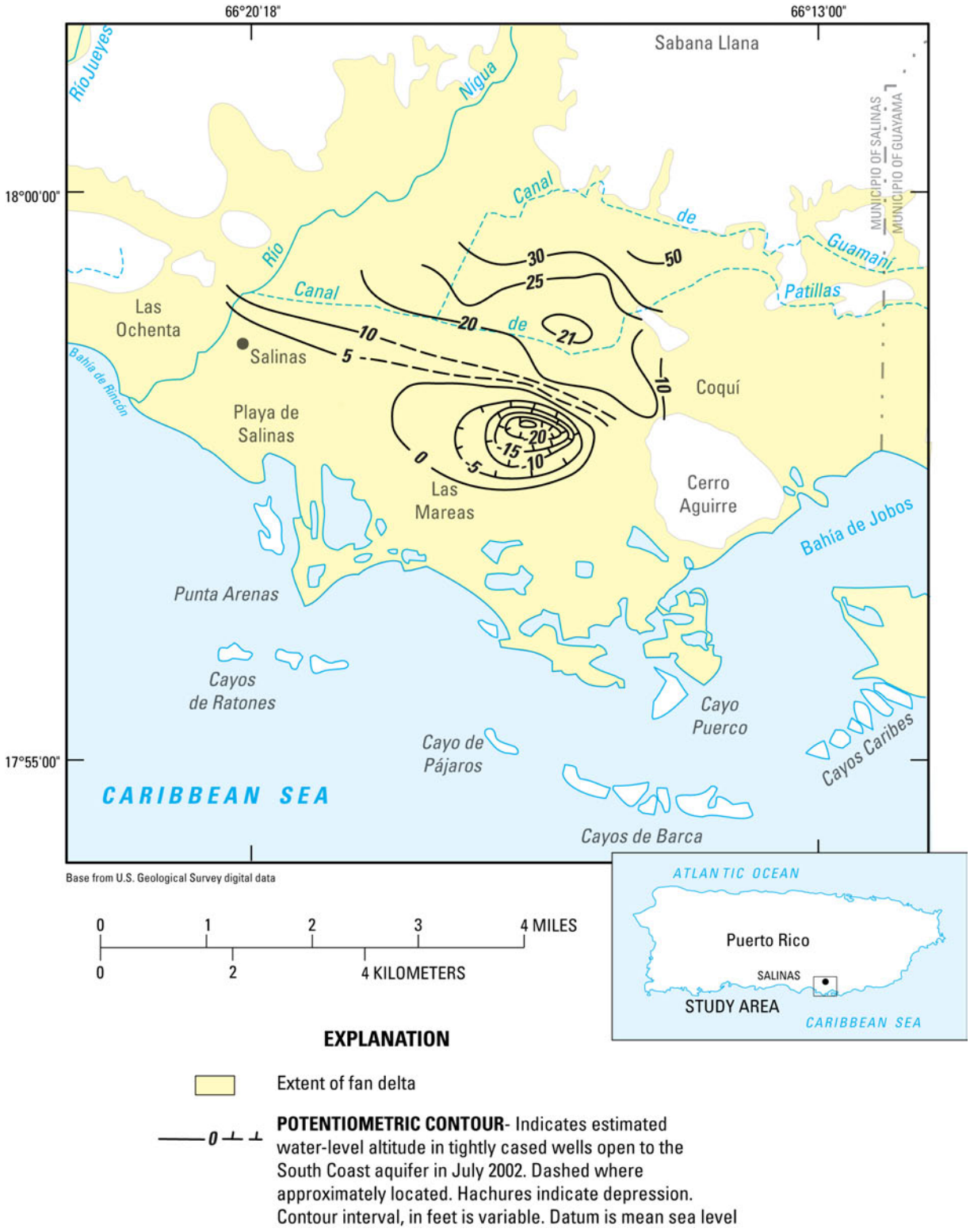

Figure 8. Potentiometric surface in the South Coast aquifer in the vicinity of Salinas during July 2002 (modified from Rodriguez, 2005).

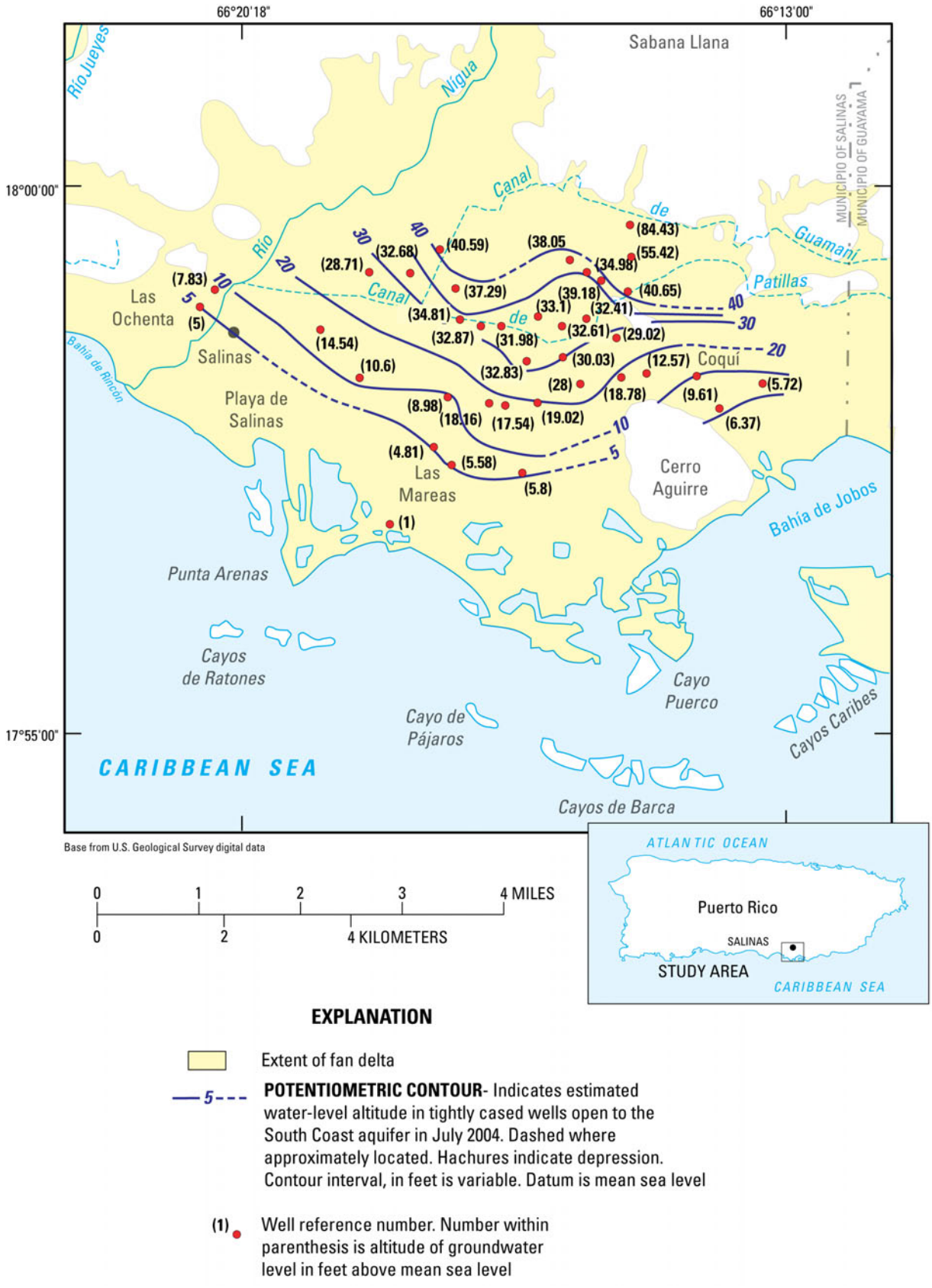

Figure 9. Potentiometric surface in the South Coast aquifer in the vicinity of Salinas during July 2004.

layers used to represent the aquifer were necessary to accurately represent the hydraulic conductivity contrasts indicated by the fence diagram (plate 4). The model grid is variably spaced, with finer spacing (802.25 ft) used near the area of interest at the coast and wider spacing (1,640.5 ft) used along the southern and eastern edges of the grid as well as the inland part of the study area (fig. 10 and plate 2).

Throughout the entire modeled area, layers 1 and 2 form the top of the aquifer. The northern extent of layer 1 is based on the northern extent of Quaternary fan-delta and alluvial deposits. Northwest of Jobos Bay, a small isolated hill (Cerro Aguirre) in the Salinas area is also included as a low permeability unit in layer 1 (fig. 10*A*). Layer 2 is active underneath much of layer 1 (fig. 10*B*), including inland areas beneath the Río Nigua, Río Lapa, and Río Majada; layer 2 is inactive north of the coastal plain where its top coincides with the top of bedrock. Layer 3 is a relatively thin layer, mostly 20-ft thick throughout, used because the clays beneath the mangrove swamp extend beneath layer 2 in part of the modeled area (fig. 10*C*). Layer 3 extends offshore into Jobos Bay where CRP data indicated possible upward freshwater discharge to the bay. The base of model layer 4 extends to the base of the aquifer, except where layer 5 is active. Model layer 5 was added to include the deepest and thickest parts of the South Coast aquifer within the Río Nigua fan-delta at Salinas, in the graben where the top of bedrock is the deepest.

The MODFLOW computer code assumes all layers are horizontal, even when a deformed grid is used. The tops and bottoms of model layers are used to calculate thickness and cross-sectional areas of model cell sides, which allows the user to verify (1) whether the simulated aquifer head is below the top of a layer for nonlinear unconfined or convertible model layers, and (2) computations associated with wet/dry functions if these options are used in the model (McDonald and Harbaugh, 1988). When thinly saturated unconfined aquifers are represented in a model, however, it can be difficult to obtain model convergence and mathematical simplification of the problem may be required (Kuniansky and Danskin, 2003). MODFLOW88/96 and MODFLOW-2000 were not designed to fully simulate flow in the unsaturated zone of an aquifer. An initial attempt was made to use an unconfined layer for layer 1 and a convertible layer for layer 2, which resulted in convergence problems. Consequently all layers were simulated as being confined to simplify the mathematical approximation of the system as a linear and more numerically stable problem. In order to constrain the transmissivity calculated by the model for layers 1 and 2 along the upper reaches of the Río Nigua basin, maximum thicknesses of 20 and 25 ft were assigned to layers 1 and 2, respectively. The saturated thickness of alluvial sediments along the upper reach of the Río Nigua is unknown. As previously indicated, the northern part of the South Coast aquifer in the modeled area (model layer 1) is unconfined and composed of highly permeable deposits, allowing streams with headwaters in the mountains to readily recharge the aquifer in this area. The top and bottom altitudes of layers 1 and 2 used in the model in the upper reach of the Río Nigua are unknown. The altitudes of the top of layer 1 and bottom of layers 1 and 2, therefore, were calculated by assigning land surface altitude as the top of layer 1, subtracting 20 ft to obtain the bottom altitude for layer 1, and subtracting 45 ft to obtain the bottom altitude for layer 2 in the upper reach of the Río Nigua, where borehole data were not available (figs. 11 and 12). The spatial discretization of the bottom altitude for all layers is shown in figure 12. In MODFLOW, the top of each layer is assumed to be equal in altitude to the base of the layer above it.

The top of layers 1 and 2 was set to land surface altitude, as estimated from digital elevation models from USGS 1:20,000 scale topographic maps (M. Santiago, U.S. Geological Survey, written commun., 2006) as shown on figure 11 except at Cerro Aguirre northeast of Jobos Bay, and along parts of the northern edge of the modeled area. In general, the potentiometric surface is below land surface in the hills. Although there were insufficient data to estimate the water-table surface altitude from land surface altitude, the water table was assigned a value that would constrain the storage properties to reasonable values for transient simulation, as discussed later.

Boundary Conditions

Boundary conditions along the top of the model grid are as follows: net recharge is applied to the top active model layer (layers 1 and 2). Net recharge is the amount of infiltration from precipitation and irrigation return flow minus evapotranspiration and surface runoff, and represents effective recharge to the saturated part of the aquifer. The spatial distribution of net aquifer recharge was based on the irrigation method used in local agricultural enterprises. Irrigation return flow from lands planted with sugarcane (using furrow irrigation) represents the highest rate of net recharge in the modeled area until 1993 when sugarcane cultivation ceased. By 2002, about 4,500 ac were used for agricultural purposes, a decrease of 4,800 ac compared to 1986 (fig. 4*A*-*B*), and drip or overhead irrigation (sprinklers and center pivot) were used for all cultivated acreage.

The Patillas and Guamaní irrigation canals are simulated in layer 1 using the River package (RIV) of MODFLOW (McDonald and Harbaugh, 1988). Along a segment of Canal de Patillas in the Salinas alluvial fan, injection wells were used to simulate infiltration

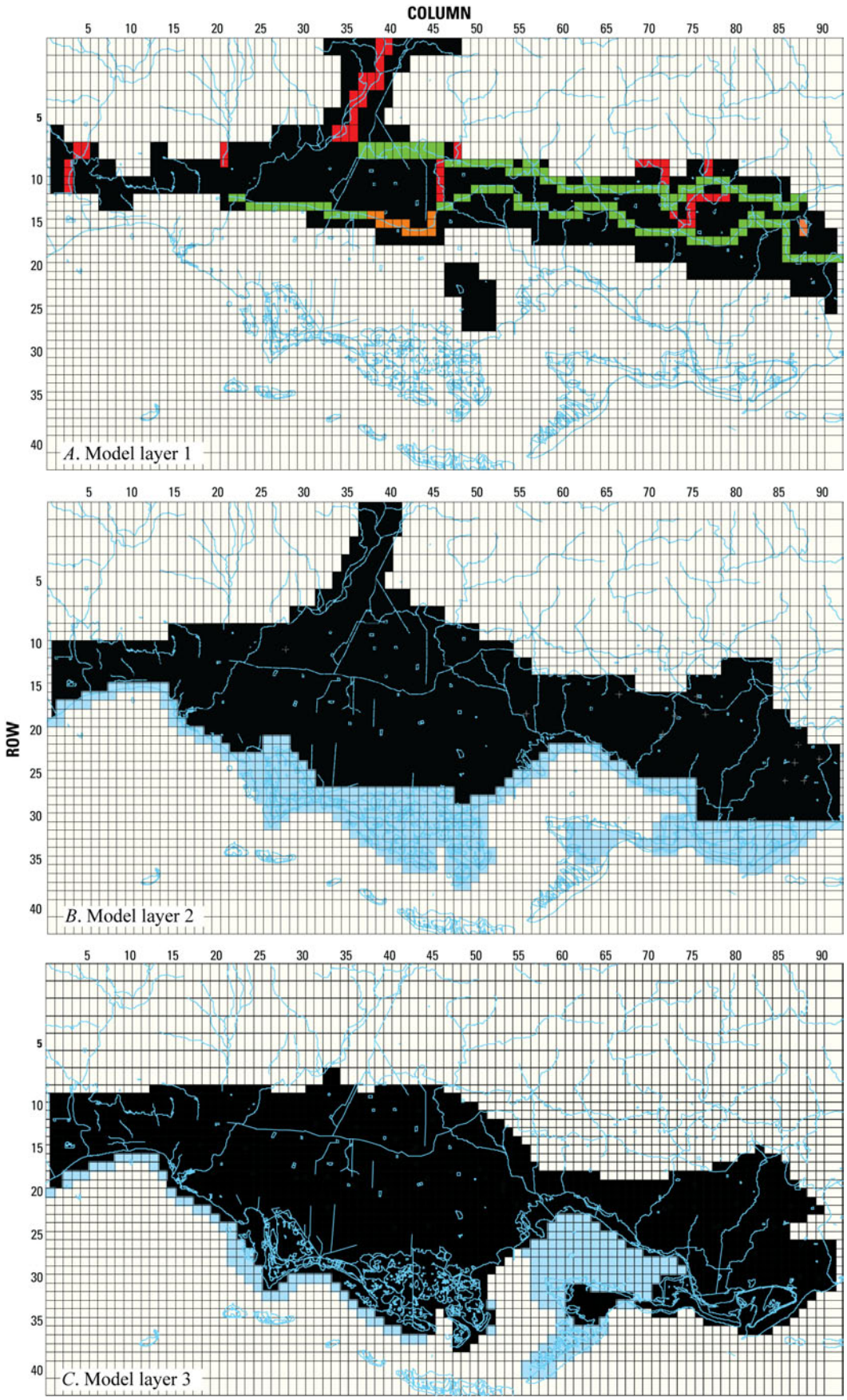
COLUMN
5 10 15 20 25 30 35 40 45 50 55 60 65 70 75 80 85 90
ROW
5 10 15 20 25 30 35 40
A. Model layer 1
B. Model layer 2
C. Model layer 3

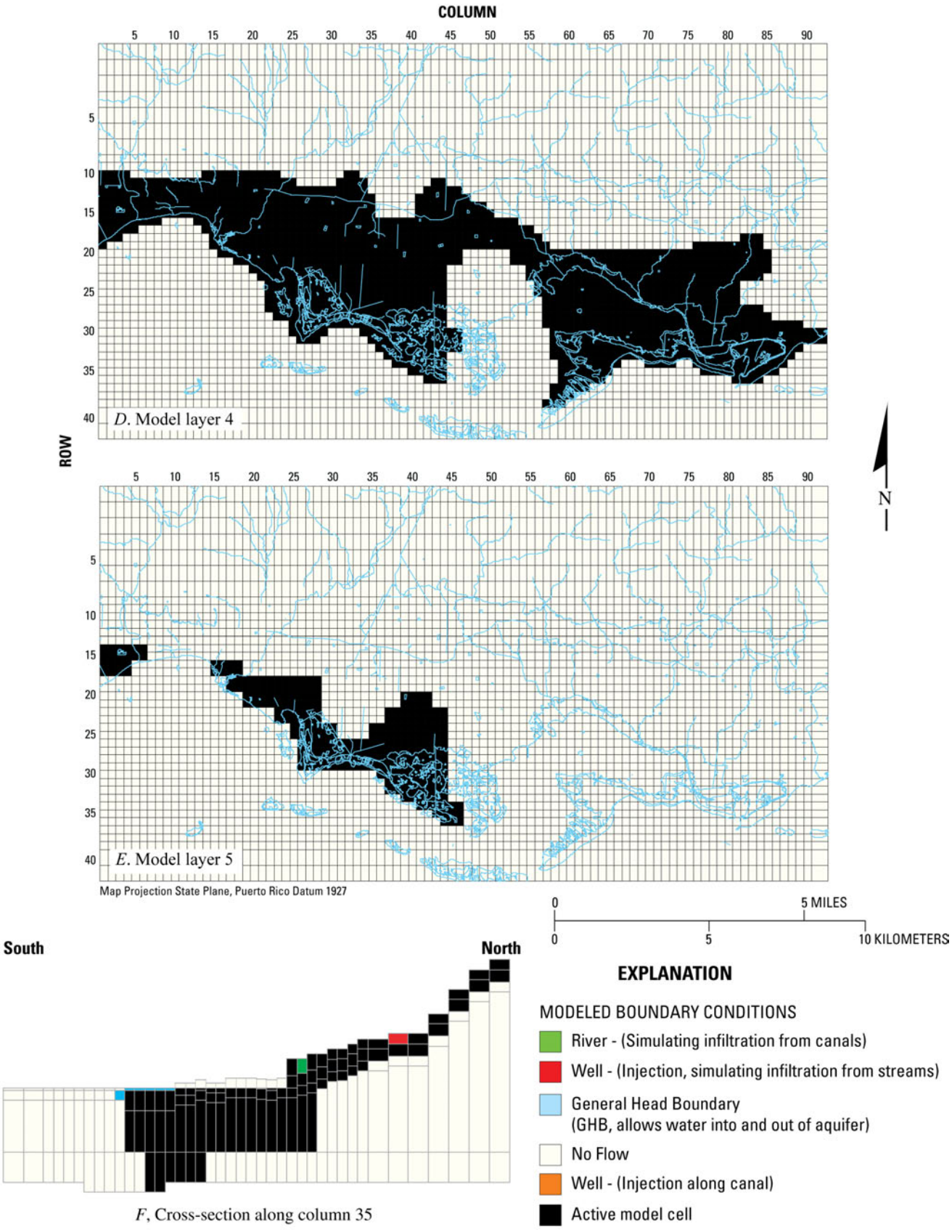

Figure 10. Finite difference grid and boundary conditions for model layers 1 through 5.

from the canal to the aquifer as estimated with stable isotopes of deuterium and oxygen-18 (Gómez–Gómez, 1991; Rodríguez, 2006). The altitude of the canal stage (RSTAGE in the River Package; McDonald and Harbaugh, 1988) was obtained from USGS 1:20,000 scale topographic maps and interpolated along the canals. The RSTAGE along the northern canal (Canal de Guamaní Oeste) ranges from 228 above mean sea level at the eastern end of the modeled area to 104 ft at the western end of the canal in the Salinas fan. The RSTAGE on the southern canal (Canal de Patillas) ranges from 97 ft above mean sea level at the eastern end of the canal to 39 ft at the western end of the canal. However, the maximum loss to the aquifer by each canal cell is constrained by setting the river bottom altitude (RBOT in the River Package; McDonald and Harbaugh, 1988) to 1 ft lower than the assigned RSTAGE. The riverbed conductance term is set such that the loss per reach is fixed for each reach by taking the total estimated loss along all of the reaches and dividing this by the number of model cells for simulating the reach. In this way, the maximum rate of inflow to the aquifer is constrained, but outflow from the aquifer to the canal is not constrained. The river cell conductance term for most of the canal model cells was set to 360 ft^2/d (square feet per day), in order to constrain the maximum leakage to the aquifer from the canals, when the simulated aquifer head drops below the canal bottom specified by the term RBOT. A few conductance terms along the Canal de Patillas were set to 4,940 ft^2/d where higher canal losses were thought to occur as indicated previously. The maximum canal losses are constrained to be less than 2 ft^3/s once the simulated aquifer head drops below the RBOT set for the RIV cells.

The estimated average annual streamflow infiltration (table 3) was injected into the aquifer using injection wells denoted as red cells in figure 10*A*. Injection wells were also placed along the part of the irrigation canal and Lago Melania, where water infiltrates the aquifer (orange cells, fig. 10*A*).

The General-Head boundary (GHB) package of MODFLOW (McDonald and Harbaugh, 1988) was used to simulate head-dependent flow to or from the mangrove swamp and coast, which is along the southern boundary of layer 2. The general head altitude was set to 0 ft (mean sea level) and the initial conductance was set at 67,280 ft^2/d (k_z was assumed to be 1 ft/d and the thickness of bed sediment 1 ft). General head boundary conditions were applied to the top of model layer 3 in Jobos Bay (as in layer 2) to adequately model those areas where the CRP data indicated freshwater discharge may be occurring to the bay (plates 6*A*-*H*; fig. 10B-*C*).

Groundwater withdrawals from the aquifer were simulated with the well package (WEL) (McDonald and Harbaugh, 1988). Pumpage was applied for the steady-state and transient simulations in layers 2 through 5 based on the screened interval penetrated by the wells (app. 3).

All of the lateral boundaries of the model are no-flow boundaries. The lateral no-flow boundaries along the coast were set at the estimated freshwater/seawater interface. This method of no-flow boundary was described by Reilly (2001). The no-flow boundary on the bottom of the system is either along the base of the permeable fan-delta and alluvial deposits, which overlies bedrock with low permeability, or at the estimated freshwater/seawater interface. The location of the freshwater/seawater interface was estimated from the freshwater lens thickness published by Renken and others (2002), Ghyben-Herzberg approximation (Bear, 1979), and the CRP data collected for the current study.

Model Calibration Strategy

Because water-use data and irrigation surveys prior to the one conducted in 1986 are less accurate than data collected during and after 1986, the process of model calibration began with developing a steady-state simulation based on the 1986 data to be used as an initial condition for transient simulation for 1986 to 2004. In March 1986, a synoptic survey of hydrologic conditions was conducted that included flow in streams and canals, groundwater withdrawals, and aquifer water-level measurements from non-pumping wells (Torres-González and Gómez-Gómez, 1987; Quiñones-Aponte and Gómez-Gómez, 1987). For transient calibration, annual stress periods were set up from 1986 through 2004. Pumpage and irrigation survey data were not available to develop transient data at a monthly resolution.

It is necessary to understand the accuracy and uncertainty of the data used for model calibration when calibrating a groundwater flow model. The match between simulated and observed data should not be expected to be closer than the accuracy of the data. Matching inaccurate observations exactly is termed "over fitting." It is also important to have estimates of fluxes to and from the groundwater system when calibrating a groundwater flow model in order to have a unique set of model parameters.

At best, the accuracy of water-level measurements for 1986 is ± 2 ft at wells where the land-surface altitude is less than about 50 ft above mean sea level, and ± 15 ft at wells where the land-surface altitude is greater than about 50 ft. In both cases, the accuracy for water-level measurements is equivalent to half the contour interval of the topographic map used by Torres-González and Gómez-Gómez (1987). Of the 66 water level measurements for 1986, about 18 are from wells where the land-surface altitude exceeded 50 ft above mean sea level. Thus, 48 measurements have an accuracy of

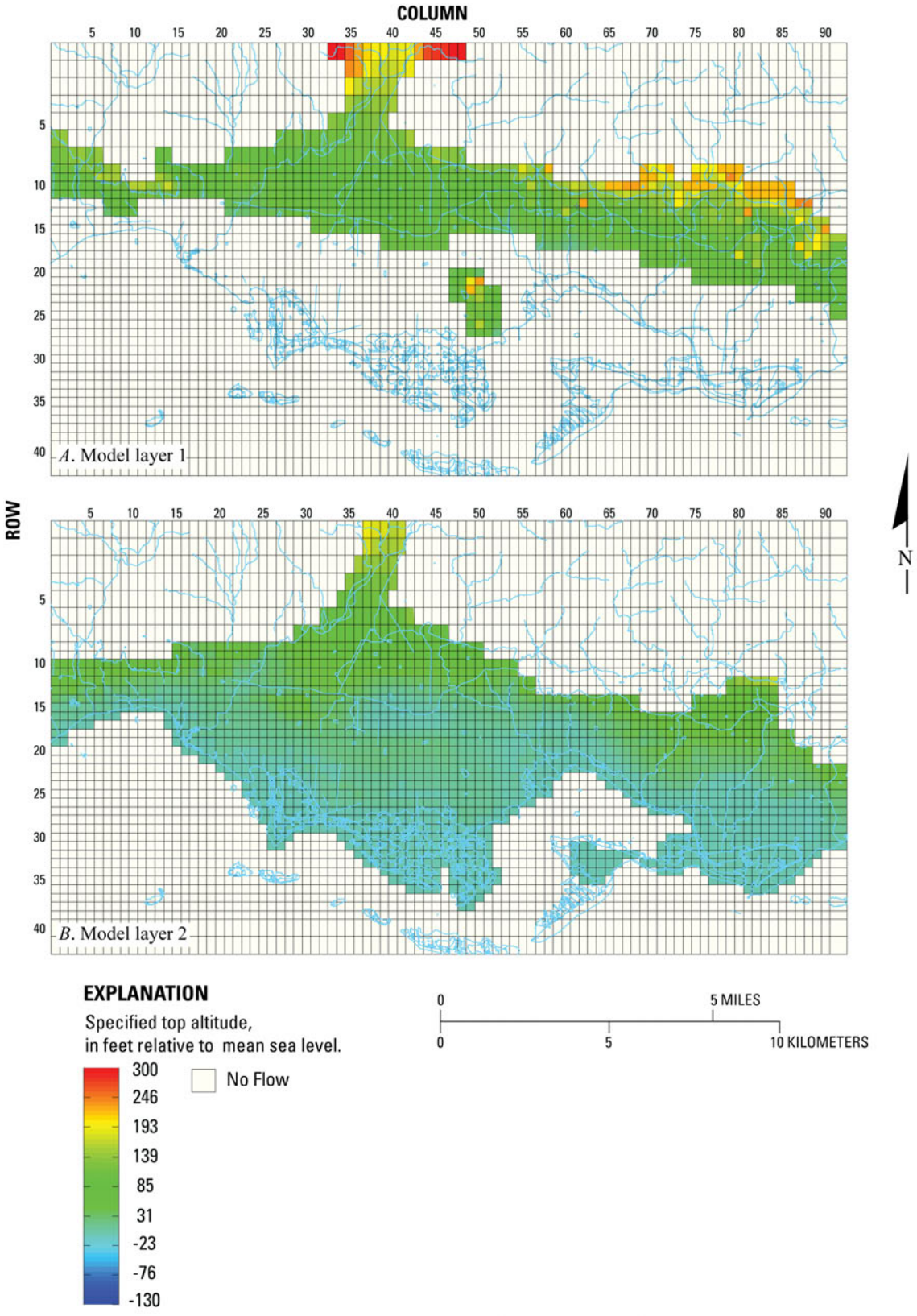

Figure 11. Specified altitudes for top of model layers 1 and 2.

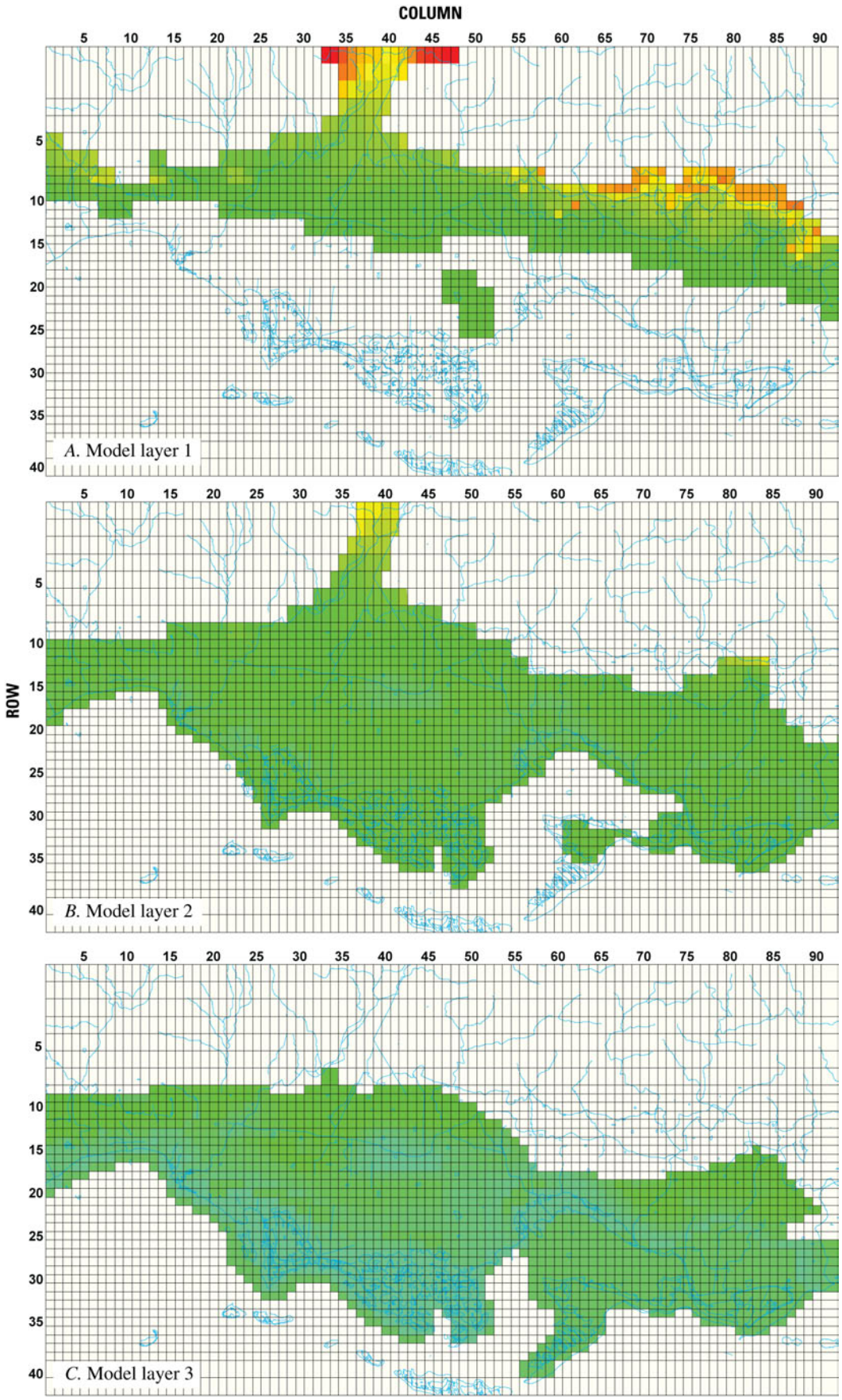
COLUMN
5 10 15 20 25 30 35 40 45 50 55 60 65 70 75 80 85 90
ROW
5 10 15 20 25 30 35 40
A. Model layer 1
B. Model layer 2
C. Model layer 3

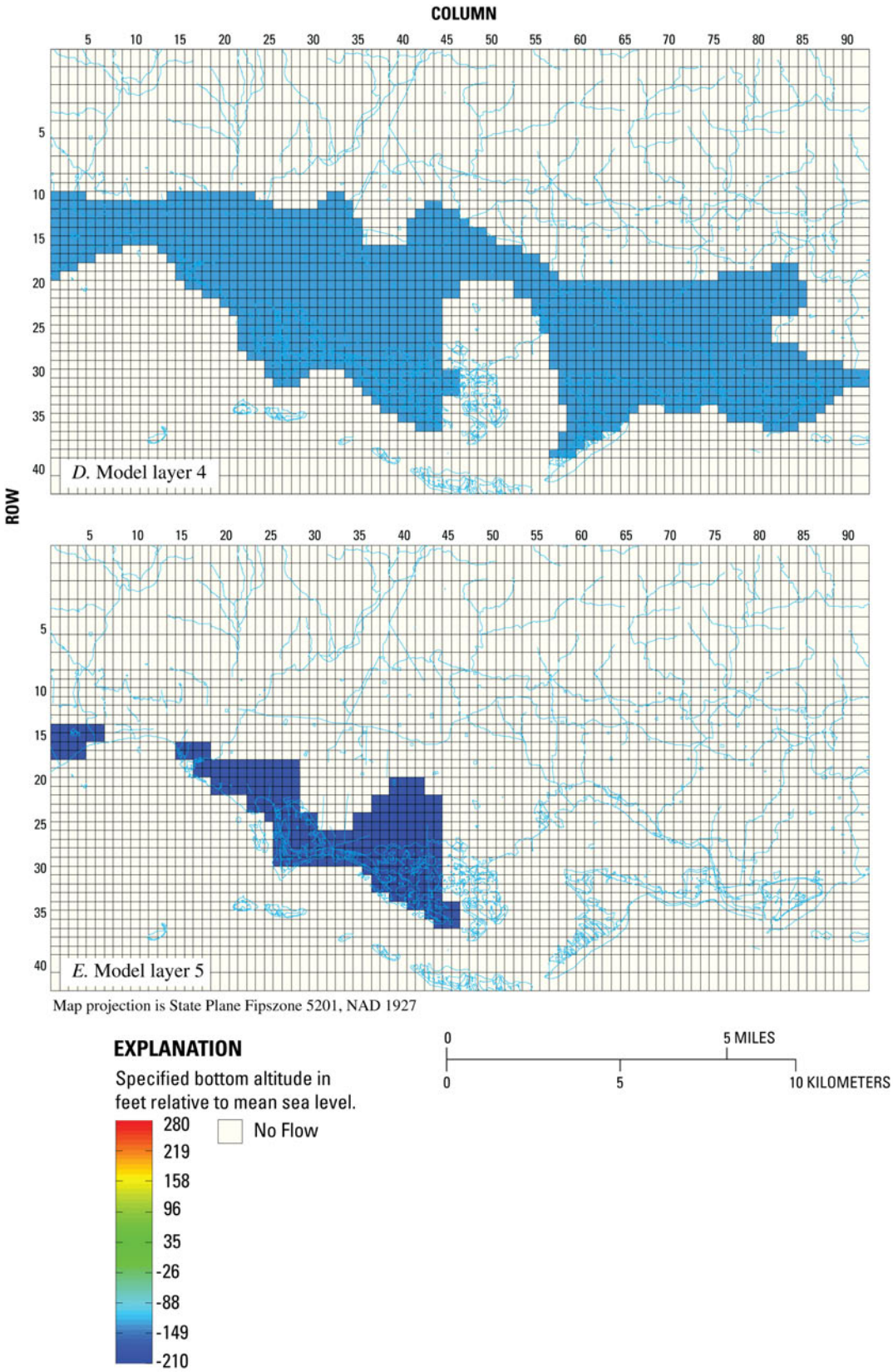

Figure 12. Specified altitudes for bottom of model layers 1 through 5.

±2 ft and 18 measurements have an accuracy of ±15 ft. The observed water-level data ranged from -18 below to 88 ft above mean sea level. Thus, the mean accuracy of the water-level observations is 5.5 ft and the standard deviation of the accuracy is 5.8 ft. There is also some error in the location of the water levels for 1986, as these were located without the benefit of modern global positioning systems (GPS). Thus, the initial condition steady-state calibration would be over fitted to the water-level data if the standard deviation of observed minus simulated water level is 6 ft or less. Because of the additional potential errors in well location for the 1986 data and the fact that the observed water levels were collected in March and the simulated water levels represent average annual conditions, it was concluded that a good fit to the observed water-level data could have a standard deviation of approximately 12 ft; this is twice the accuracy standard deviation, which would indicate that approximately two thirds of the residual errors are less than 12 ft.

Another useful statistic, which is dimensionless, is the standard deviation of residuals divided by the range in the data. This statistic is useful because the range of the observed water-level data used for calibration is accounted for. Generally, if the range of water-level data is large, there is usually a larger standard deviation in residual error. Thus, a good fit to the data would be reflected in a ratio of approximately 1/10 or less.

There is uncertainty in the estimates of spatially distributed recharge, irrigation return flow, and groundwater withdrawals for both irrigation, and public supply, which has no requirement for accurate metering. For this model, the initial estimates of net aquifer recharge were based on the previous model study and calibration of the adjacent area (Kuniansky and others, 2004). Irrigation return flow of as much as 30 percent was also applied to areas formerly in sugarcane crops as estimated by Kuniansky and others (2004). Irrigation withdrawals were considered to be less accurate than public and industrial withdrawals; because irrigation withdrawals are estimated from crop water requirements minus precipitation and surface-water application, whereas public and industrial withdrawals are generally metered. The estimates of streamflow infiltration for this model are considered reasonable, but conservative, as they are based on estimates of daily base flow and precipitation data (table 3).

The range in horizontal hydraulic conductivity of the sediments is probably the best understood property for the upper 200 ft of the aquifer, and areally ranges from 2 to 500 ft/d. The distribution of hydraulic conductivity if sorting from low to high is as follows; 10 percentile of 7 ft/d, 25 percentile of 20 ft/d, 50 percentile of 50 ft/d, 75 percentile of 90 ft/d, and 90 percentile of 200 ft/d (table 5). The spatial distribution of hydraulic conductivity values for the model should reflect the mapped hydraulic conductivity shown in figure 6. This map mimics the areal distribution of sand and gravel percentages in figure 5, with larger hydraulic conductivities in fan-delta deposits and areas of higher sand and gravel percentages and low conductivities in the inter-fluvial areas between the fan-delta lobes (Renken and others, 2002).

For the steady-state initial calibration condition, the initial hydraulic conductivity was set to the mid-range value for zones of hydraulic conductivity (fig. 6). Additionally, the ranges in recharge were tested and some of the initial pumping estimates (as reported for conditions during March 1986) were also reviewed and modified as necessary.

Sensitivity analysis was performed to gain some insight into which parameters and stresses could be evaluated with parameter estimation. Only parameters for which the observed data set is sensitive can be estimated with parameter estimation. MODFLOW-2000 with parameter estimation was used to test different zoning schemes of hydraulic conductivity or net aquifer recharge.

Because the groundwater flow equation is based on Darcy's law, recharge (flux) and hydraulic conductivity are usually correlated in the parameter estimation process and cannot be estimated simultaneously without better prior information (tighter bounds on the estimated parameters or stresses) about recharge and irrigation return flow than previously mentioned. The prior information functions for hydraulic conductivity adequately constrained these parameter estimates. As a result of parameter correlation and poor prior information for net aquifer recharge and groundwater withdrawals, attempts to estimate hydraulic conductivity and recharge parameters simultaneously with MODFLOW-2000 resulted in what appear to be unreasonable recharge rates for the steady-state initial condition. Thus, a combination of trial and error and parameter estimation was utilized in model calibration for steady-state conditions.

Once the steady-state simulation was calibrated, with a good fit achieved between observed and simulated water levels, the simulated water levels were used as the initial condition for the transient simulation (1986-2004). Some modifications to the hydraulic conductivity and storage coefficients were made to improve the transient model match to data from seven observation wells. If hydraulic conductivity was modified, then the initial steady-state model was run with the new hydraulic conductivity value, the residuals for the steady-state simulation were examined, and a new initial condition was generated.

During the calibration process, the initial estimate of irrigation withdrawals from 1986 to 1993 was reduced by 20 percent to obtain a better fit for the simulated

water-level hydrographs. The original estimate for all other groundwater withdrawals was not modified.

Water-level observations and the simulated residual errors for the March 1986, July 2002, and May 2004 potentiometric maps are provided in appendix 6. The final calibrated initial condition for the 1986 data had a mean residual error of -0.75 ft, a residual standard deviation of 9.52 ft, and the standard deviation divided by the range in observed data of 0.09, which was considered satisfactory. The simulated 1986 potentiometric surface with posted residuals are shown in figure 13. A positive error means that the simulated water level is too low and a negative error means that the simulated water level is too high.

For the transient simulation, seven observation well hydrographs with a daily water level were available to fit simulated water levels. The hydrographs for observed and simulated water levels are shown in figure 14; the simulation had annual stress periods with multiple time steps. The residual error is interpolated in time for the simulated value to be compared to the observed daily value. The mean residual error for all of the hydrographs observations in figure 14 is 6.01 ft. The residual standard deviation is 7.36 ft and the standard deviation divided by the range of the data is 0.076. The calibration statistics are similar to the calibration statistics for 1986 potentiometric map data, and the results were within the calibration criteria considered acceptable. In general, the simulated water levels are lower than the observed water levels in the hydrographs, resulting in the positive mean residual error. Only four of the hydrographs (fig. 14*A-D*) have water-level data through the 2003 storm event. Although the simulated water levels are generally lower than the observed water levels, the increases in simulated and observed water levels following the November 2003 storm event are similar.

The simulated water-level map for 2002 and posted residuals (fig. 15) indicate a worse fit than the fit to the 1986 data, but one that is within the established calibration criteria. As with the 1986 steady-state simulation, the 2002 simulated values are again lower than the observed values. The observed water levels for 2002 represent conditions during July, whereas the simulated water levels represent average conditions for 2002. The mean residual error was 12.76 ft, the residual standard deviation was 16.53 ft, and the standard deviation divided by the range in observed data was 0.13.

The simulated water-level map for 2004 and posted residuals (fig. 16) indicate a fit that is within the calibration criteria, and closer in magnitude to the fit obtained for the 1986 data than for the 2002 data. The observed water levels represent data collected during May, whereas the simulated water levels represent average conditions for 2004. The mean residual error was 3.07 ft, the residual standard deviation was 9.49 ft, and the standard deviation divided by the range in observed data was 0.11.

The final horizontal hydraulic conductivity, K_h, assigned to each layer are shown in figure 17. Over the coastal plain, the range in K_h is 1 to 200 ft/d. In the upper reaches of the Río Nigua and its tributaries, the Río Lapa and Río Majada, high K_h values of 200 and 400 ft/d are assigned to layers 1 and 2. The vertical hydraulic conductivity (K_v) was set equal to one tenth of K_h value except in areas beneath the two high K_h zones along the upper reaches of the Río Nigua and its tributaries (Río Lapa and Río Majada) where coarse-grained deposits of sand, gravel, and cobbles constitute the permeable aquifer unit. For these two high K_h zones, K_v is set equal to half of K_h. The spatial distribution of K_h zones assigned to each layer reflects the information in the borehole lithologic descriptions and the depositional framework of higher K_h zones along the major streams, which create the fan-delta deposits within the South Coast aquifer, and lower K_h zones in the inter-fluvial areas.

It was necessary to include aquifer storage properties in the transient simulation only, and these properties mainly affect the amplitude of the hydrographs shown on figure 14. In MODFLOW-2000, a constant specific storage value, rather than multiple storage coefficients, was assigned to the model layers. The storage coefficient (S) can be defined as the volume of water that an aquifer releases or uptakes per unit surface area of aquifer per unit change of head. The storage coefficient of an unconfined aquifer is approximately equal to the specific yield (S_Y), which is generally related to the amount of water that can be released by gravity drainage. S_y is usually less than the porosity, as a result of some water adhering to the sediment grains, but can approach the porosity of coarse-grained material. S_y can range from 0.07 for sandy clay to 0.35 for gravelly sand (Johnson, 1967). In confined aquifers, the storage coefficient is related to the compressibility of the aquifer and fluid and the thickness of the aquifer. Storage coefficients for confined aquifers generally range from 0.00001 to 0.001 (Bouwer, 1978; Fetter, 1994). Specific storage (S_S) is related to the storage coefficient by $S = S_S b$, where S_S is the volume of water an aquifer releases or uptakes per unit volume of an aquifer per unit change of head and b is the thickness of the aquifer. Specific storage is also known as the elastic storage coefficient and is a function of the density of water, the constant for the acceleration of gravity, the compressibility of the aquifer skeleton, porosity, and the compressibility of water. Specific storage has a dimension of inverse length (L^{-1}) and is generally greater than 10^{-6} ft^{-1} and less than 10^{-4} ft^{-1}.

Because all model layers were simulated as confined, the specific storage for layer 1 was set to 0.0025, such that this would result in a storage

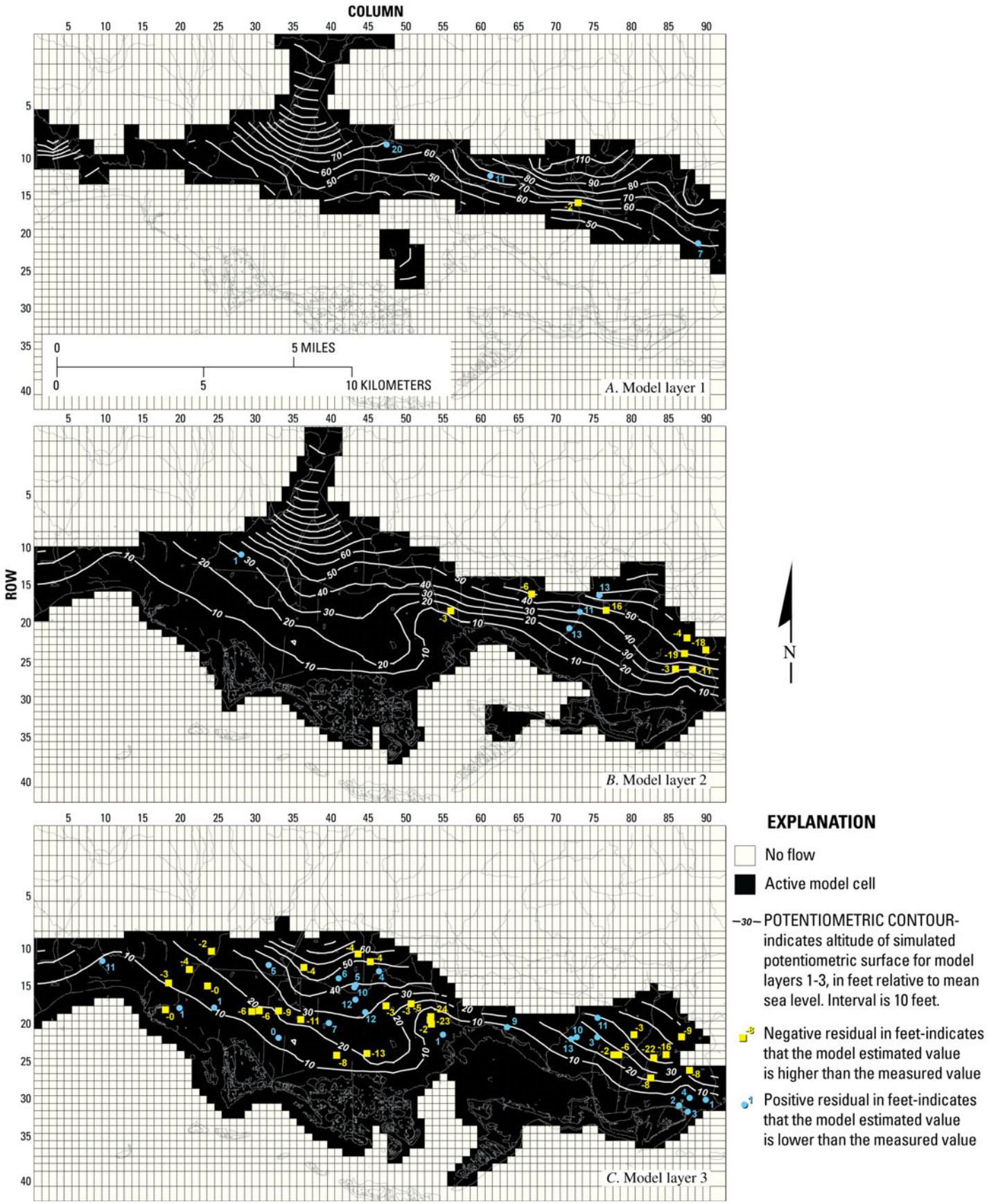

Figure 13. Simulated potentiometric surface for model-calibrated conditions during March 1986.

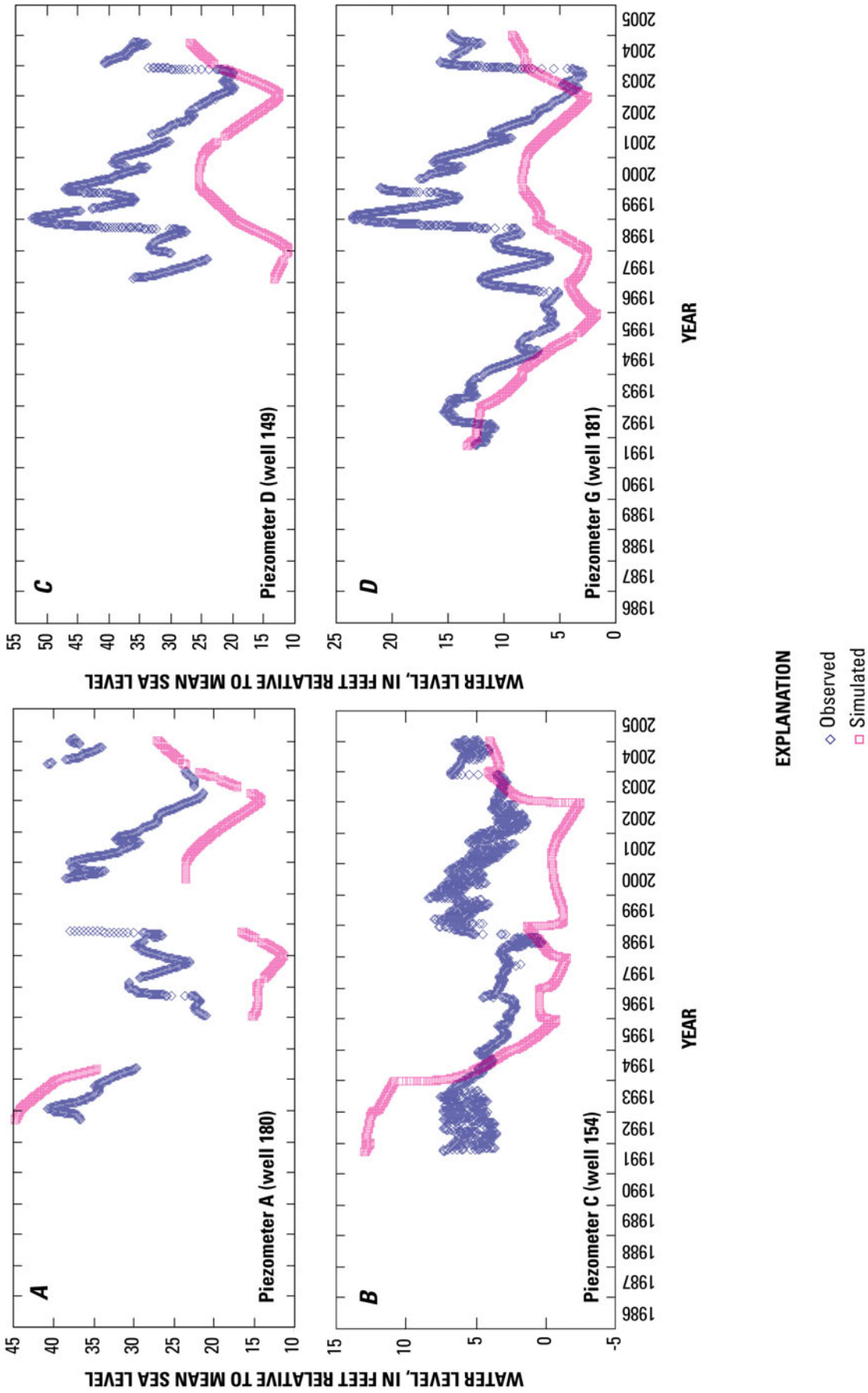

Figure 14. Observed and simulated water levels between 1986 and 2004 at selected wells within the study area.

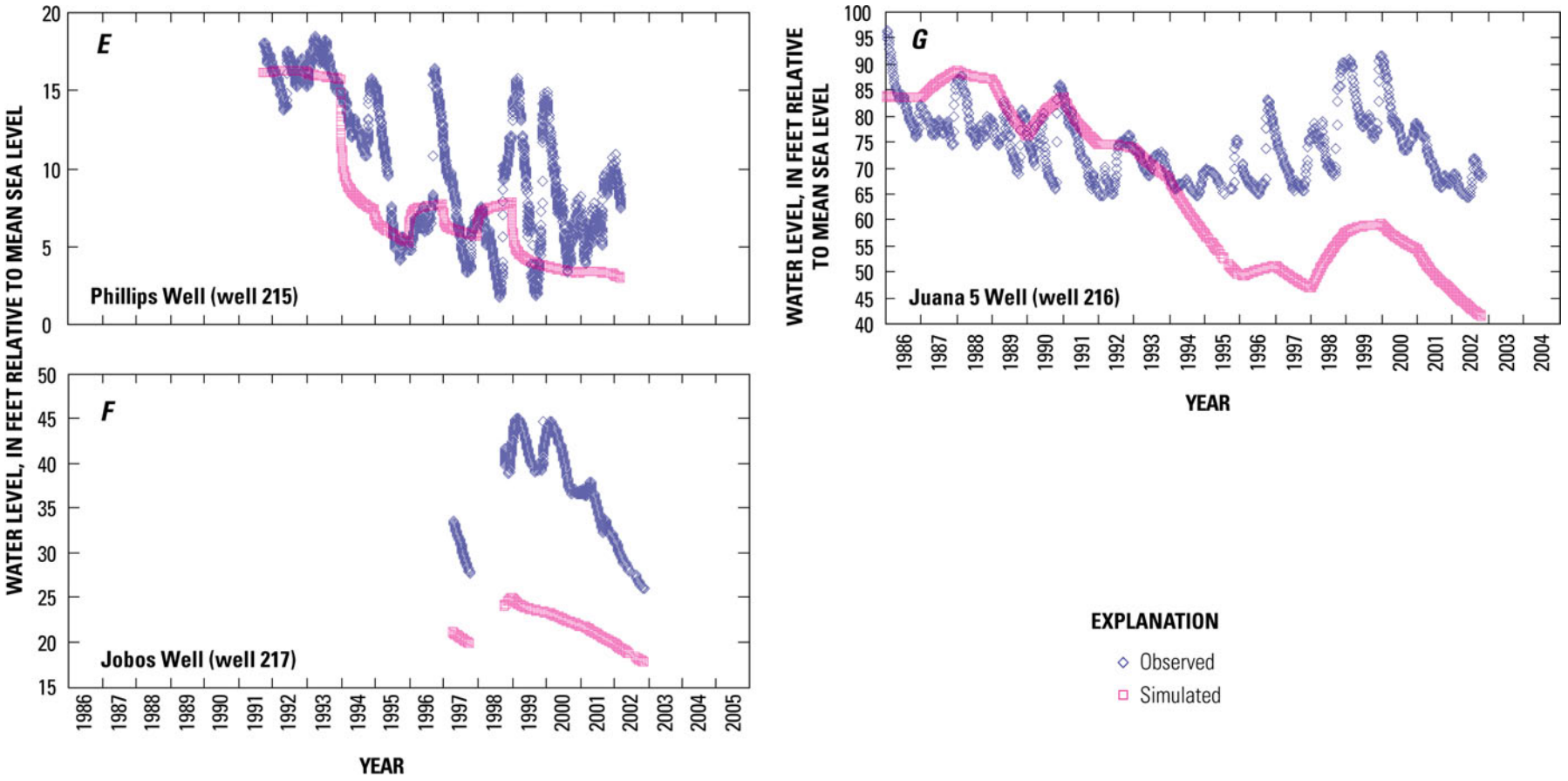

Figure 14. Observed and simulated water levels between 1986 and 2004 at selected wells within the study area—Continued.

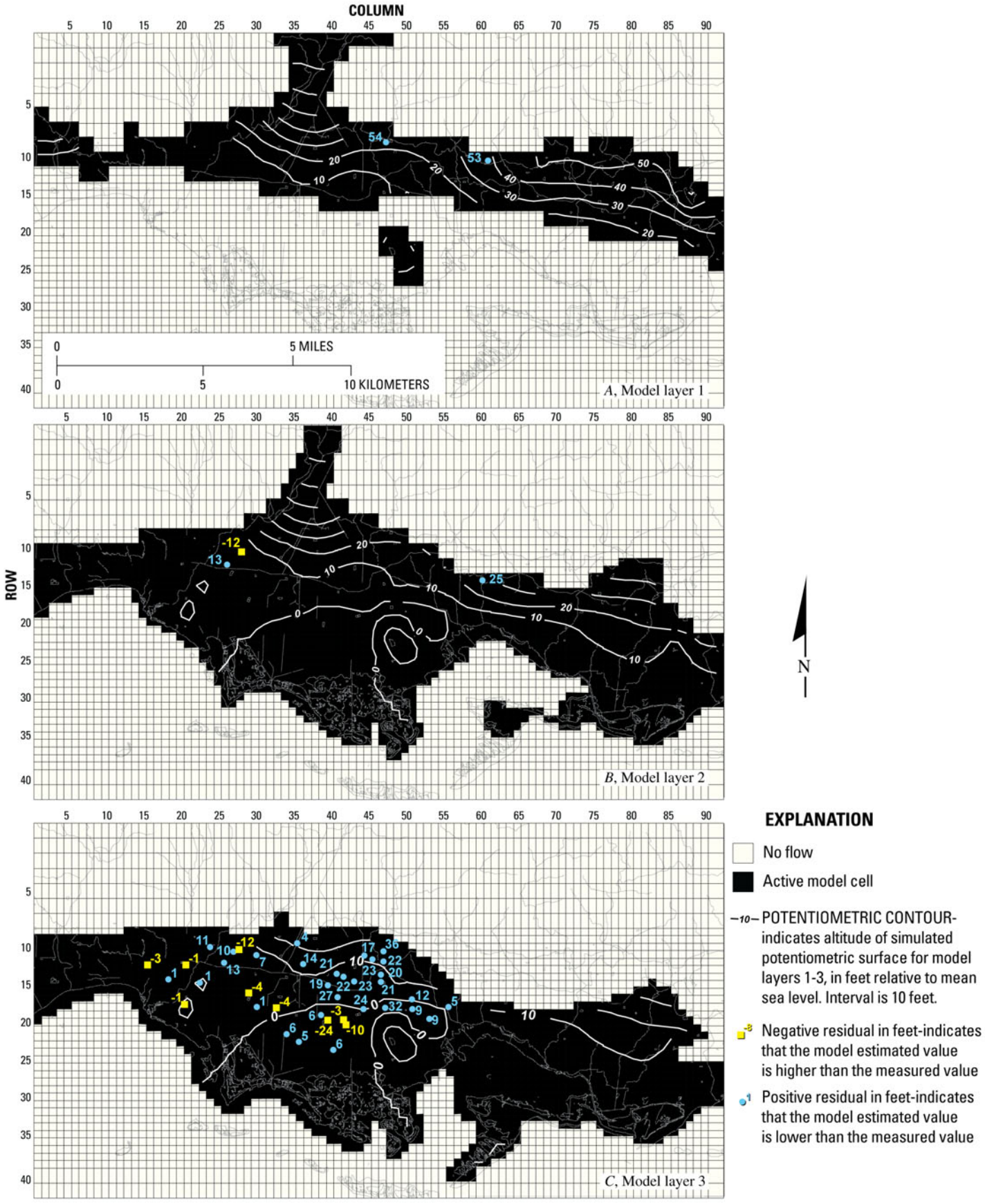

Figure 15. Map showing simulated potentiometric surface for model-calibrated conditions during 2002.

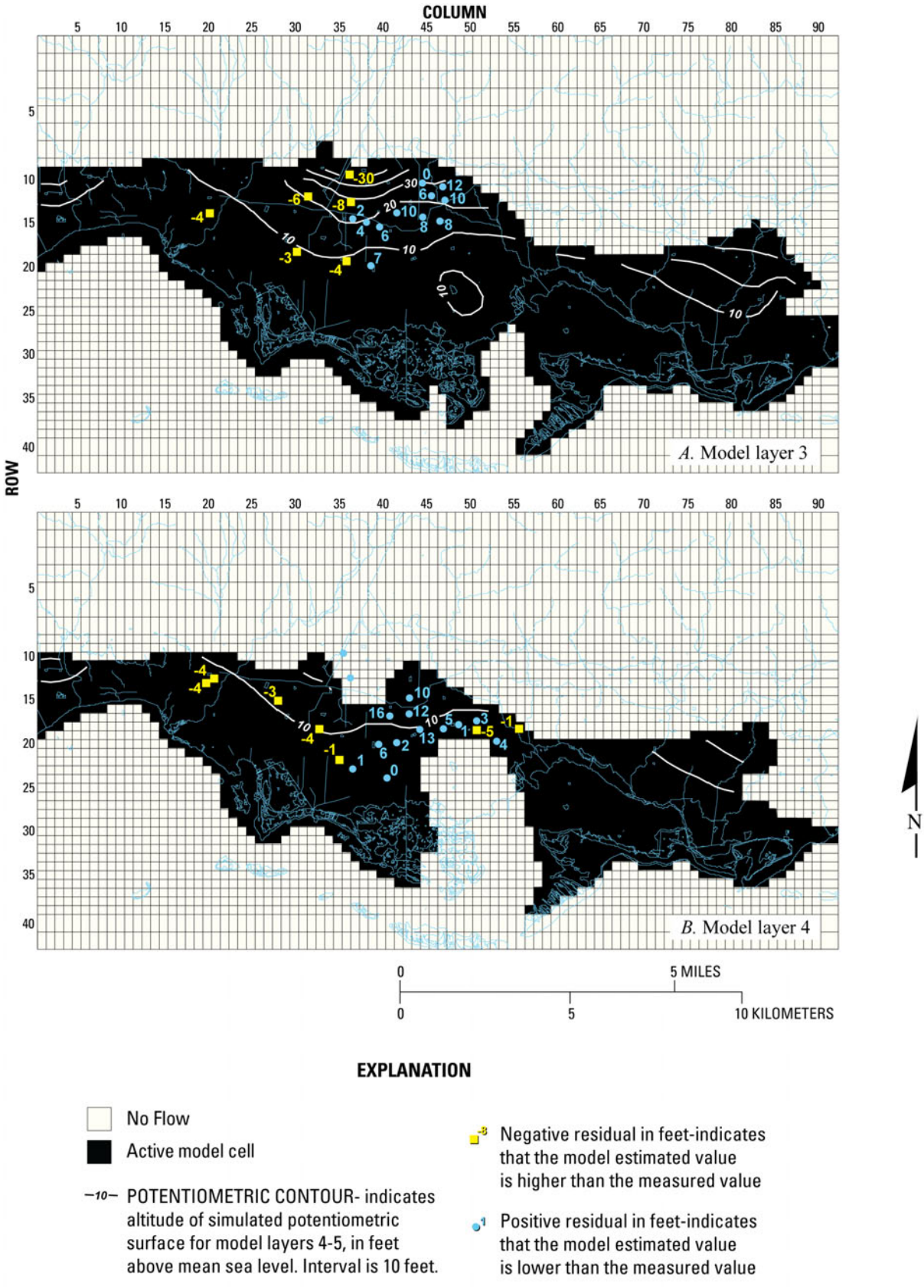

Figure 16. Simulated potentiometric surface for model-calibrated conditions during 2004 and posted residuals.

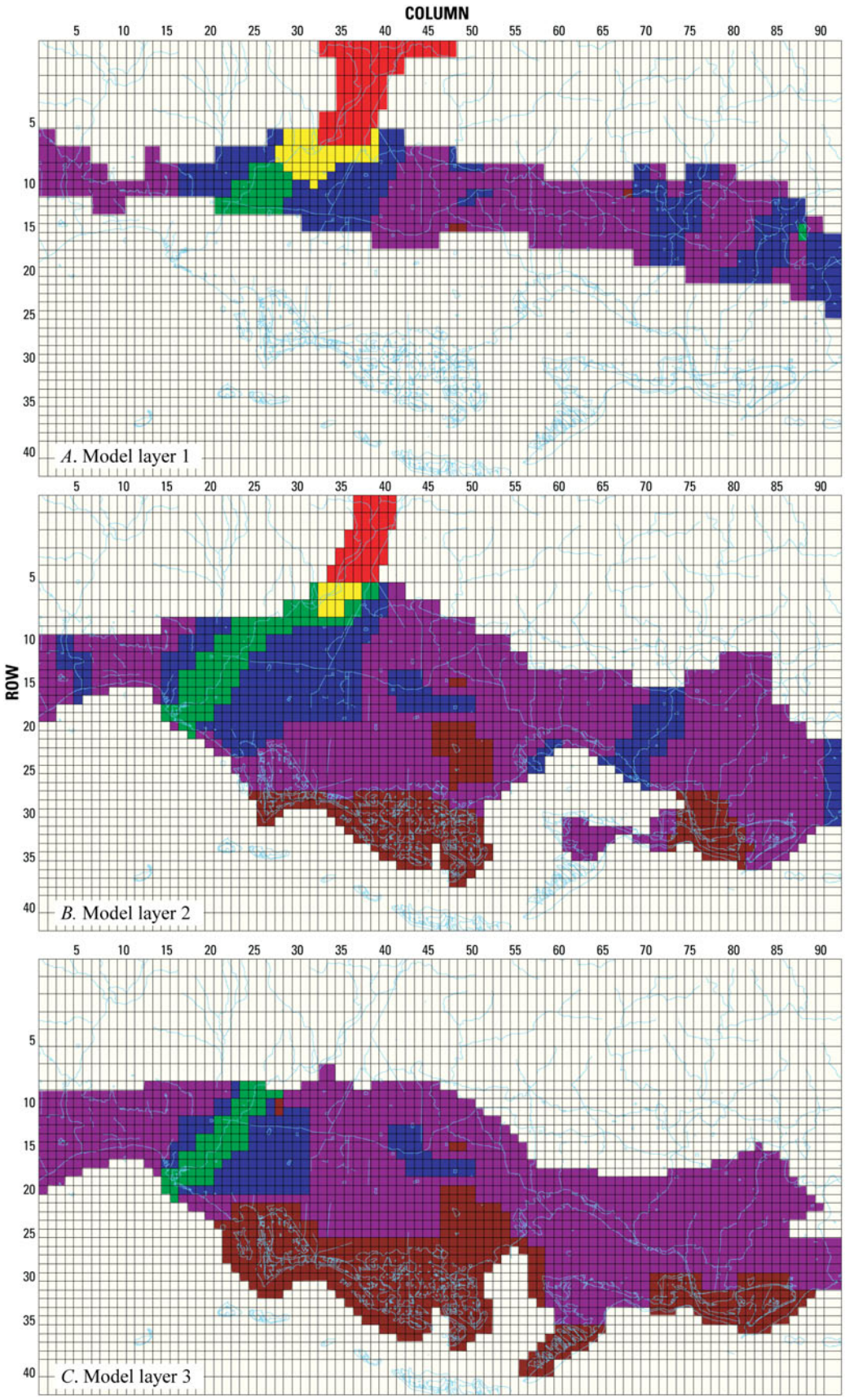
COLUMN
ROW
A. Model layer 1
B. Model layer 2
C. Model layer 3

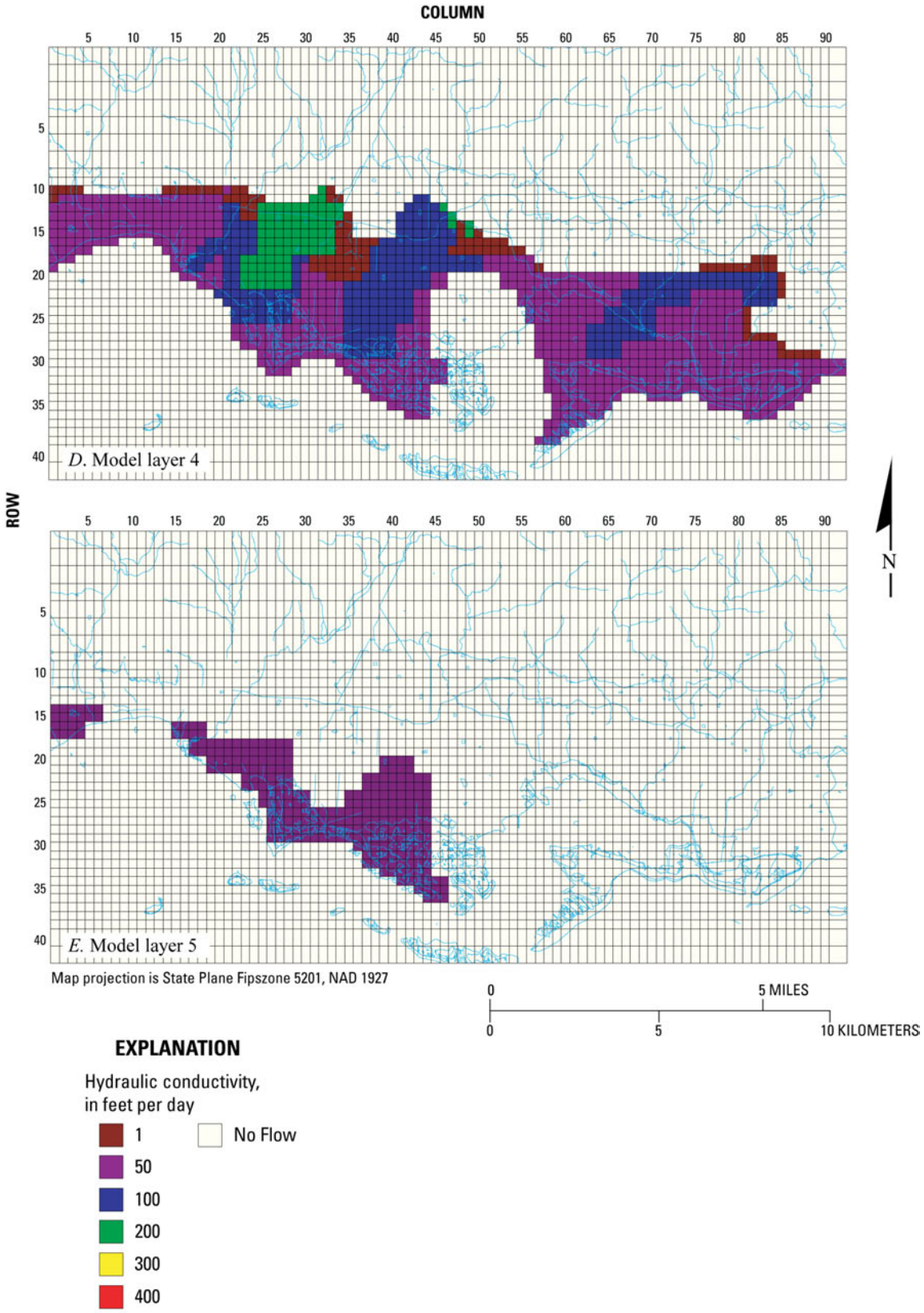

Figure 17. Final calibrated horizontal hydraulic conductivity values assigned to each of the five model layers for the South Coast aquifer between the Río Jueyes and Río Guamaní, southern Puerto Rico.

coefficient value closer to a specific yield of 0.05 over most of the layer (the specific storage times a thickness of 20 ft). Figure 18*A*, shows the range of storage coefficients assigned to each cell in model layer one, which range from 0.05 to 0.325. As mentioned earlier, the altitude of the top of layer 1 was set to a value below land surface altitude in hilly areas to constrain the storage property to 0.325 or less, which is the upper reasonable limit for specific yield in an unconfined system (Johnson, 1967; Bouwer, 1978). Specific storage was set to 0.0005 for layer 2, and 0.00001 for layers 3 through 5. Specific storage values were set at the upper range of specific storage in confined aquifers for layer 2 because these are fairly recent alluvial sedimentary deposits, which are more elastic than indurated sedimentary rock. Additionally, the thin clay and silt lenses within these deposits increase the elastic storage within this layer. The deeper sediments (represented by layers 3 through 5) were assigned specific storage values that are more typical of confined aquifers. Because the storage coefficient for each model cell is calculated by multiplying specific storage by layer thickness, the value of the storage coefficient varies as the thicknesses of the layers are not constant. The range, however, is not wide because most of the layers have almost constant thickness. Layers 1 and 2 have the widest range in thickness as the top and bottom of these layers are based on land surface altitude and the estimated altitude of the base of the unconsolidated clay/silt zone overlying the bedrock unit. Additionally, layer 2 was set to be only 5 ft thick beneath the mangroves along the coast.

Sensitivity Testing and Analysis

Groundwater modeling results are affected by various modeling parameters, stresses, and assumptions, including the (1) geometry of the hydrogeologic units, (2) vertical and horizontal spacing of the model grid, (3) types and locations of model boundaries, (4) magnitudes and areal distributions of stresses such as groundwater recharge and withdrawals, (5) conductance of river and general head boundary cells, and (6) horizontal and vertical hydraulic conductivities of aquifers and confining units. Transient simulation results are affected by the time-step size, number of stress periods, or the storativity of the aquifers and confining units. Ideally, a complete sensitivity analysis would determine model sensitivity to all of these parameters and assumptions, but only model sensitivity to the parameters and stresses were determined for this model. For this study, the model response tested for goodness of fit is the simulated water level, because most fluxes to or from the system are calculated or reported values. This model is considered sensitive to a parameter or stress when a small change (perturbation) of the model-assigned parameter or stress causes a large change in the simulated water level. Sensitivity analysis is useful for indicating where errors in the calibrated set of parameters and stresses are most likely, or the simulated groundwater head is sensitive to the parameter or stress. If the model is sensitive to changes in the parameter or stress, the calibrated value is more likely to be accurately estimated through simulation. If the model is insensitive to changes in a parameter or stress, then it is not known if the calibrated value is close to the actual value, and that parameter or stress cannot be estimated through simulation or automated parameter estimation.

This model was calibrated using a combination of parameter estimation and trial-and-error analysis. Automated parameter estimation was used with the steady-state model. Composite-scaled sensitivity analysis was performed for some of the parameters for the steady-state data (table 6). The composite-scaled sensitivity is a dimensionless measure of the change in calculated head with respect to the value of a parameter, and is independent of the actual values of the observations (Hill, 1998). Composite-scaled sensitivities are calculated for each parameter using the scaled sensitivities for all observations, and indicate the total amount of information provided by the observations and the parameter. When the sensitivity process is used with the final set of parameters incorporated in the calibrated model, the sensitivities indicate which parameters will result in the greatest change in observation types. For the steady-state model, only 66 water-level observations were available. Thus, the sensitivity testing provides information on how the parameters and stresses affect water levels. Although 18 of the measurements were ±15 ft and 48 were ±2 ft, weighting was not used in the sensitivity analysis. Weighting is critical for calibration and sensitivity analysis if there are different observation types, such as flux observations, water levels, or water-level differences (Hill, 1998). For this model, all of the observations available were water levels because the fluxes are all calculated or reported. Therefore, weighting the observations does not provide more information about sensitivity, although weighting would have given the appearance of better calibration statistics because the worst residual errors were at wells with the lowest associated accuracy. The larger the composite scaled sensitivity number, the greater the model sensitivity to that parameter. The parameters in table 6 are sorted from largest to smallest composite-scaled sensitivity.

For the steady state simulation, recharge was applied to the highest active area in three zones—1 (furrow irrigation area in green - zone 2), 2 (net

Table 6. Composite scaled sensitivity for selected parameters, steady-state simulation for existing conditions in 1986.

Parameter name	Description	Composite scaled sensitivity
rch2	Net recharge zone 2 (furrow irrigation area)	23.60
kx2	Horizontal hydraulic conductivity zone 2	16.84
kx3	Horizontal hydraulic conductivity zone 3	9.69
rch1	Net recharge zone 1	7.35
kx4	Horizontal hydraulic conductivity zone 4	4.57
kx5	Horizontal hydraulic conductivity zone 5	1.31
kz1	Vertical hydraulic conductivity zone 1	0.92
kz2	Vertical hydraulic conductivity zone 2	0.37
kx6	Horizontal hydraulic conductivity zone 6	0.30
kx1	Horizontal hydraulic conductivity zone 1	0.26
rch4	Net recharge zone 4 (hill in coastal plain)	0.22
kz3	Vertical hydraulic conductivity zone 3	0.08
kz4	Vertical hydraulic conductivity zone 4	0.07
kz5	Vertical hydraulic conductivity zone 5	0.00
kz6	Vertical hydraulic conductivity zone 6	0.00

recharge from rainfall area in yellow - zone 1) and 3 (net recharge at Cerro Aguirre area in blue – zone 4) (fig. 19). Two recharge areas are most important—areas of net recharge with no irrigation (zone 1 in yellow) and the areas with furrow irrigation (zone 2 in green) (fig. 19). Of lesser importance is recharge to (zone 4) Cerro Aguirre, where the bedrock projects above the alluvial plain. The bedrock unit in this area has a lower permeability that that of surrounding areas and it was assigned a net recharge equal to half the net recharge for the non-irrigated area.

The parameters with the greatest composite-scaled sensitivity, in order of decreasing sensitivity, are net recharge to zone 2 (furrow irrigation area), K_x for zone 2, K_x for zone 3, net recharge to zone 1 (net recharge from precipitation over most of the area), K_x for zone 4, and K_x for zone 5 (table 6). The steady-state simulation is fairly insensitive to K_z in general, K_x for zones 1 and 6, and net recharge in zone 4.

Sensitivity analysis was performed by perturbing zoned parameters and stresses for the transient simulation. Results of the analysis show the residual standard deviation between observed and simulated water-levels as a function of multipliers applied to the calibrated value (fig. 20). The model was most sensitive to the reduction of horizontal hydraulic conductivity of zone 2 (fig. 20*A*), which represents the lower permeability sediments between the higher permeability fan-delta deposits. A K_x of 50 ft/d was assigned to zone 2, because increases beyond this value did not affect simulated heads. The model was fairly insensitive to most other hydraulic conductivity parameters, and was least sensitive to the assigned vertical hydraulic conductivity (K_z).

For the transient simulation, recharge decreased beginning in 1986 as the furrow irrigation return flows diminished and then ceased after 1993 (app. 5). From 1993 to 2004, net recharge was limited to rainfall; infiltration from streams and canals were considered separately in the sensitivity analysis. The transient simulation is mostly sensitive to recharge in zone 1 (fig. 20*B*), which represents recharge from rainfall in the area without furrow irrigation in the upper part of the coastal plain. The transient simulation was somewhat sensitive to reductions in the storage of layer 2, as this layer is composed of poorly compacted and coarser sediments, and it is reasonable to assume that its storage value is in the upper range.

The transient simulation was highly sensitive to reductions below 1.0 and increases above 1.4 times the calibration value of infiltration from the Río Nigua (fig. 20*C*). In general, the transient simulation was not significantly sensitive to infiltration from other streams (simulated as injection wells) and conductance of canals and general head boundaries.

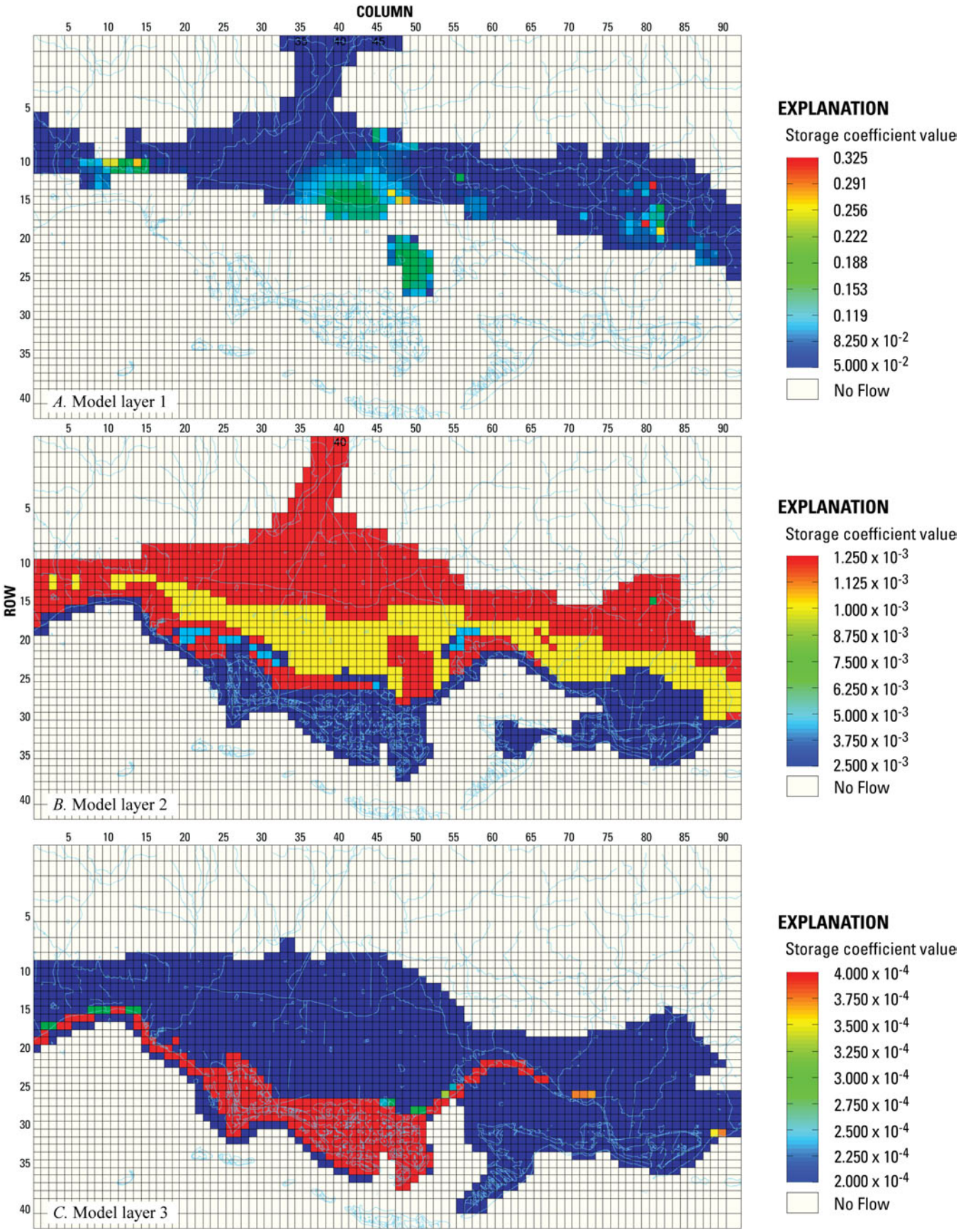
COLUMN
ROW
A. Model layer 1
B. Model layer 2
C. Model layer 3
EXPLANATION
Storage coefficient value
0.325
0.291
0.256
0.222
0.188
0.153
0.119
8.250 x 10-2
5.000 x 10-2
No Flow
EXPLANATION
Storage coefficient value
1.250 x 10-3
1.125 x 10-3
1.000 x 10-3
8.750 x 10-3
7.500 x 10-3
6.250 x 10-3
5.000 x 10-3
3.750 x 10-3
2.500 x 10-3
No Flow
EXPLANATION
Storage coefficient value
4.000 x 10-4
3.750 x 10-4
3.500 x 10-4
3.250 x 10-4
3.000 x 10-4
2.750 x 10-4
2.500 x 10-4
2.250 x 10-4
2.000 x 10-4
No Flow

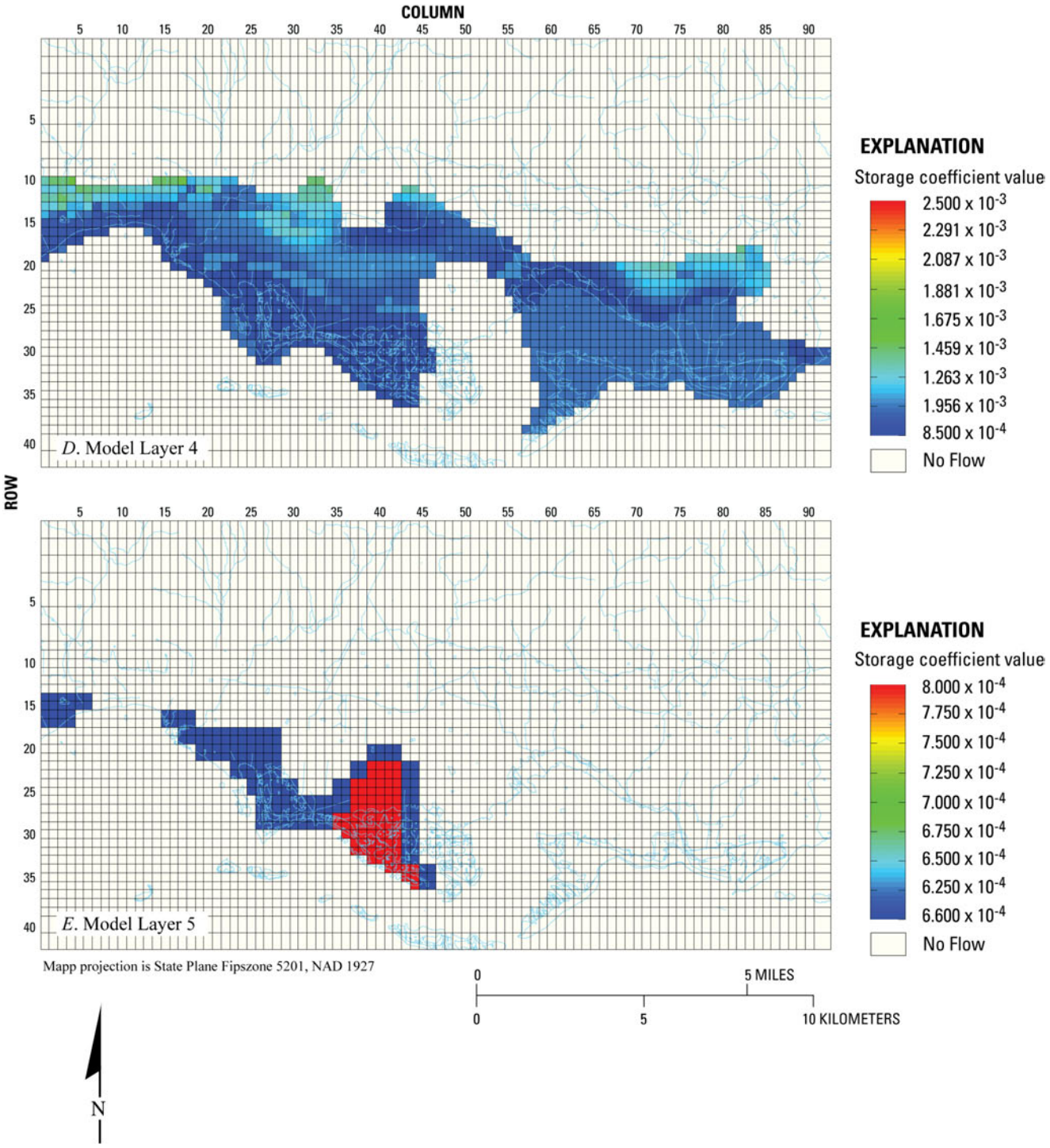

Figure 18. Final storage values assigned to each of the five model layers for the South Coast aquifer between the Río Jueyes and the Río Guamaní, southern Puerto Rico.

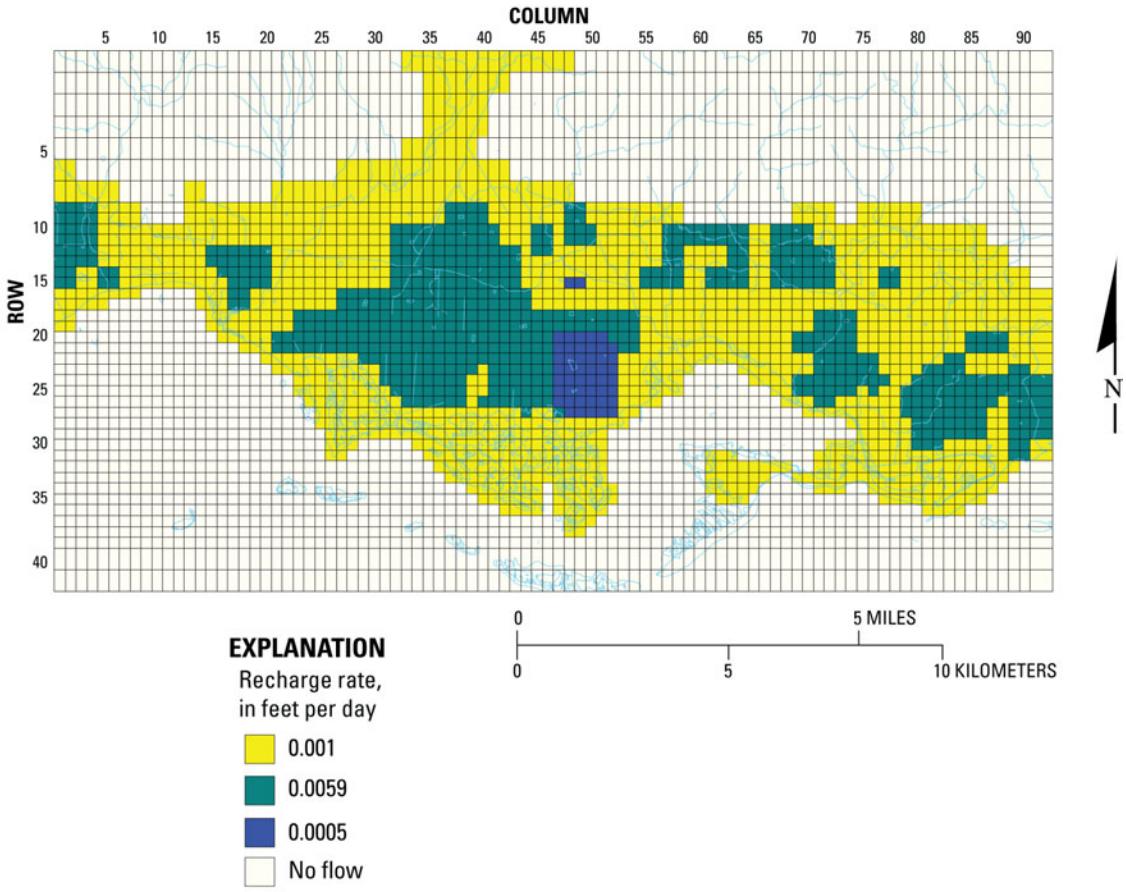

Figure 19. Recharge rates assigned to uppermost active layer (layer 1 or 2) for the 1986 steady state simulation.

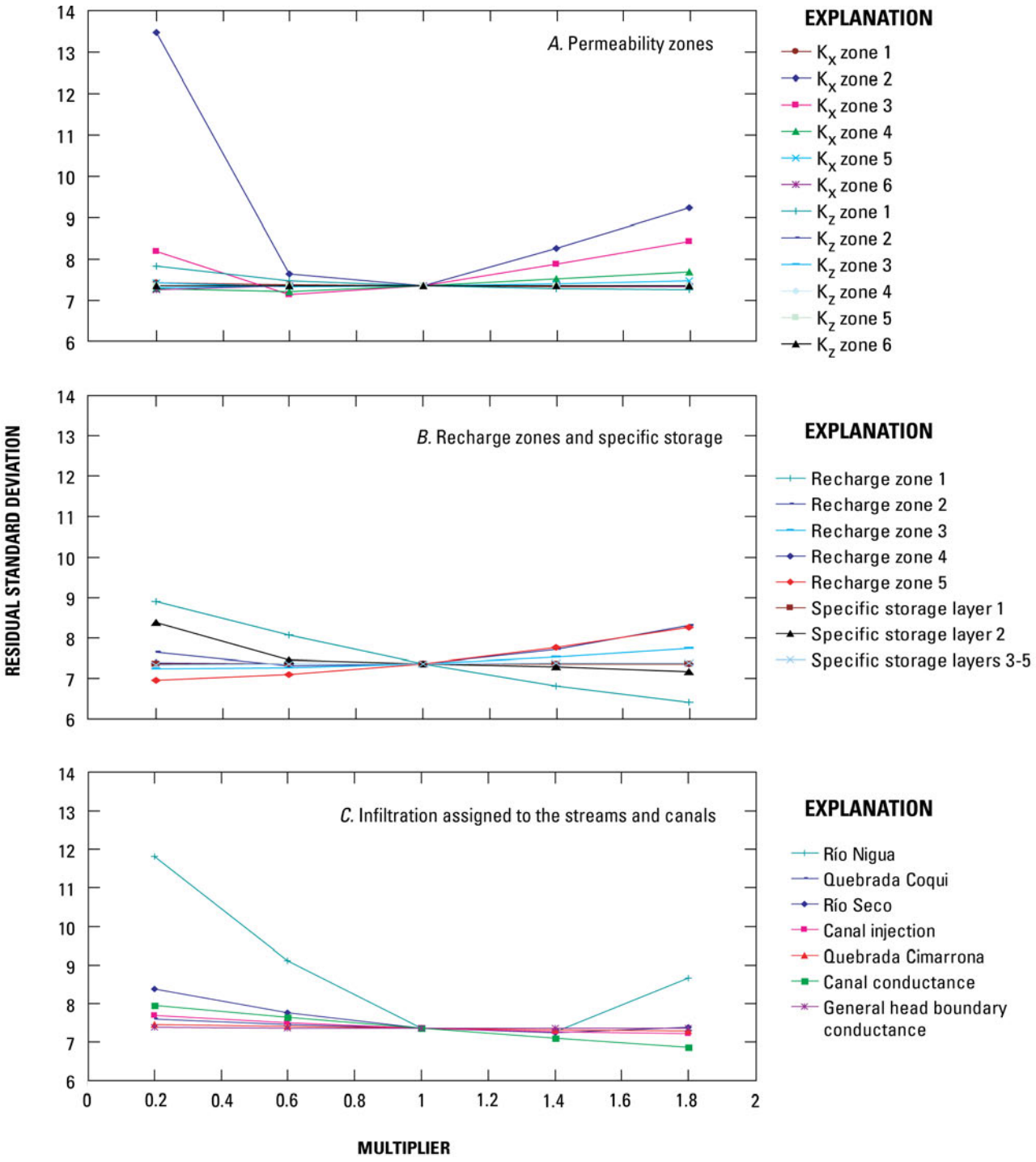

Figure 20. Sensitivity analysis based on transient simulation using the residual standard deviation from water-level hydrographs.

Effects of Water-Resources Development

The effect that changes in water-resources development have on the groundwater flow system in the study area is best described by examining changes in water budgets derived from the groundwater flow model. The model-derived water budget for the steady-state simulation is shown in table 7 and the water budget for the calibrated transient (1986-2004) simulation is shown in figure 21.

The initial steady-state simulation of 1986 represents a wetter than average year in which streamflow infiltration was higher than average (16.78 ft^3/d, table 3). Annual rainfall at the Jájome Alto rainfall station was 83 in., which is greater than the average annual rainfall of 77 in. at this station. Unfortunately, there were too many days of missing record at the Aguirre Central rain gage in 1986 to obtain the measured annual total. However, based on data from other rainfall stations in the area, the estimated annual rainfall for 1986 at the Aguirre Central rain gage was 41 in., which is comparable to the average annual rainfall of 40 in. Additionally, 1985 was a relatively wet year in which 57 in. of rainfall was measured at the Aguirre Central rain gage. As a result, the water level in the aquifer was fairly high in 1986 for the initial condition, and as simulated by the model, there was upward flow from the aquifer to the coastal swamps and the Jobos Bay, representing as much as 63 percent of the simulated aquifer discharge (24.61 Mgal/d) through the general head boundary cells (table 7). The remaining 37 percent of discharge from the aquifer (14.40 Mgal/d) was from groundwater withdrawals, with minor flow into some of the canals simulated with the river package (0.23 Mgal/d). Net areal recharge represented 67 percent of inflow (26.22 Mgal/d), streamflow infiltration represented 30 percent of the inflow (11.96 Mgal/d), and the canals simulated with the river package provided 3 percent of the inflow (1.05 Mgal/d).

The transient model water budgets show the rates of flow to and from sources and sinks at the end of each annual stress period (fig. 21). In general, there is greater total flow through the system from 1986 through 1993 as a result of the irrigation return flow. The average net aquifer recharge rate applied to the model from 1986 through 1993 was 21 Mgal/d, which decreased to an average of only 6 Mgal/d from 1994 through 2004 as a result of the switch from furrow irrigation to more efficient irrigation practices discussed earlier. Although irrigation withdrawals were greatest during the period of furrow irrigation, some of the irrigation water was supplied from surface-water sources outside of the model area by way of the irrigation canals; therefore, the irrigation return flow more than offset the irrigation pumpage. The average groundwater withdrawal rate for all pumpage was estimated at 15 Mgal/d for 1986 through 1993 and 10 Mgal/d for 1994 through 2004 as a result of the decreased irrigation withdrawals. The change in irrigation practices primarily affected recharge and freshwater discharge to the coast, reducing both after 1993. The simulated average discharge to the coast was 19 Mgal/d prior to 1994 and 7 Mgal/d from 1994 through 2004, a reduction of 63 percent. The average annual rainfall at the Aguirre Central raingage was 38 in. for both 1986 through 1993 and 1994 through 2004. Therefore, the difference in the modeled water budgets for these two periods is probably related to the cessation of furrow irrigation rather than a difference in rainfall between periods.

Table 7. Model derived water budget for the steady-state simulation for 1986.

[Mgal/d, million gallons per day]

Description	Inflow (Mgal/d)	Outflow (Mgal/d)
Recharge	26.22	0.00
River Cells assigned to the irrigation canals	1.05	0.23
General Head Boundary Cells	0.00	24.61
Wells (Streamflow Infiltration)	11.96	0.00
Wells (Withdrawal)	0.00	14.40
Total	39.23	39.23

Although the water budget for the entire model volume is revealing, it does not provide information specific to the changes in groundwater leakage for the mangrove swamp in the JBNERR area. Figure 22*A* shows the rates of flow between model layer 2 and the general head boundary cells at the end of each stress period for the JBNERR at Mar Negro. Groundwater discharge is generally small (less than 1.2 Mgal/d) because most of the pumping wells are near the center of the Salinas fan delta, which is near the JBNERR, and because water from the estuary may infiltrate the aquifer during some years, as indicated by the model (fig. 22*A*). Flow from the estuary to the aquifer only occurs after furrow irrigation ceases and both annual rainfall and streamflow infiltration are below average (table 8).

An additional transient model run was made with the pumpage set to zero. Figure 22*B* shows the flux to the mangroves (out of the aquifer) in light blue (fig. 22*B*) superimposed with the flux in and out of the aquifer from the calibrated transient simulation shown fig. 22*A*. The period of furrow irrigation (1986-1993) still has the increased recharge from irrigation return flow included (fig. 22*B*). The hypothetical simulation shows a large

increase in outward flow from the aquifer to the estuary, and there is never any simulated flow of water from the estuary to the aquifer. The average flow from the aquifer to the estuary is 2.5 Mgal/d if all pumping is removed for 1994 to 2004. With pumping for this same period, the flow into the aquifer from the estuary averages 0.1 Mgal/d and the average flow from the aquifer to the estuary is 0.2 Mgal/d. These water budgets indicate that pumping at the Salinas fan is capturing groundwater flow that would otherwise discharge through the mangroves. As noted earlier, the irrigation return flow more than offsets the groundwater withdrawals from 1986 through 1993.

Two additional hypothetical simulations were extended to year 2014 by adding a 10-year stress period to the end of the 1986-2004 simulation using 2004 pumping rates. The first simulation assumed average (1986-2004) precipitation with average net recharge and no irrigation return flow, and average surface-water infiltration from streams; the second simulation assumed a 25 reduction in precipitation. The flux to the mangrove swamp in the additional 10-year stress period is also shown on figure 22*B*. The hypothetical simulations indicate that without a reduction in pumping rates, slightly dryer than average period would result in almost no freshwater discharge to the mangroves at the JBNERR and potential saline-water movement from the estuary into the aquifer. These two simulations were rerun assuming no pumpage (fig. 22*B*).

Alternative Strategies for Groundwater Management

Alternatives for groundwater management in the aquifer near the JBNERR include reducing groundwater withdrawals, implementing artificial recharge measures, or a combination of both. Artificial recharge is defined as any method used to increase recharge to an aquifer by introducing water that would not naturally be present (American Society of Civil Engineers, 2001). Artificial recharge can be accomplished by increasing surface-water infiltration using “in-channel” or “off-channel” means. In-channel methods can include in-stream dams and weirs or levees to impound water across the flood plain. Off-channel methods involve the development of canals or other structures that divert floodwater from streams to adjacent fields. Additionally, artificial recharge may be accomplished by using injection wells to pump freshwater or treated wastewater into the aquifer. It is not within the scope of this study to determine which alternative approach is most feasible or determine the source of freshwater or treated waste water. However, the model can be used to investigate how to increase groundwater flow (to the mangroves) up to the 2-Mgal/d rate simulated for no-pumping conditions. Because it may not be practical to achieve the simulated flux of 2 Mgal/d at the mangroves, the alternatives were tested by running the calibrated transient model with a 10-year stress period under average climate conditions with a goal of achieving 70 percent or 1.4 Mgal/d of groundwater flow toward the mangroves at the JBNERR.

Five alternatives for achieving a 1.4-Mgal/d discharge to the mangroves were evaluated: (1) artificial recharge using injection wells north of the JBNERR boundary (figs. 23 and 24), (2) artificial recharge by flooding fields in areas north of the JBNERR (figs. 23 and 25), (3) termination of groundwater withdrawals near the affected mangroves (figs. 23 and 26), (4) reduction of groundwater withdrawals by 50 percent at irrigation wells (figs. 23 and 27), and (5) a combination of alternatives 2 and 4 (figs. 23 and 28).

The objective of the first alternative was to determine the spacing and rate of injection required to obtain discharge to the mangrove area of approximately 1.4 Mgal/d. Through trial and error it was determined that eight wells injecting a total of 1,040 gal/min (gallons per minute) to layers 2 and 3 (each well operating at an injection rate of 130 gal/min) for a total of about 1.5 Mgal/d resulted in a total flux to the mangrove area of about 1.4 Mgal/d.

The second alternative was tested by flooding agricultural fields north of the JBNERR and south of Highway 3. This alternative involves determining the rate of increased recharge to agricultural fields, and possibly using water from Canal de Patillas. The number of flooded cells in agricultural fields and the increased rate of recharge required to provide a groundwater discharge to the mangrove area of about 1.4 Mgal/d was determined by trial and error. This rate can be achieved if the recharge over approximately 958 ac is increased from 0.00072 to 0.0059 ft/d—the net recharge value used for the period when sugarcane was the principal crop in the area. The net recharge applied to the 958 ac represents 1.84 Mgal/d. This alternative, however, will require additional water if the area is cultivated. The irrigation requirement for the cultivation of sugarcane is 4 ft/yr (an area of 938 ac would require 3.4 Mgal/d). Thus, if sugarcane were planted, the total water requirement would be at least 3.4 Mgal/d.

The third alternative was tested by ceasing groundwater withdrawals from all wells located in an area bounded by the Canal de Patillas, the JBNERR, Hacienda Magdalena, and Cerro Aguirre. The model simulation indicated that the aquifer flux to the mangrove area will be about 1.34 Mgal/d. This alternative may require importing at least 2.44 Mgal/d of water from other sources to compensate for the shutdown of 2 public-supply wells, 4 industrial wells, and 6 agricultural wells that withdraw about 0.56, 1.07 and 0.81 Mgal/d, respectively.

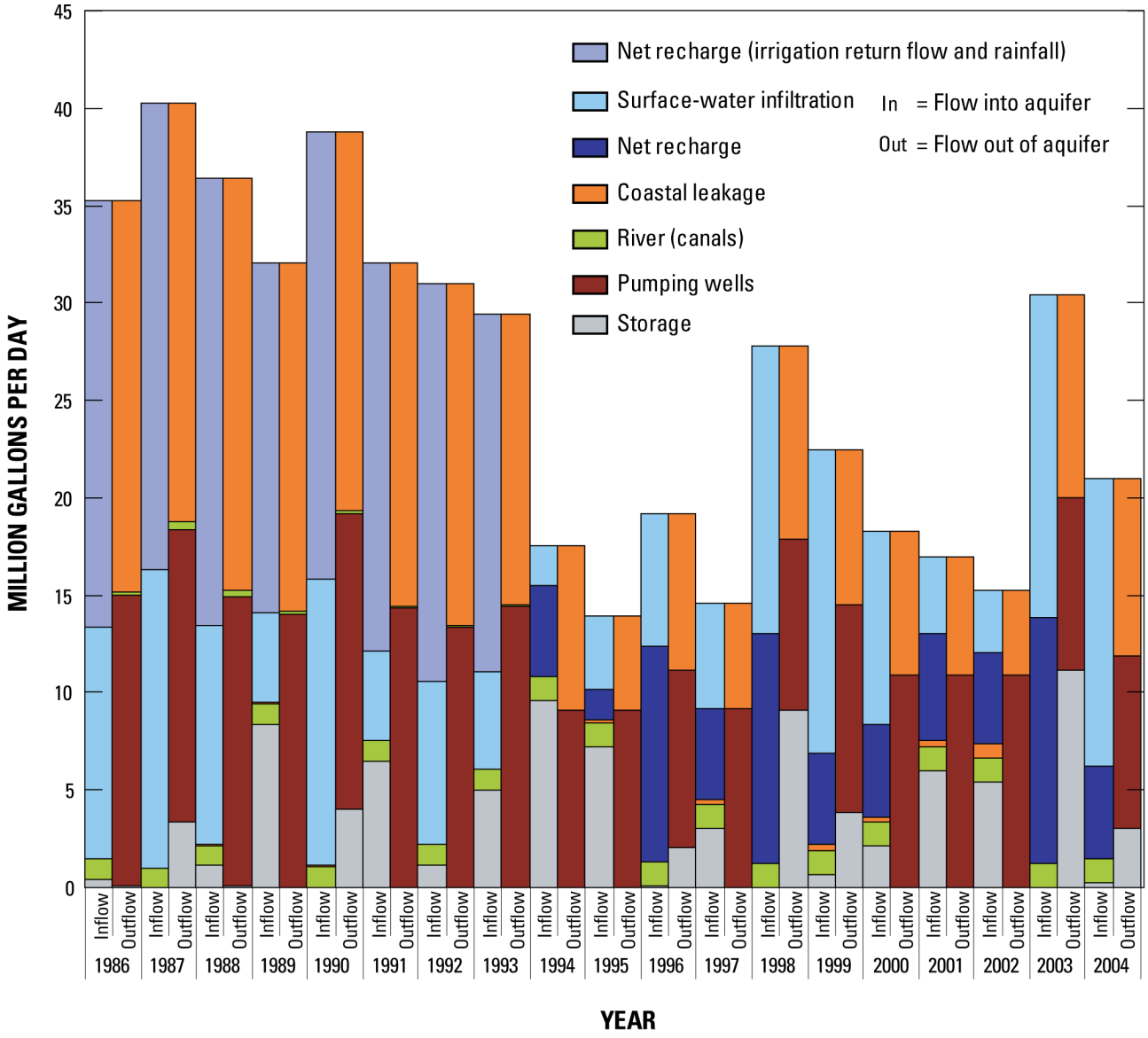

Figure 21. Calibrated transient model simulated water budget for annual stress periods 1986 through 2004.

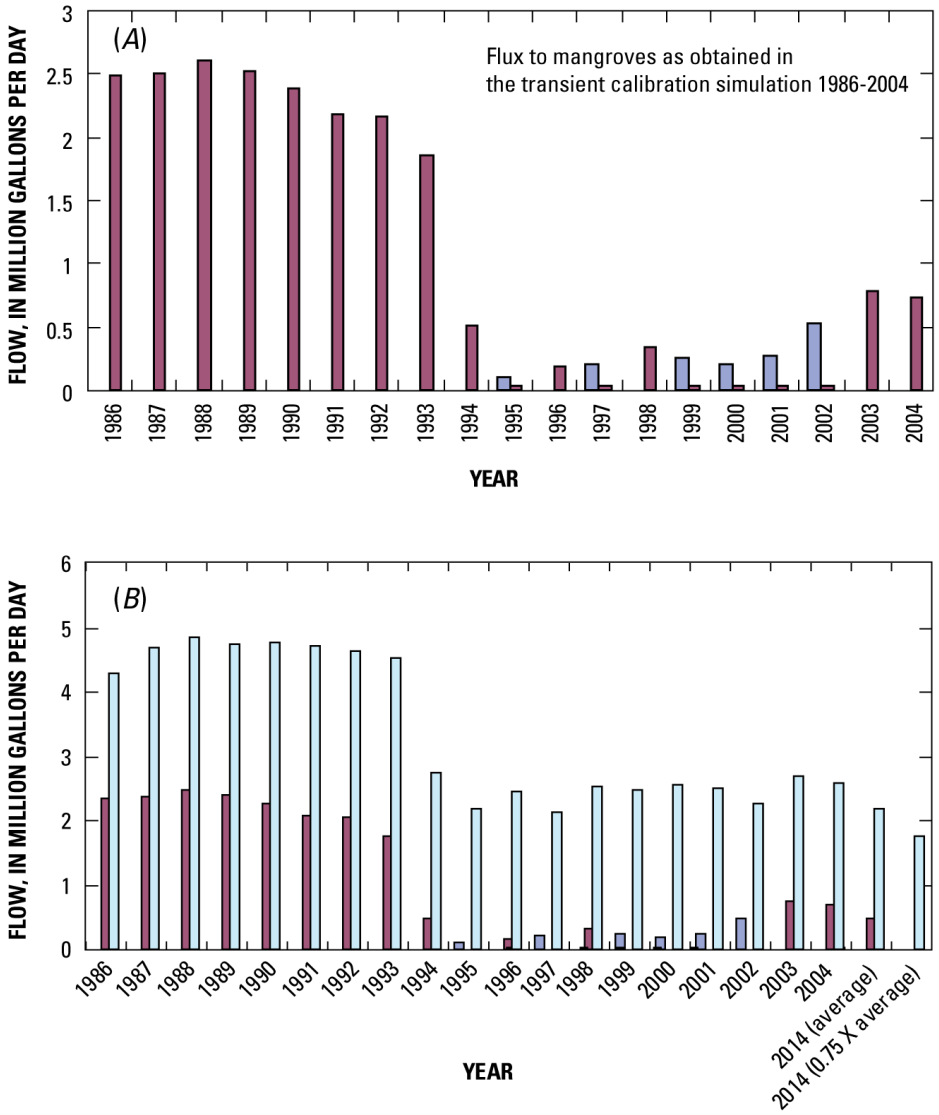

Figure 22. Model simulated flow to the mangroves (part of the general-head boundary cells in model layer 2) in the Jobos Bay National Estuarine Research Reserve near Salinas, Puerto Rico (*A*) as obtained in calibrated transient model and (*B*) flux to mangroves with a 10-year stress period added while maintaining 2004 pumping rates with average precipitation and with 75 percent of average precipitation.

Table 8. Summary of years where irrigation return flow occurs, precipitation conditions are less than average, and model simulated water budget indicates estuary water enters the South Coast aquifer.

Year	Irrigation return flow from furrow irrigation	Annual rainfall at Aguirre less than average	Estimated annual streamflow infiltration less than average	Rainfall and streamflow infiltration less than average	Model simulated water budget indicates estuary water flows into the aquifer
1986	X				
1987	X				
1988	X				
1989	X	X	X	X	
1990	X				
1991	X	X	X	X	
1992	X	X			
1993	X	X	X	X	
1994		X	X	X	
1995		X	X	X	X
1996			X		
1997		X	X	X	X
1998					
1999		X			X
2000		X			X
2001		X	X	X	X
2002		X	X	X	X
2003					
2004					

The fourth alternative was tested by reducing the groundwater withdrawals by 50 percent from all agricultural wells within the aquifer. The simulation indicated that this reduction in groundwater withdrawals will result in a discharge to the mangrove area of about 0.80 Mgal/d. This amount, however, is less than the 1.4 Mgal/d goal required for discharge to the mangrove area. The fourth alternative will require about 1.26 Mgal/d of water from other sources to compensate for the reduction in pumpage from 15 agricultural wells.

The fifth alternative was tested using a combination of the previous simulated alternatives of reduction of groundwater withdrawals and artificial recharge over agricultural areas. The reduction of groundwater withdrawals was the same as in alternative 4; however, the flooded agricultural fields covered an area of 587 ac, which is 61 percent of the area used in alternative 2. The results from the model simulation indicated that the discharge to the mangrove area will be about 1.37 Mgal/d. The net recharge applied over the agricultural field is 0.0059 ft/d, which is the same as for alternative 2, and equivalent to 1.13 Mgal/d. As in alternative 2, the water requirement from other sources will depend upon whether the area is cultivated or if it is flooded without cultivation. Using the irrigation requirements for sugarcane cultivation (4 ft/yr) in 587 ac, approximately 2.1 Mgal/d would be required. This alternative will require an additional 1.26 Mgal/d of water from other sources to compensate for the reduction in pumpage from agricultural wells.

A summary of the water requirements from artificial recharge sources and simulated discharge to the mangroves for each of the tested alternatives is given in figure 23. The first and fourth alternatives require the least amount of artificial recharge. However, the fourth alternative does not substantially increase flow to the mangroves. Thus, the first alternative requires the

least amount of water and yields the target amount of discharge to the mangroves.

The potentiometric surfaces resulting from all five simulated alternatives described previously (figs. 24-28) indicate how water levels and the shape of the contours change from the 2004 simulated surface for model layer 2. In particular, the implementation of alternatives 1, 2, and 3 may create groundwater mounds and increase groundwater levels, above those of the 2004 potentiometric surface, by more than 5 ft near the mangrove swamps (figs. 24-26). These increases in groundwater levels could increase the potentiometric surface to the point of saturating soils. In conjunction with the groundwater level increases, a pronounced southward component in the direction of groundwater flow results from all of the five alternatives evaluated.

The groundwater altitudes measured at observation wells 154, 177, and 96 (plate 2 and apps. 3 and 4) near the northern border of the JBNERR (USGS Piezometer C, JBNERR West, and JBNERR East, respectively), could be used to identify periods when groundwater discharge to the mangrove areas declines. These piezometers may also serve to monitor the temporal and spatial effects of the applied water-management alternative(s) on groundwater levels. These wells could also be used for collecting water samples to detect changes in groundwater chemical composition.

Limitations of the Model

All groundwater flow models are an over-simplification of the actual aquifer system. Three major simplifications involved in this modeling effort are (1) simplified hydraulic conductivity zones for the five model layers, (2) the assumption of a correctly located and static freshwater/seawater interface represented in the model as a no-flow boundary, and (3) use of non-varying general head boundaries along the coast. The greatest sources of error in the model calibration process result from a lack of accuracy in groundwater withdrawal rates, especially from irrigation wells; a lack of continuous streamflow gaging stations along upstream and downstream segments of streams that lose flow to the aquifer (especially the Río Nigua); and a lack of seepage studies for the irrigation canals.

The hydraulic conductivity is undoubtedly more heterogeneous in the study area than in the simplified zones used in the calibrated model. However, the final distribution of hydraulic conductivity is within reasonable ranges of the known distribution, based on specific capacity tests, and mimics the current understanding of the depositional environment (table 5; Renken and others, 2002).

The errors introduced by approximating the freshwater/seawater interface as a stationary no-flow boundary are believed to be small (Reilly, 2001). This is common practice, especially for simulations involving short time scales. No effort was made to test this boundary condition.

The non-varying general head boundary in layers 2 and 3 along the coast may have some effect on leakage to or from the aquifer to the mangroves and the sea. The conductance term is calculated from the estimates of horizontal hydraulic conductivity of the coastal sediments divided by 10 (to represent vertical hydraulic conductivity) and the cell area. Because the grid spacing is fairly small, the conductance terms are not large, and therefore, they do not result in forcing a constant head and should provide a reasonable estimate of groundwater flow to or from the coast (Kuniansky and Danskin, 2003). The general head at the coast is set to mean sea level, even though the actual head would rise and fall with the tides. However, tidal fluctuations in southern Puerto Rico are small, with a diurnal range of 0.8 ft (Arroyo NWS station). Thus, the non-varying specified head along the coast is a reasonable approximation, especially because annual stress periods were used.

Calibration of the model would be improved with more accurate information about the major components of the water budget. The two major components with missing information are non-metered groundwater withdrawals and continuous streamflow. Better knowledge of these fluxes would help constrain the model calibration and provide much more confidence in the calibrated set of aquifer properties and net recharge. This information would result in a more limited set of model parameters and stresses. Despite this limitation, final estimates of these water-budget components are within ranges estimated by previous studies.

Because of the uncertainty in major water-budget components, the groundwater management alternatives examined herein are primarily illustrative rather than quantitative examples of how fresh groundwater flux may be increased to mangroves in the JBNERR. The rates of groundwater withdrawal reduction, rates of net recharge applied, and injection rates determined from the simulation of the alternatives should not be considered precise estimates. However, the analysis of the relation between groundwater withdrawal reductions and net recharge increases, and the injection rate required to increase fresh groundwater discharge to the mangroves in the JBNERR, should prove useful in evaluating available water-management alternatives.

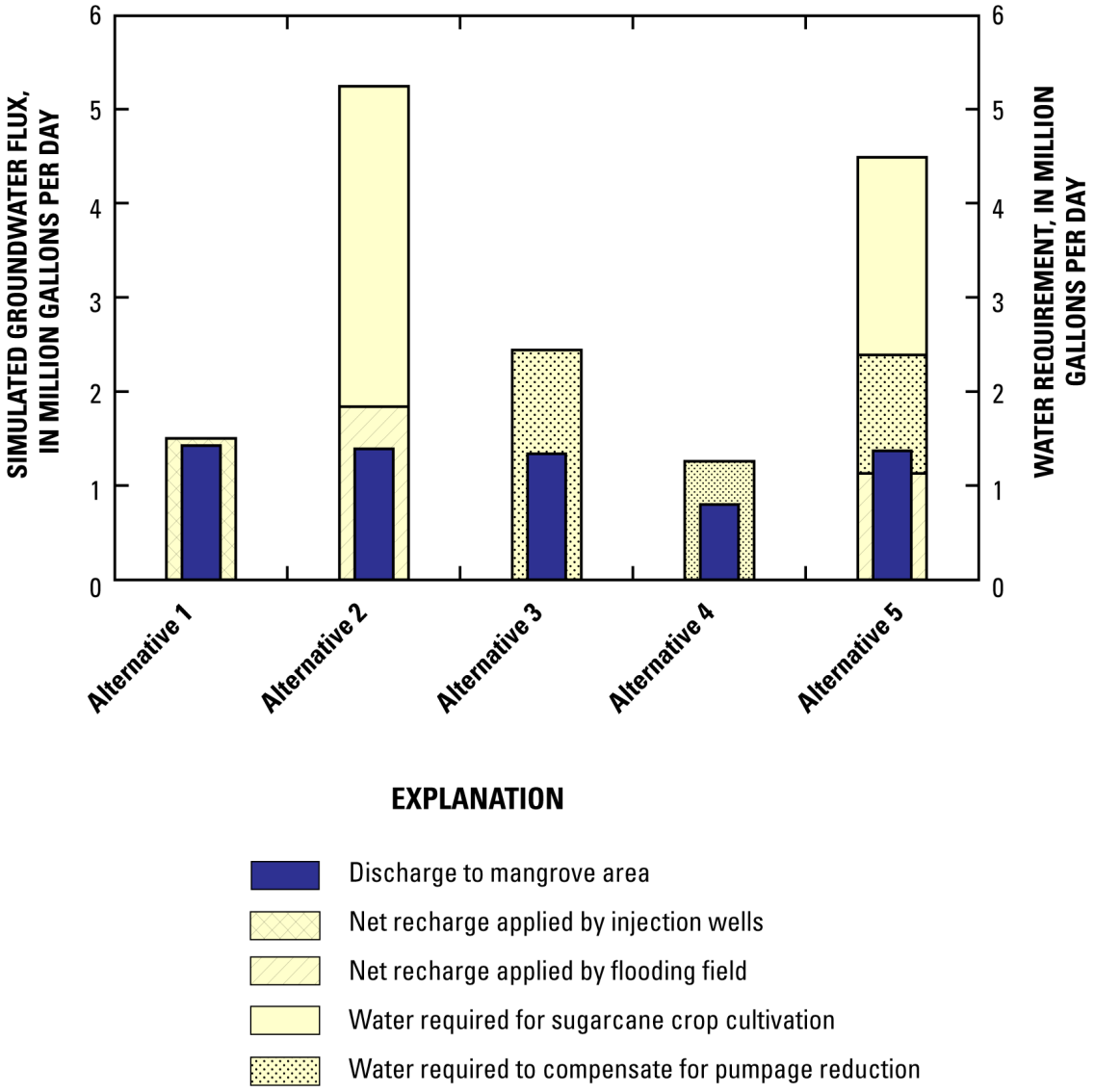

Figure 23. Model simulated groundwater flux to the mangrove area in the Jobos Bay National Estuarine Research Reserve and required water from sources for each of the groundwater management strategies tested.

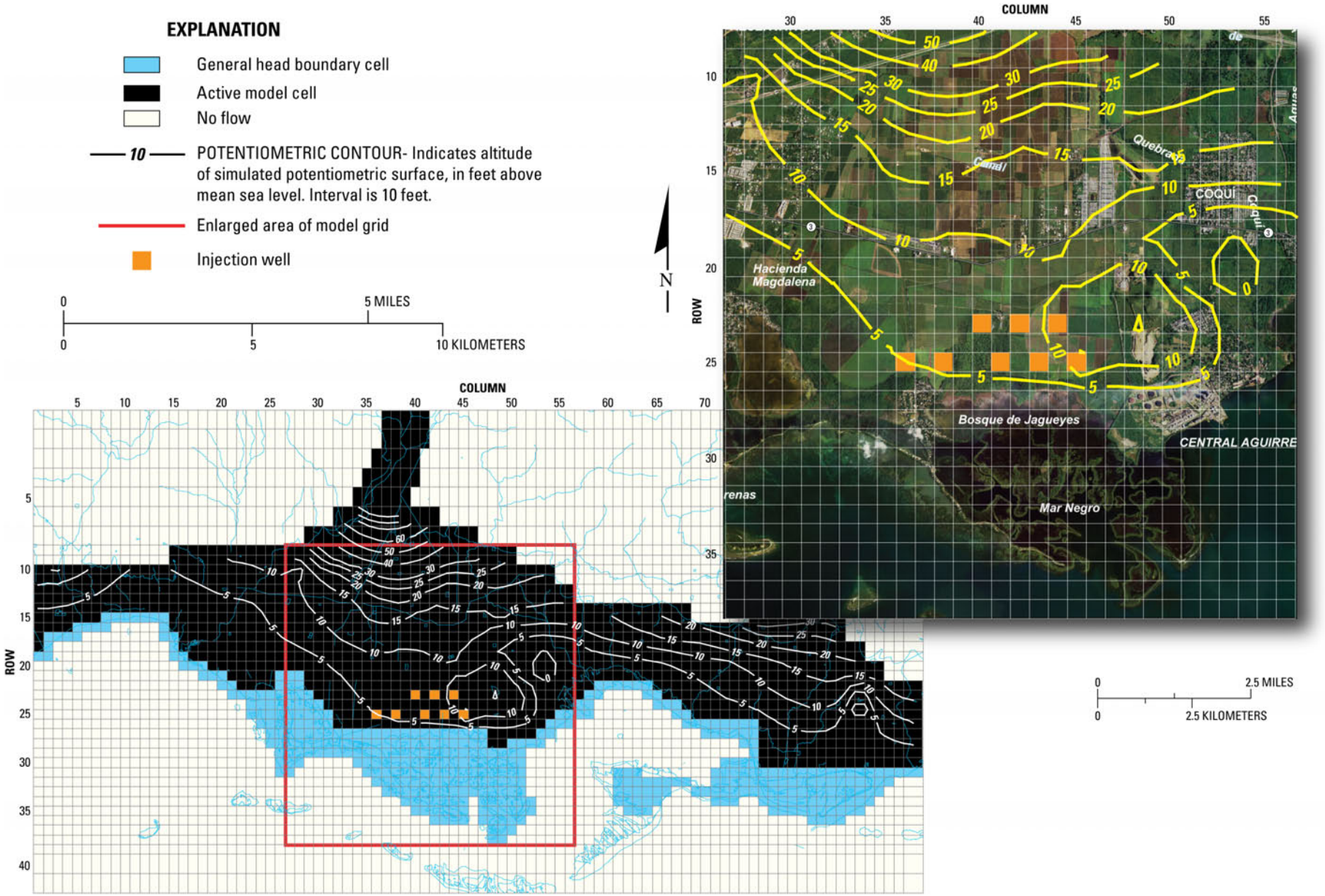

Figure 24. Model-simulated potentiometric surface in the South Coast aquifer after 10-years of average rainfall recharge and 2004 pumpage with artificial recharge by use of injection wells located north of Jobos Bay National Estuarine Research Reserve boundary, Salinas , Puerto Rico (alternative 1)..

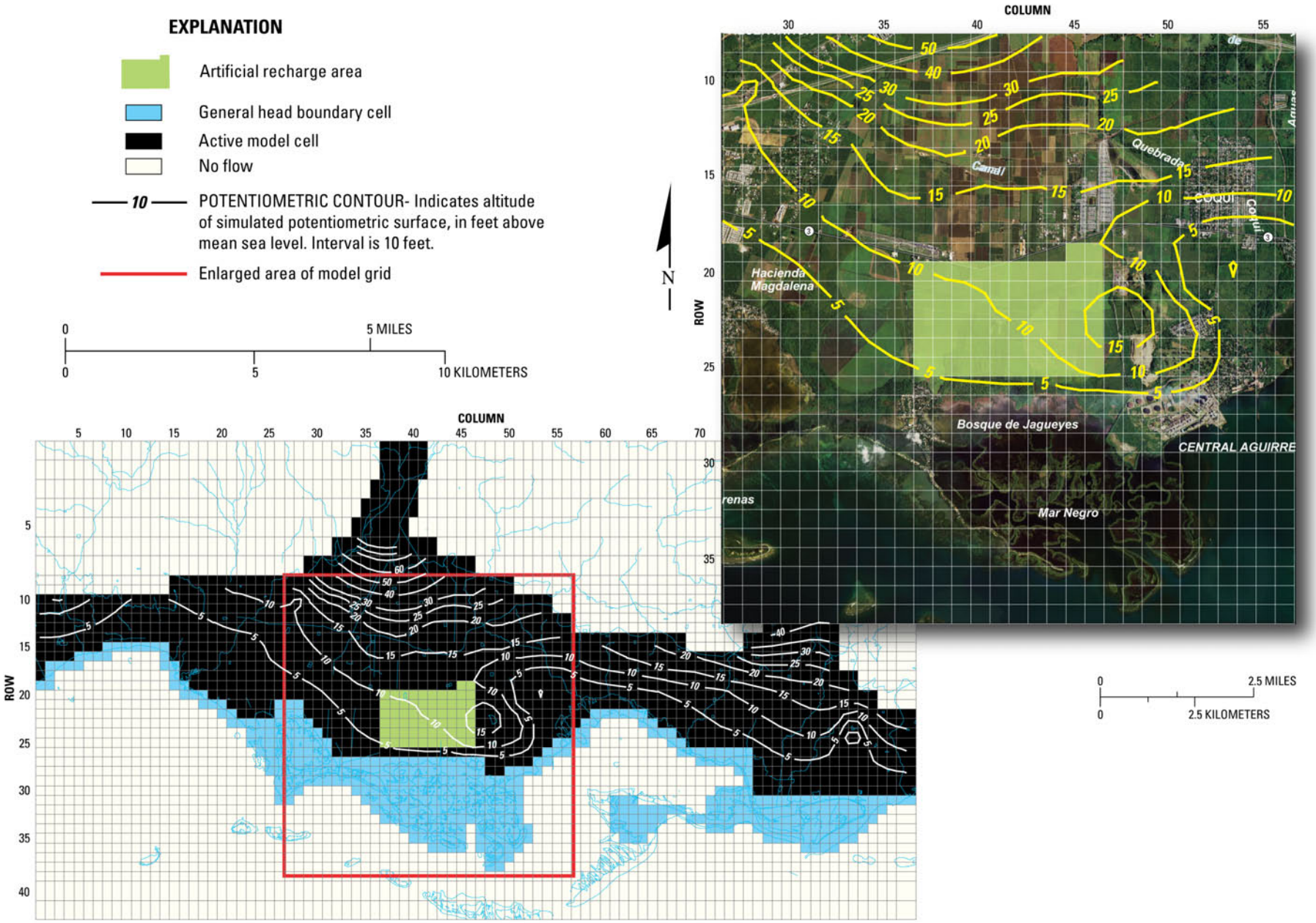

Figure 25. Model-simulated potentiometric surface in the South Coast aquifer for 2014 following 10 years of average recharge and 2004 pumpage rates, and incorporating artificial recharge applied over agricultural areas north of Jobos Bay National Estuarine Research Reserve, Salinas, Puerto Rico. (alternative 2).

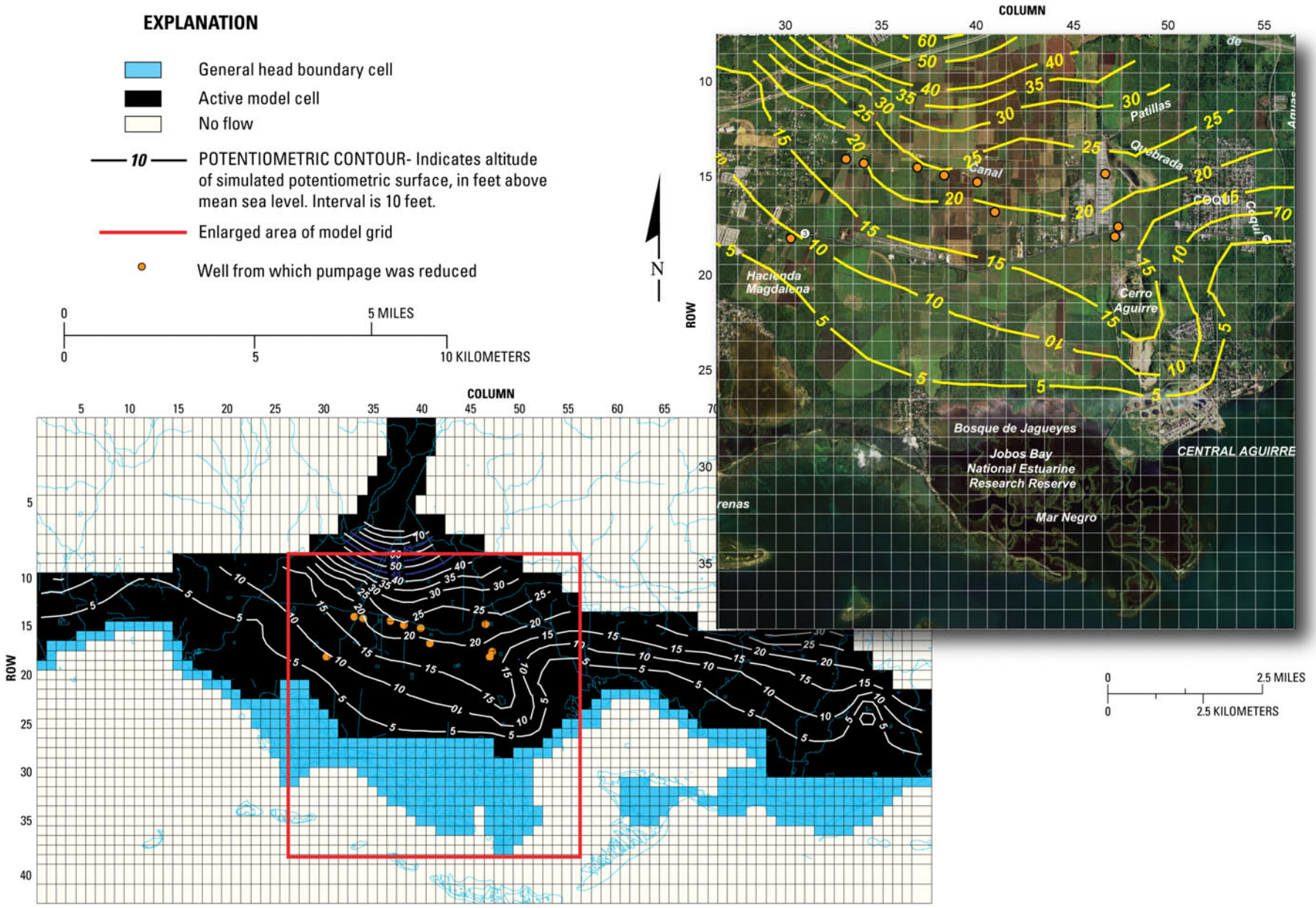

Figure 26. Model-simulated potentiometric surface in the South Coast aquifer for 2014 following 10 years of average recharge and 2004 pumpage rates, except at wells located in the area bounded by Canal de Patillas, Jobos Bay National Estuarine Research Reserve, Hacienda Magdalena , and Cerro Aguirre (alternative 3).

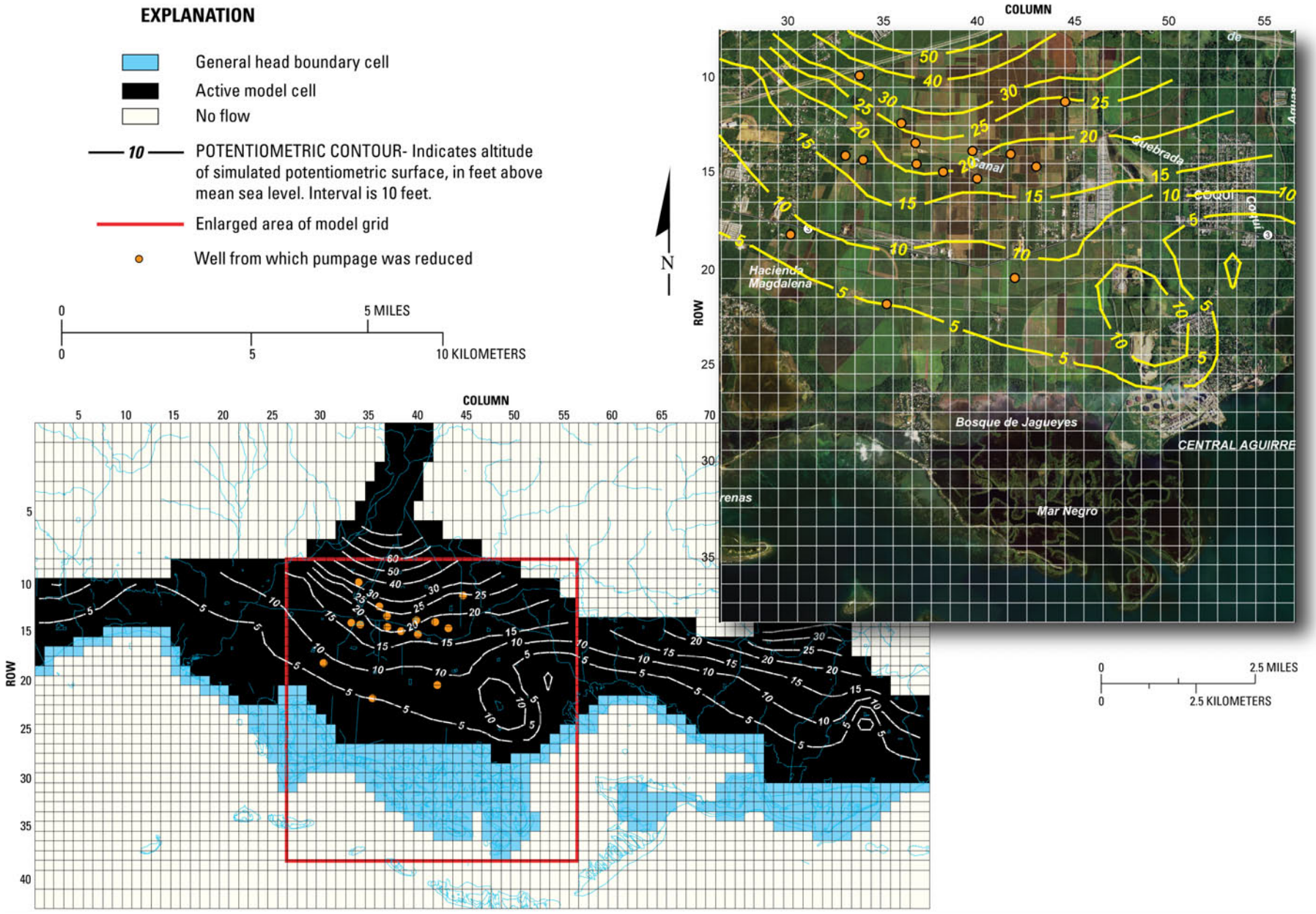

Figure 27. Model-simulated potentiometric surface in the South Coast aquifer for 2014 following 10 years of average recharge and a 50 percent reduction in 2004 pumpage rates from agricultural use wells (alternative 4).

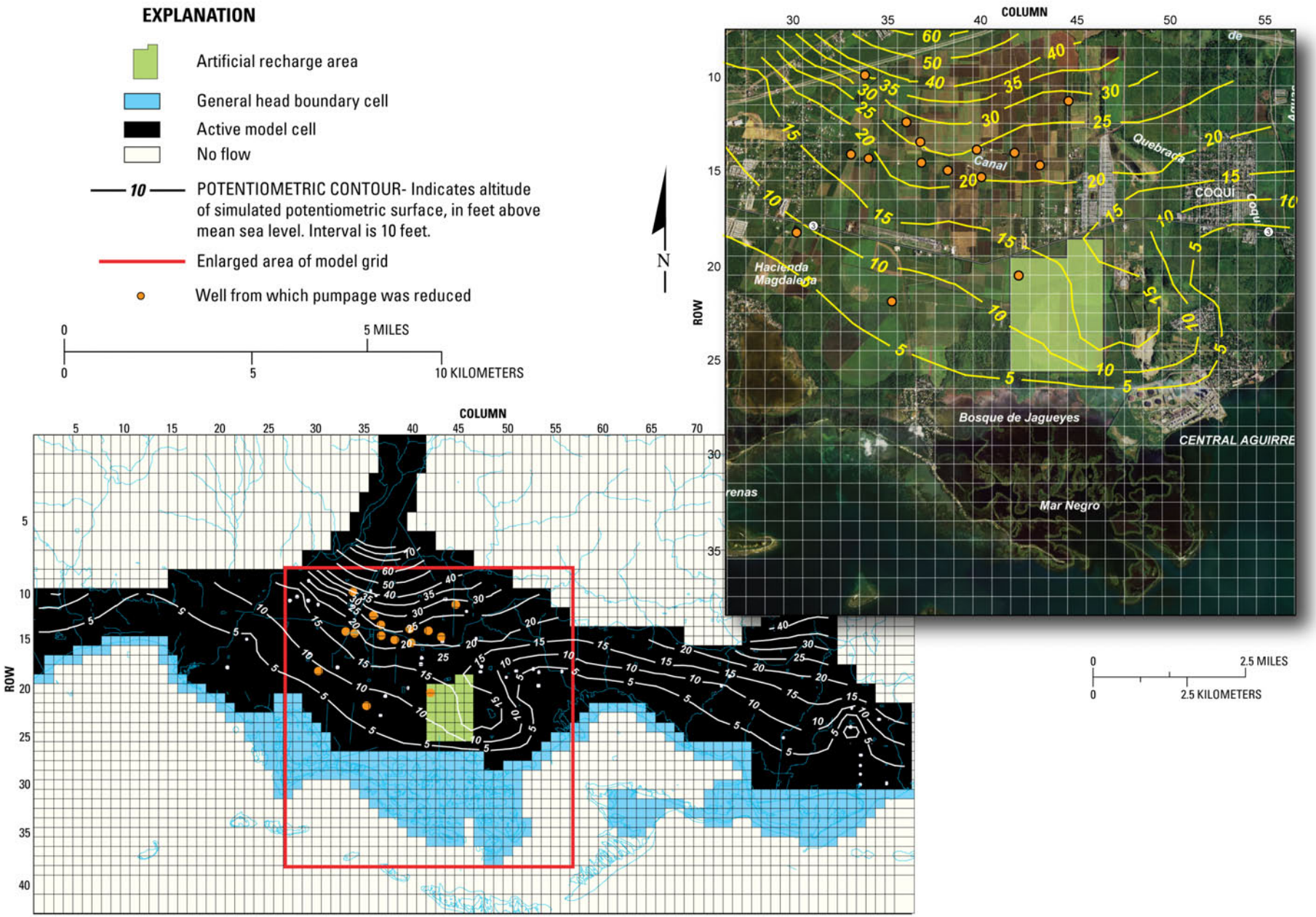

Figure 28. Model-simulated potentiometric surface in the South Coast aquifer for 2014 following 10 years of average recharge incorporating artificial recharge applied over an area of about 587 acres north of the Jobos Bay National Estuarine Research Reserve and a 50 percent reduction in 2004 pumpage rates from agricultural use wells (alternative 5).

Summary

Since about 1990, about 75 ac of mature black mangroves have died in the JBNERR. Many factors can contribute to the mortality of mangroves, including hurricanes, storms, tsunamis, droughts, changes in hydrology, erosion and subsidence, hypersalinity, and pollution. However, changes in irrigation practices, rainfall, and water use between 1986 and 2002 have resulted in approximately 25 ft of drawdown in the potentiometric surface of the aquifer near the JBNERR by 1995. To address these concerns, the USGS, in cooperation with the Puerto Rico Department of Natural and Environmental Resources, conducted a study to determine how aquifer development and changes in irrigation practices may have affected the groundwater flow to the JBNERR.

The objectives of this study were accomplished by gathering and analyzing data and developing a three-dimensional groundwater flow model of the aquifer. Although the domain of the groundwater model emphasizes the JBNERR area, it extends to hydrogeologic boundaries of rivers to the west and east, as well as to the northern and basal boundaries of alluvial deposits on the coastal plain. The collection of continuous resistivity profiles along the coast at the JBNERR and in Jobos Bay helped define the freshwater/seawater interface that forms the coastal boundary as well as freshwater discharge locations to the bay.

The model was calibrated to annual stress periods from 1986 to 2004. The steady-state initial condition of 1986 was representative of the existing hydrologic conditions, when furrow irrigation was exclusively used in the area (furrow irrigation ceased by 1994). By simulating annual hydraulic head distributions and groundwater budgets from 1986 to 2004, it was possible to quantify the changes in groundwater flow to the JBNERR, particularly the groundwater discharge into the mangrove areas, and determine how replacing furrow irrigation with micro-drip irrigation affected groundwater flux through the mangroves.

Simulations indicate that the upward groundwater flow to the mangrove swamps in the JBNERR could have been as high as 25 Mgal/d in 1986, equivalent to 63 percent of the total simulated aquifer discharge. Net areal recharge during 1986 may have been as high as 26 Mgal/d, which includes irrigation return flow and is equivalent to 67 percent of the total simulated aquifer inflow. Simulated streamflow infiltration for 1986 was 12 Mgal/d, equivalent to 30 percent of the simulated aquifer inflow.

Transient simulations indicate that the switch from furrow irrigation to drip irrigation primarily reduced freshwater discharge the coast. Prior to 1994, furrow irrigation was still predominant and irrigation return flows increased the net recharge to the aquifer. This additional recharge more than offset the effect of groundwater withdrawals, and the simulated average discharge to the coast was 19 Mgal/d. From 1994 through 2004, furrow irrigation was completely replaced by drip irrigation, resulting in reduced groundwater withdrawals. However, the reduced withdrawals did not offset the loss of recharge from irrigation return flows, and the simulated average coastal discharge declined to only 7 Mgal/d, a reduction of 63 percent. The average annual rainfall at the Aguirre Central rainfall station remained relatively constant, averaging 38 in., for both the 1986 to 1993 and 1994 to 2004 periods, thus minimizing the possibility that the difference in simulated water budgets for the two periods was the result of comparing a wet period to a dry period. The simulated average groundwater discharge to the mangrove swamps at the JBNERR from 1994 to 2004 was less than 0.2 Mgal/d, compared to an average of 2 Mgal/d for the 1986 to 1993 period when irrigation return flow occurred. The groundwater discharge to the mangrove swamps exceeded 0.5 Mgal/d during 2003-2004 because of higher than average annual rainfall during these 2 years. The transient simulation also indicated that if pumpage from the aquifer is not reduced and conditions are slightly drier than average during a given period, then little freshwater discharge to the Mar Negro at JBNEER will occur, and saline water from the estuary may move into the aquifer.

Sensitivity analyses indicate that the steady-state simulation is most sensitive to net recharge in furrow irrigation areas and horizontal hydraulic conductivity in zone 2, and fairly insensitive to vertical hydraulic conductivity. The horizontal hydraulic conductivity of zone 2 represents the lower permeability sediments between higher permeability fan deposits. The transient simulation is most sensitive to reductions in the horizontal hydraulic conductivity of zone 2 and streamflow infiltration along Río Nigua.

The groundwater flow model was used to test five alternatives for increasing groundwater discharge to the coastal mangrove swamps to approximately 1.4 million gallons per day: (1) artificially recharging the aquifer with injection wells or (2) increasing irrigation return flow by going back to furrow irrigation; (3) termination of groundwater withdrawals near the mangroves; (4) reduction of groundwater withdrawals at irrigation wells by 50 percent; and (5) a combination of alternatives 2 and 4 increasing irrigation return flows and decreasing irrigation withdrawals. Each alternative assumed average climatic conditions and groundwater withdrawals at 2004 rates. Alternative 1 required 1.5 Mgal/d of injected water. Alternative 2 required flooding 958 acres with a rate of 1.84 Mgal/d if no crops are grown. Alternative 3 required the termination of 2.44 Mgal/d of withdrawals to achieve

1.34 Mgal/d of discharge to the mangroves. Alternative 4 did not achieve the objective with only 0.80 Mgal/d of simulated discharge to the mangroves, while requiring a 1.26 Mgal/d reduction in groundwater withdrawals. Alternative 5 required flooding fields with an additional 1.13 Mgal/d and the same reduction in groundwater withdrawals, but did achieve the objective of about 1.4 Mgal/d discharge to the mangroves. Alternative 1, incorporating injection wells near the reserve required the least amount of water to raise groundwater levels and maintain discharge of 1.4 Mgal/d through the mangroves.

Selected References

American Society of Civil Engineers, 2001, Standard guidelines for artificial recharge of ground water: Environmental and Water Resources Institute American Society of Civil Engineers Report 34-01, 106 p.

Bear, Jacob, 1979, Hydraulics of Groundwater: New York, McGraw-Hill, 567p.

Bennet, G.D., 1976, Electrical analog simulation of the aquifers along the south coast of Puerto Rico: U.S. Geological Survey Open-File Report 76-4, 99 p.

Bennet, G.D., and Guisti, E.V., 1971, Coastal groundwater flow near Ponce, Puerto Rico: Geological Survey Research 1971, Chapter D: U.S. Geological Survey Professional Paper 750-D, p. D206-D211.

Bouwer, Herman, 1978, Groundwater hydrology: New York, McGraw-Hill, 480 p.

Cintrón, Gilberto, Lugo, A.E., Pool, D.J., and Morris, Greg, 1978, Mangroves in Puerto Rico and adjacent islands: Biotropica, v. 10, no. 2, p. 110-121.

Díaz, J.R., 1974, Coastal salinity reconnaissance and monitoring system-south coast of Puerto Rico: U.S. Geological Survey Open-File Report 74-1, 28 p.

Díaz, J.R., 1977a, Groundwater levels on the south coast of Puerto Rico, February 1974 to February 1975: U.S. Geological Survey Open-File Report 76-625, 30 p.

Díaz, J.R., 1977b, Ground water in alluvium on the south coast of Puerto Rico, February 1977: U.S. Geological Survey Open-File Report 77-696, 6 p.

Díaz, J.R., 1979a, Groundwater levels in alluvium on the south coast of Puerto Rico, February 1978: U.S. Geological Survey Open-File Report 79-1272, 18 p.

Díaz, J.R., 1979b, Seawater intrusion, south coast of Puerto Rico, 1966-77: U.S. Geological Survey Open-File Report 79-1334, 20 p.

Fetter, C.W., 1994, Applied hydrogeology: New York, Macmillan, 691 p.

Giusti, E.V., 1971, Water resources of the Coamo area, Puerto Rico: Commonwealth of Puerto Rico Water-resources Bulletin 8, 43 p.

Gómez-Gómez, Fernando, 1979, Reconnaissance of six solid waste disposal sites in Puerto Rico and effects on water quality: U.S. Geological Survey Open-File Report 79-1338, 10 p.

Gómez-Gómez, Fernando, 1987, Planning report for the Caribbean Islands Regional Aquifer-System Analysis Project: U.S. Geological Survey Water-Resources Investigations Report 86-4074, 50 p.

Gómez-Gómez, Fernando, 1991, Hydrochemistry of the South Coastal Plain aquifer system of Puerto Rico and its relation to surface-water recharge, *in* Gómez-Gómez, Fernando, Quiñones-Aponte, Vicente, and Johnson, A.I., eds., Regional aquifer systems of the United States—Aquifers of the Caribbean Islands: American Water Resources Association Monograph Series no. 15, p. 57-75.

Graves, R.P., 1992, Geohydrology of the Aguirre and Pozo Hondo area, southern Puerto Rico: U.S. Geological Survey Water-Resources Investigations Report 91-4124, 43 p.

Harbaugh, A.W., and McDonald, M.G., 1996, User's documentation for MODFLOW-96, An update to the U.S. Geological Survey modular finite-difference groundwater flow model: U.S. Geological Survey Open-File Report 96-485, 56 p.

Harbaugh, A.W., Banta, E.R., Hill, M.C., and McDonald, M.G., 2000, MODFLOW-2000, The U.S. Geological Survey modular groundwater model User guide to modularization concepts and the Groundwater Flow Process: U.S. Geological Survey Open-File Report 00-92, 121 p.

Heisel, J.E., and Gonzalez, J.R., 1979, Water budget and hydraulic aspects of artificial recharge, south coast of Puerto Rico: U.S. Geological Survey Water-Resources Investigations Report 78-58, 102 p.

Helmer, E.H., Ramos, O., del Mar-Lopez, T., Quiñones, M., and Díaz, W., 2002, Mapping forest type and land use of a biodiversity hotspot: International Institute of Tropical Forestry, U.S. Department of Agriculture, 36 p.

Hem, J.D., 1985, Study and interpretation of the chemical characteristics of natural water (3d ed.): U.S. Geological Survey Water-Supply Paper 2254, 263 p.

Hill, M.C., 1998, Methods and guidelines for effective model calibration: U.S. Geological Survey Water-Resources Investigations Report 98-4005, 90 p.

Hill, M.C., Banta, E.R., Harbaugh, A.W., and Anderman, E.R., 2000, MODFLOW-2000, The U.S. Geological Survey modular groundwater model; user guide to the observation, sensitivity, and parameter-estimation processes and three post-processing programs: U.S. Geological Survey Open-File Report 00-184, 209 p.

Jimenez, J.A., Lugo, A.E., and Cintron, Gilberto, 1985, Tree mortality in mangrove forests: Biotropica, v. 17, no. 3, p. 177-185.

Johnson, A.I., 1967, Specific yield—Compilation of specific yields of various materials: U.S. Geological Survey Water-Supply Paper 1662-D.

Krushensky, R.D., and Schellekens, J.H., 2001, Geology of Puerto Rico, *in* Bawiec, W.J., ed., Geology, Geochemistry, Geophysics, Mineral Occurrence, and Mineral Resource Assessment for the Commonwealth of Puerto Rico: U.S. Geological Survey Open-File Report 98-38, CD-ROM.

Kuniansky, E.L., and Danskin, W.R., 2003, Models gone bad—Common modeling problems and how to solve them, *in* Poeter, Eileen, Zheng, Chunmiao, Hill, Mary, and Doherty, John, eds., MODFLOW and More 2003—Understanding through Modeling, Conference Proceedings: Golden, Colo., Colorado School of Mines, p. 356-360.

Kuniansky, E.L., Gómez-Gómez, Fernando, and Torres-González, Sigfredo, 2004, Effects of aquifer development and changes in irrigation practices on groundwater availability in the Santa Isabel area, Puerto Rico: U.S. Geological Survey Water-Resources Investigations Report 03-4303, 56 p.

McClymonds, N.E., and Díaz, J.R., 1972, Water resources of the Jobos area, Puerto Rico: Commonwealth of Puerto Rico Water-Resources Bulletin 13, 32 p.

McClymonds, N.E., and Ward, P.E., 1966, Hydrologic characteristics of the alluvial fan near Salinas, Puerto Rico: U.S. Geological Survey Professional Paper 550-C, p. C231-C234.

McDonald, M.G., and Harbaugh, A.W., 1988, A modular three-dimensional finite-difference groundwater flow model: U.S. Geological Survey Techniques of Water-Resources Investigations book 6, chap. A1, 586 p.

National Oceanic and Atmospheric Administration, 2005, Climatological Data Annual Summary, Puerto Rico and the Virgin Islands, v. 51, no. 13.

Pool, D.J., Snedaker, S.C., and Lugo, A.E., 1977, Structure of mangrove forests in Florida, Puerto Rico, Mexico, and Costa Rica: Biotropica, v. 9, no. 3, p. 195-212.

Puerto Rico Water Resources Authority, 1972, Geological and geophysical investigations of the proposed Aguirre nuclear station in the Aguirre power plant complex environmental report: 101 p.

Quiñones-Aponte, Vicente, 1989, Horizontal anisotropy of the principal groundwater flow zone in the Salinas alluvial aquifer, Puerto Rico: Ground Water, v. 27, no. 4, p. 491-500.

Quiñones-Aponte, Vicente, 1991, Water resources development and its influence on the water budget for the aquifer system in the Salinas to Patillas area, Puerto Rico, *in* Gómez-Gómez, Fernando, Quiñones-Aponte, Vicente, and Johnson, A.I., eds., Regional aquifer systems of the United States—Aquifers of the Caribbean Islands: American Water Resources Association Monograph Series no. 15, p. 37-55.

Quiñones-Aponte, Vicente, and Gómez-Gómez, Fernando, 1987, Potentiometric surface of the Salinas alluvial aquifer and the hydrologic conditions in the Salinas quadrangle, Puerto Rico, March 1986: U.S. Geological Survey Water-Resources Investigations Report 87-4161, 1 sheet.

Quiñones-Aponte, Vicente, Gómez-Gómez, Fernando, and Renken, R.A., 1996, Geohydrology and simulation of groundwater flow in the Salinas to Patillas area, Puerto Rico: U.S. Geological Survey Water-Resources Investigations Report 95-4063, 37 p.

Ramos-Ginés Orlando, 1994, Effects of changing irrigation practices on the groundwater hydrology of the Santa Isabel-Juana Díaz area, south central Puerto Rico: U.S. Geological Survey Water-Resources Investigations Report 91-4183, 22 p.

Reilly, T.E., 2001, System and boundary conceptualization in groundwater flow simulation: U.S. Geological Survey Techniques of Water-Resources Investigations, book 3, chap. B8, 26 p.

Renken, R.A., Gómez -Gómez, Fernando, Quiñones-Aponte, Vicente, and Dacosta, Rafael, 1995, Structure and depositional patterns and their influence on the hydraulic conductivity of fan-deltas in southern Puerto Rico, *in* Miller, R.L., Escalante, G., Reinemund, J.A., and Bergin, M.J., eds., Energy and Mineral Potential of the Central American-Caribbean Region: Circum-Pacific Council for Energy and Mineral Resources, Earth Science Series, Springer-Verlag, v. 16, p. 369-377.

Renken, R.A., Ward, W.C., Gill, I.P., Gómez-Gómez, Fernando, and Rodriguez-Martínez, Jesús, 2002, Geology and hydrogeology of the Caribbean Islands Aquifer System of the Commonwealth of Puerto Rico and the U.S. Virgin Islands: U.S. Geological Survey Professional Paper 1419, 139 p.

Robert, M.L., 2001, Evaluación de fuentes dispersas de contaminación en la cuenca hidrográfica de la Reserva Estuarina de la Bahía de Jobos y su posible asociación con los altos niveles de nitratos en sus aguas subterráneas: Universidad de Puerto Rico, Recinto Ciencias Médicas, Escuela Graduada de Salud Pública.

Rodríguez, J.M., 2005, Potentiometric surface of the fan-delta aquifer and hydrologic conditions at the Río Nigua de Salinas fan delta, Salinas, Puerto Rico, July 9-11, 2002: U.S. Geological Survey Scientific Investigations Map 2910, 1 pl.

Rodríguez, J.M., 2006, Evaluation of hydrologic conditions and nitrate concentrations in the Río Nigua de Salinas fan delta Aquifer, Salinas, Puerto Rico, 2002-2003: U.S. Geological Survey Scientific Investigations Report 2006-5062, 38 p.

Rodriguez, J.M., and Gomez-Gomez, Fernando, 2008, Historical ground-water development in the Salinas alluvial fan area, Salinas, Puerto Rico, 1900-2005: U.S. Geological Survey Scientific Investigation Map 2008-3032

Rodriguez, J.M., and Gomez-Gomez, Fernando, 2009, Groundwater quality survey of the South Coast aquifer of Puerto Rico, April 2 through May 30, 2007: U.S. Geological Survey Scientific Investigation Map 2009-3032

Rutledge, A.T., 1993, Computer programs for describing the recession of groundwater discharge and for estimating mean groundwater recharge and discharge from streamflow records: U.S. Geological Survey Water-Resources Investigations Report 93-4121, 45 p.

Theis, C.V., Brown, R.H., and Meyer, R.R., 1963, Estimating the transmissibility of aquifers from the specific capacity of wells: U.S. Geological Survey Water-Supply Paper 1536-1, 331-341 p.

Torres-González, Sigfredo, and Gómez-Gómez, Fernando, 1987, Potentiometric surface of the fan-delta aquifer and hydrologic conditions in the central Aguirre quadrangle, Puerto Rico, March, 1986: U.S. Geological Survey Water-Resources Investigations Report 87-4160, 1 sheet.

Yamauchi, H., 1984, Impact on groundwater resources of conversion from furrow to drip irrigation: Water Resources Bulletin, no. 4, v. 20, p. 557-563.

Appendix

Appendix 1. Estimated average annual rates of groundwater withdrawals in the Río Jueyes to Río Guamaní part of the South Coast aquifer from 1986 to 2004.

Reference map number	Well name	Discharge (gallons per minute)	Discharge (million gallons per day)																		
			1986	1987	1988	1989	1990	1991	1992	1993	1994	1995	1996	1997	1998	1999	2000	2001	2002	2003	2004
18	PRASA Puente Jobos	160	0.23	0.23	0.23	0.23	0.00	0.00	0.00	0.00	0.00	0.00	0.00	0.00	0.00	0.00	0.00	0.00	0.00	0.00	0.00
33	Phillips (8 wells)	na	0.80	0.80	1.05	1.20	1.16	1.16	1.16	1.18	0.00	0.00	0.00	0.00	0.00	0.00	0.00	0.00	0.00	0.00	0.00
40	Salich 1	3,000	0.98	0.98	0.86	0.81	0.86	0.98	0.86	0.98	0.00	0.00	0.00	0.00	1.20	1.20	1.20	1.20	1.20	0.00	0.00
41	Aguirre 3	1,650	0.00	0.00	0.00	0.00	0.00	0.00	0.00	0.00	0.70	0.70	0.70	0.70	0.70	0.70	0.70	0.70	0.70	0.70	0.70
42	Fortuna 1	970	0.32	0.32	0.32	0.32	0.32	0.32	0.32	0.32	0.40	0.40	0.40	0.40	0.40	0.40	0.40	0.40	0.40	0.40	0.40
49	Magdalena 2	550	0.00	0.00	0.00	0.00	0.00	0.00	0.00	0.00	0.00	0.00	0.00	0.00	0.00	0.00	0.10	0.10	0.10	0.10	0.10
50	Esperanza 3	2,000	0.66	0.66	0.54	0.48	0.54	0.66	0.54	0.66	0.00	0.00	0.00	0.00	0.00	0.00	0.00	0.00	0.00	0.00	0.00
51	Magdalena 1	1,300	0.43	0.43	0.43	0.25	0.43	0.43	0.31	0.43	0.00	0.00	0.00	0.00	0.10	0.10	0.10	0.10	0.10	0.10	0.10
52	Carmen 2	1500	0.49	0.49	0.49	0.31	0.49	0.49	0.49	0.49	0.00	0.00	0.00	0.00	0.00	0.00	0.00	0.00	0.00	0.00	0.00
54	Salinas 1	650	0.80	0.80	0.80	0.80	0.80	0.80	0.80	0.80	0.60	0.60	0.60	0.60	0.60	0.60	0.60	0.60	0.60	0.60	0.60
55	Salinas 2	700	0.10	0.10	0.10	0.10	0.10	0.10	0.10	0.10	1.00	1.00	1.00	1.00	1.00	1.00	1.00	1.00	1.00	1.00	1.00
70	Amadeo 2	800	0.00	0.00	0.00	0.00	0.00	0.00	0.00	0.00	0.50	0.50	0.50	0.50	0.50	0.50	0.50	0.50	0.50	0.50	0.50
71	Godreau 6	1,690	0.55	0.55	0.44	0.38	0.44	0.55	0.44	0.55	0.00	0.00	0.00	0.00	0.00	0.00	0.00	0.00	0.00	0.00	0.00
72	Godreau 5	1,100	0.36	0.36	0.36	0.18	0.36	0.36	0.36	0.36	0.00	0.00	0.00	0.00	0.00	0.00	0.00	0.00	0.00	0.00	0.00
110	Godreau 2	665	0.22	0.22	0.22	0.04	0.22	0.22	0.22	0.22	0.00	0.00	0.00	0.00	0.00	0.00	0.00	0.00	0.00	0.00	0.00
111	Godreau 4	1,300	0.43	0.43	0.43	0.25	0.43	0.43	0.43	0.43	0.00	0.00	0.00	0.00	0.00	0.00	0.00	0.00	0.00	0.00	0.00
114	AEE 6	1,000	0.60	0.24	0.24	0.24	0.24	0.24	0.24	0.24	0.24	0.24	0.24	0.24	0.24	0.24	0.24	0.24	0.24	0.24	0.24
115	AEE 7	650	0.40	0.40	0.40	0.40	0.40	0.40	0.40	0.40	0.40	0.40	0.40	0.40	0.40	0.40	0.40	0.40	0.40	0.40	0.40
116	AEE 9	790	0.00	0.00	0.00	0.00	0.00	0.00	0.00	0.00	0.47	0.47	0.47	0.47	0.47	0.47	0.47	0.47	0.47	0.47	0.47
126	PRASA Villodas	360	0.52	0.52	0.52	0.52	0.52	0.52	0.52	0.52	0.52	0.52	0.52	0.52	0.00	0.00	0.00	0.00	0.00	0.00	0.00
127	PRASA Perpetuo	50	0.08	0.10	0.11	0.11	0.11	0.11	0.11	0.11	0.16	0.16	0.17	0.30	0.27	0.27	0.27	0.27	0.27	0.27	0.27
128	Aguirre 1	na	0.00	0.00	0.00	0.00	0.00	0.00	0.00	0.10	0.13	0.13	0.13	0.13	0.13	0.13	0.13	0.13	0.13	0.00	0.00
129	Fortuna 1	1,500	0.49	0.49	0.37	0.37	0.25	0.25	0.00	0.00	0.00	0.00	0.00	0.00	0.00	0.00	0.00	0.00	0.00	0.00	0.00
130	Adela 1	1,000	0.33	0.33	0.33	0.33	0.33	0.33	0.33	0.33	0.41	0.41	0.41	0.41	0.41	0.41	0.41	0.41	0.41	0.41	0.41
131	Lanausse 2	200	0.00	0.00	0.00	0.00	0.00	0.00	0.00	0.00	0.08	0.08	0.08	0.08	0.08	0.08	0.08	0.08	0.08	0.08	0.08
142	Salinas 4 (Coco 2)	320	0.46	0.37	0.43	0.43	0.43	0.46	0.46	0.20	0.21	0.21	0.21	0.21	0.21	0.21	0.21	0.21	0.21	0.21	0.21
143	PRASA Campamento	113	0.16	0.16	0.16	0.16	0.16	0.20	0.20	0.20	0.20	0.20	0.16	0.10	0.10	0.10	0.10	0.10	0.00	0.00	0.00
151	Magdalena 3	560	0.00	0.00	0.00	0.00	0.00	0.00	0.00	0.00	0.00	0.00	0.00	0.00	0.23	0.23	0.23	0.23	0.23	0.23	0.23
156	Fortuna 4	600	0.00	0.00	0.00	0.00	0.00	0.00	0.00	0.00	0.17	0.17	0.17	0.17	0.17	0.17	0.17	0.17	0.17	0.17	0.17

Appendix 1. Estimated average annual rates of groundwater withdrawals in the Río Jueyes to Río Guamaní part of the South Coast aquifer from 1986 to 2004.—Continued

Reference map number	Well name	Discharge (gallons per minute)	Discharge (million gallons per day)																		
			1986	1987	1988	1989	1990	1991	1992	1993	1994	1995	1996	1997	1998	1999	2000	2001	2002	2003	2004
159	PRASA Godreau 2	190	0.00	0.00	0.00	0.00	0.00	0.00	0.00	0.33	0.35	0.35	0.35	0.58	0.58	0.58	0.58	0.58	0.58	0.58	0.58
160	PRASA Coco 3	130	0.36	0.36	0.36	0.36	0.36	0.36	0.36	0.36	0.36	0.36	0.36	0.36	0.36	0.36	0.36	0.36	0.36	0.36	0.36
161	PRASA Las Margaritas	200	0.29	0.29	0.29	0.29	0.29	0.29	0.29	0.29	0.29	0.29	0.29	0.29	0.29	0.29	0.29	0.29	0.29	0.29	0.29
162	Deestano	na	0.00	0.00	0.00	0.00	0.00	0.00	0.00	0.00	0.07	0.07	0.07	0.07	0.07	0.07	0.07	0.07	0.07	0.07	0.07
163	AEE 5	900	0.60	0.60	0.60	0.60	0.60	0.60	0.60	0.60	0.20	0.20	0.20	0.20	0.20	0.20	0.20	0.20	0.20	0.20	0.20
170	Magdalena 4	300	0.1	0.1	0.1	0.1	0.05	0.05	0.05	0.05	0.00	0.00	0.00	0.00	0.00	0.00	0.00	0.00	0.00	0.00	0.00
172	PRASA AEE	300	0.32	0.44	0.50	0.48	0.44	0.50	0.40	0.40	0.41	0.41	0.41	0.41	0.41	0.41	0.41	0.41	0.41	0.41	0.41
173	PRASA San Felipe	100	0.15	0.15	0.15	0.15	0.15	0.15	0.16	0.20	0.21	0.21	0.21	0.21	0.21	0.21	0.21	0.21	0.21	0.21	0.21
176	PRASA Las Mareas	60	0.09	0.11	0.11	0.11	0.11	0.11	0.14	0.14	0.15	0.15	0.15	0.15	0.15	0.15	0.15	0.15	0.15	0.15	0.15
201	Fortuna 10	250	0.00	0.00	0.00	0.00	0.00	0.00	0.00	0.00	0.1	0.10	0.10	0.10	0.10	0.10	0.10	0.10	0.10	0.10	0.10
202	Fortuna 5	360	0.00	0.00	0.00	0.00	0.00	0.00	0.00	0.00	0.11	0.11	0.11	0.11	0.11	0.11	0.11	0.11	0.11	0.11	0.11
206	PRASA Godreau 1	270	0.00	0.00	0.00	0.37	0.50	0.65	0.40	0.33	0.39	0.39	0.39	0.39	0.39	0.39	0.39	0.39	0.39	0.39	0.39
207	Esperanza 2	1,800	0.59	0.59	0.59	0.41	0.59	0.59	0.47	0.59	0.00	0.00	0.00	0.00	0.00	0.00	0.00	0.00	0.00	0.00	0.00
208	Godreau 1	250	0.00	0.00	0.00	0.00	0.00	0.00	0.00	0.00	0.04	0.04	0.04	0.04	0.04	0.04	0.04	0.04	0.04	0.04	0.04
209	Santa Fe 1	200	0.00	0.00	0.00	0.00	0.00	0.00	0.00	0.00	0.08	0.08	0.08	0.08	0.08	0.08	0.08	0.08	0.08	0.08	0.08
210	Santa Fe 2	400	0.00	0.00	0.00	0.00	0.00	0.00	0.00	0.00	0.00	0.00	0.00	0.00	0.08	0.08	0.08	0.08	0.08	0.08	0.08
211	Gonzalez 2	500	0.00	0.00	0.00	0.00	0.00	0.00	0.00	0.00	0.13	0.13	0.13	0.13	0.13	0.13	0.13	0.13	0.13	0.13	0.13
212	Aguirre 6	1,800	0.59	0.55	0.55	0.55	0.55	0.55	0.55	0.55	0.00	0.00	0.00	0.00	0.20	0.20	0.20	0.20	0.20	0.00	0.00
213	Ayerst	na	0.00	0.00	0.00	0.00	0.22	0.25	0.25	0.28	0.31	0.30	0.29	0.31	0.31	0.27	0.30	0.30	0.30	0.30	0.30
214	Fibers Superfund	na	0.00	0.00	0.00	0.00	0.00	0.00	0.00	0.00	0.00	0.00	0.00	0.00	0.00	0.65	0.65	0.65	0.65	0.65	0.65

Appendix 2*a*. Lithologic description for test boring SC-2 at Salinas, Puerto Rico, March 16-17, 1987.

[Lithologic description by Jesús Rodríguez-Martínez. Latitude 17°57'38", longitude 66°24'11"; horizontal datum: North American Datum 1927; land surface altitude: about 23 feet above mean sea level]

Depth interval (feet)	Lithologic description
0-10	Claystone, light brownish yellow, locally dark, locally orange and black stained, well indurated, slightly calcareous, with pebbly lithic clasts.
10-15	Sand, clayey, dark yellowish brown.
15-26	Claystone, moderate yellowish brown, locally silty and sandy.
26-38	Volcanic gravel, with minor cobbles and a coarse to very coarse dark lithic sand.
38-48	Claystone, pale yellowish brown and very pale orange, sandy and pebbly.
48-58	Gravel, cobbly, with very coarse volcanic and quartzose sand.
58-68	Claystone, moderate brown, locally pebbly coarse sandy and silty, locally with weathered lithic clasts.
68-89	Claystone, moderate brown, moderate to well indurated, silty and pebbly in part.
89-99	Claystone, moderate brown to dark brownish yellow, locally dusky yellow mottled, silty in part.
99-116	Gravel, volcanic, cobbly, with a matrix of volcanic and minor very coarse quartzose sand.
116-125	Gravel, volcanic, multi-colored, sub-angular to sub-rounded, moderately weathered, with a minor quartzose and volcanic sand.
125-142	Sand, volcanic and quartzose, very coarse to cobbly, with a minor quartz fraction.
142-164	Sand, volcanic and quartzose, very coarse to pebbly.
164-178	Claystone, moderate brown with an assorted mixture of volcanic pebbles, cobbles and coarse sand.
178-194	Claystone, moderate to dark yellowish brown, locally sandy, silty and pebbly.
194-203	Sand, volcanic, dusky brown to dark yellow, very coarse grained, to pebbly and cobbly.
203-210	Claystone, moderate brown, locally volcanic pebbly.
210-229	Sand, volcanic, very coarse grained, clayey
229-257	Claystone, moderate brown, sandy, locally with volcanic cobbles and pebbles
257-273	Sand, clayey, dark yellowish brown locally pebbly.
273-280	Conglomerate, sandy, with a minor clayey matrix
280-294	Sand, moderate dark yellowish, very coarse grained, pebbly,clayey,
294-300	Conglomerate, volcanic clasts, brownish yellow to yellowish orange, black mottled, in a very coarse grained and pebbly sand.
300-303	Claystone, dark yellowish brown, silty, locally sandy and pebbly.
303-321	Sand, coarse grained, clayey and pebbly, with multi-colored volcanic clasts.
321-336	Claystone, reddish brown, black mottled, sandy, locally with volcanic pebbles.
336-349	Sand, dark yellowish brown to moderate brown, coarse grained, clayey and pebbly.
349-366	Claystone, moderate brown, locally grading to a clayey sand, locally pebbly.
366-410	Conglomerate, volcanic clasts, in a clayey coarse grained sand matrix.
410-416	Claystone, moderate brown to medium reddish brown, black mottled.
[F]inal depth 416 feet	

Appendix 2b. Lithologic description for test boring SC-3 at Guayama, Puerto Rico, March 19-20, 1987.

[Lithologic description by Jesús Rodríguez-Martínez. Reference number 89 in appendix 3. Latitude 17°58' 01", longitude 66°10'52"; horizontal datum: North American Datum 1927. Land surface altitude about 48 feet above mean sea level]

Depth interval (feet)	Lithologic description
0-9	Sand, volcanic, medium to very coarse grained, locally silty and clayey, locally with cobbles, with a minor quartz fraction (possibly artificial fill).
9-16	Conglomerate, volcanic cobbles with a matrix of very coarse grained and pebbly sand.
16-21	Claystone, dusky brown, slightly calcareous, sandy and silty, locally with volcanic pebbles.
21-27	Claystone, as above, dark and moderate yellowish brown, slightly to moderately calcareous.
27-44	Claystone, as above, becoming pale and medium bluish green mottled with heavily altered limestone clasts.
44-54	Pebbly, very coarse volcanic sand, locally with volcanic cobbles.
54-65	Claystone with volcanic gravel.
65-69	Sand, volcanic, dark gray, black, locally green volcanic, very coarse grained, pebbly.
69-80	Claystone, medium reddish brown, grayish green, greenish gray mottled, internally black mottled, partially wet, locally slightly calcareous, reddish brown downward, locally with cobbles.
80-103	Sandstone, poorly consolidated, very coarse grained, subangular to subrounded, locally with volcanic pebbles and cobbles,
103-108	Generally as above, and increasingly pebbly.
108-113	Claystone, moderate brown to medium reddish brown, black and light greenish gray mottled internally, silty, locally pebbly.
113-124	Sand, volcanic, very coarse grained, pebbly.
124-128	Claystone, moderate brown to medium yellowish gray, black mottled locally, silty.
128-135	Sand, volcanic, sand, dark gray, medium green, very coarse grained, pebbly, with a minor quartz fraction.
135-139	Claystone, medium-reddish brown, silty.
139-148	Conglomerate, volcanic, medium green, dark-brownish red, angular- subangular, slightly to moderately altered in a minor to coarse sand fraction.
148-160	Generally as above, but locally with silt.
160-178	Claystone, silty, with volcanic weathered material.
178-196	Sand, volcanic, very coarse grained, with angular volcanic pebbles of medium dark green color and with red and yellow tones.
196-204	Igneous basement, medium to dark green, with dark green phenocrysts (ferromagnesium) and veinlets (irregular pattern) of calcite and silica, yellowish red-oxidized zones and veinlets (hematite?).

[F]inal depth, 204 feet

Appendix 3. General information for wells in the South Coast aquifer between the Río Jueyes and Río Guamaní used in this study.

[Superscripts in left column represent the following: a, well used in fence diagram; b, well used in map of thickness of surficial clay and silt; c, well used in delineation of base of permeable material; d, well used to obtain hydrologic and hydraulic data such as water level, specific capacity data, and others; na, data not available; ddmmss, degrees minutes seconds]

Well name and reference number	USGS site identifier[1]	Latitude (ddmmss)	Longitude (ddmmss)	Land surface datum (feet above mean sea level)	Depth, (feet below land surface)	Open interval, (feet above mean sea level)
Benito 1 (1)a,d	175854066114900	175854	661149	69	60	26-60
San Felipe (2)a,b,c,d	175816066125400	175816	661254	10	54	33-54
PRASA Coquí #1 (3)a,b,c,d	175826066134400	175826	661344	26	80	na
Templo Glove (4)a,b,c,d	175830066135400	175830	661354	33	80	na
Bomba Coquí 2 (5)a,b,c,d	175813066133100	175813	661331	16	150	na
Aguirre Sugar 9 (6)a,b,c,d	175810066145300	175810	661453	43	128	0-128
PRWRA 1 (7)a,b,c,d	175824066142300	175824	661423	47	250	na
Hacienda Vieja 3 (8)a,b,c	175755066143000	175755	661430	36	94	na
Pozo Aguirre 2 (9)a,b,c	175759066144400	175759	661444	16	87	na
Hacienda Vieja T-01 (10)a,b,c	175754066144500	175754	661445	20	115	na
Cautiño 3 (11)a,b,c,d	175822066104300	175822	661043	66	130	na
Cautiño 4 (12)a,b,c	175810066105800	175810	661058	51	131	na
Sucn González (13)a,b,c	175822066105300	175822	661053	61	94	na
Benito 2 (14)a,b,c	175751066105900	175751	661059	38	125	na
Bomba Coquí 4 (15)a,b,c,d	175757066131800	175757	661318	8	189	na
Josefa Norte (16)a,b,c,d	175732066091900	175732	660919	30	100	na
La Ana at Josefa (17)a,b,c,d	175756066095700	175756	660957	49	195	0-196
PRASA Puente Jobos (18)a,b,c,d	175724066095600	175724	660956	27	150	60-87
A-02-Test Well (19)a,b,c	175722066090200	175722	660902	33	32	na
Guamani 3 (20)a,b,c	175758066104000	175758	166104	39	150	na
Las Mareas 2 (21)a,b,c	175627066084000	175627	660840	2	30	na
Bomba Mercedes 8 (22)a,b,c	175648066080600	175648	660806	7	110	na
Merced Batt Well 2 (23)d	175648066081600	175648	660816	7	110	na
Luce Co. 4 (24)a,b,c,d	175646066082100	175646	660821	7	110	na
USGS 1 (25)a,b,c	175642066083700	175642	660837	7	52	17-50
USGS 2 (26)a,b,c	175645066092300	175645	660923	2	52	na
Luce Co. 3 (27)a,b,c,d	175741066082100	175741	660821	52	44	na

Appendix 3. General information for wells in the South Coast aquifer between the Río Jueyes and Río Guamaní used in this study.—Continued

[Superscripts in left column represent the following: a, well used in fence diagram; b, well used in map of thickness of surficial clay and silt; c, well used in delineation of base of permeable material; d, well used to obtain hydrologic and hydraulic data such as water level, specific capacity data, and others; na, data not available; ddmmss, degrees minutes seconds]

Well name and reference number	USGS site identifier[1]	Latitude (ddmmss)	Longitude (ddmmss)	Land surface datum (feet above mean sea level)	Depth, (feet below land surface)	Open interval, (feet above mean sea level)
Cabassa 1 (28)a,b,c	175718066082300	175718	660823	46	120	na
Aguirre Sugar 2 (29)a,b,c	175718066080700	175718	660807	39	175	na
Reunión Batt (30)a,b,c	175740066085000	175740	660850	49	86	na
Melania (31)a,b,c,d	175755066084800	175755	660848	62	105	na
Reunión 3 (32)a,b,c	175735066085900	175735	660859	43	132	22-130
Phillips #7 (33)a,b,c,d	175718066083900	175718	660839	41	151	25-51
Fibers 1 (34) (Inter Fibers 1)a,b,c	175754066084100	175754	660841	61	120	20-120
Phillips Dom #2 (35)a,b,c	175716066083400	175716	660834	39	150	25-150
Inter Fibers 3 (36)a,b,c	175755066085700	175755	660857	56	150	na
C-01-Test (37)a,b,c	175732066084500	175732	660845	49	41	na
PRASA Fibers 3 (38)d	175735066090500	175735	660905	51	na	na
Phillips core well (39)a,b,c	175720066084000	175720	660840	43	110	na
Salich #1 (40)a,b,c,d	175748066160400	175748	661606	25	162	32-96
Aguirre 3 (41)a,b	175804066150700	175804	661507	32	150	0-150
Fortuna 1 (42)a,b,c,d	175810066155400	175810	661554	70	140	0-140
Caraballo (43)d	175856066151000	175856	661510	70	140	na
Esperanza #1 (44)a,b,c,d	175810066153500	175810	661535	39	150	0-103
Lanause 3 (45)a,b,c	175840066153700	175840	661537	54	160	na
SC-2 (46)a,b,c	175750066152000	175750	661520	23	416	na
Teresa 1 (47)a,b,c	175829066163000	175829	661630	33	140	na
Magdalena 1 (48)a,b,c	175859066162200	175859	661622	58	180	na
Magdalena #2 (49)a,b,c,d	175855066161400	175855	661614	56	150	na
Providencia 1 (50)a,b,c	175851066163000	175851	661630	52	119	0-99
Aguirre 2 (51)a,b	175835066162600	175835	661626	46	126	0-126
Carmen #2 (52)a,b,c	175837066165400	175837	661654	40	173	54-172
Salinas Airfield (53)a,b,c,d	175819066160600	175819	661606	51	90	30-90

Appendix 3. General information for wells in the South Coast aquifer between the Río Jueyes and Río Guamaní used in this study.—Continued

[Superscripts in left column represent the following: a, well used in fence diagram; b, well used in map of thickness of surficial clay and silt; c, well used in delineation of base of permeable material; d, well used to obtain hydrologic and hydraulic data such as water level, specific capacity data, and others; na, data not available; ddmmss, degrees minutes seconds]

Well name and reference number	USGS site identifier[1]	Latitude (ddmmss)	Longitude (ddmmss)	Land surface datum (feet above mean sea level)	Depth, (feet below land surface)	Open interval, (feet above mean sea level)
Salinas 1 (54)a,b,c,d	175851066174600	175851	661746	29	120	25-120
Salinas 2 (55)a,b,d	175850066154500	175850	661545	29	120	25-120
Antonneti #1 (56)a,b,c,d	175821066182100	175821	661821	11	60	0-60
Margarita #3 (57)a,b,c,d	175839066180700	175839	661807	20	154	12-154
Las Pozas-2 TW (58)a,b,c	175852066185500	175852	661855	6	171	na
U.S. Army #1 (59)a,b,c,d	175928066171500	175928	661715	57	165	32-65
U.S. Army-1 TW (60)a,b,c	175942066170100	175942	661701	66	48	38-48
Vélez #1 (61)a,b,c,d	175928066174000	175928	661740	107	46	21-101
Pueblito (62)a,b,c,d	175905066172000	175905	661720	126	44	32-112
Coco Alvarado (63)a,b,c	175840066181200	175840	661812	18	69	9-57
Isadora #2 (64)a,b,c,d	175908066180500	175908	661804	31	180	na
Pozas 1 (65)a,c	175903066192000	175903	661920	16	160	0-160
Pozas Test #1 (66)a,b,c,d	175848066190100	175848	661901	6	168	9-104
Sabater Viejo (67)a,b,c,d	175926066141100	175926	661411	89	200	24-56
Providencia 2 (DW) (68)a,b,c,d	175904066163700	175904	661637	56	137	na
Burgos (69)a,b,c	175811066155900	175903	661650	54	120	30-120
Amadeo #2 (70)a,b,c	175933066161800	175933	661618	82	175	na
Godreau 6 (71)a,b,c,d	175921066165500	175921	661655	62	150	na
Godreau 5 (72)a,b,c,d	175930066160300	175930	661603	84	146	na
U.S. Army #2 (73)a,b,c,d	175952066162400	175952	661624	89	165	30-123, 125-157
Porrata (74)a,b,c,d	175943066150600	175943	661506	95	272	na
Coco Test 1 (75)a,b,c	175957066153800	175957	661538	112	66	na
Río Jueyes #1 (76)a,b,c	175857066203000	175857	662030	26	196	na
Texidor 1 (77)a,b,c	175916066202700	175916	662027	52	168	20-167
Palés (78)a,b,c	175916066203300	175916	662033	49	160	na
San José #2 (79)a,b,c	175956066200400	175956	662004	135	175	na

Appendix 3. General information for wells in the South Coast aquifer between the Río Jueyes and Río Guamaní used in this study.—Continued

[Superscripts in left column represent the following: a, well used in fence diagram; b, well used in map of thickness of surficial clay and silt; c, well used in delineation of base of permeable material; d, well used to obtain hydrologic and hydraulic data such as water level, specific capacity data, and others; na, data not available; ddmmss, degrees minutes seconds]

Well name and reference number	USGS site identifier[1]	Latitude (ddmmss)	Longitude (ddmmss)	Land surface datum (feet above mean sea level)	Depth, (feet below land surface)	Open interval, (feet above mean sea level)
Sostre #2 (80)a,b,c,d	175959066201200	175959	662012	145	236	96-142
Sostre #1 (81)a,b,c,d	175956066205400	175956	662054	148	146	46-136
Coco 1 (82)a,b,c,d	180044066153500	180044	661535	141	120	32-53
Santini-1 (83)a,b,c	180059066151900	180059	661519	157	100	68-100
Defense Dept (84)a,b,c	180136066153800	180136	661538	187	114	na
Municipio Salinas (85)a,b,c	180141066150900	180141	661509	57	100	na
Theater 1 (86)a,b,c,d	180023066175400	180023	661754	131	80	0-180
Peñuelas (87)a,b,c	180007066203000	180007	662030	154	115	55-115
Ballester (88)a,b,c	180041066222900	180041	662229	174	33	na
SC-3 (89)a,b,c	175801066105200	175801	661052	48	204	na
Pozo Hondo (90)a,b,c	175951066102900	175951	661029	246	106	na
Aguirre Norte (91)a,b,c	175954066122900	175954	661229	210	na	na
Merced TW (92)d	175748066081300	175748	660813	59	101	na
Aguirre Sugar 1A (93)d	175747066075800	175747	660758	3	75	na
Godreau 7 (94)d	175903066165000	175903	661650	54	120	na
Amadeo Gonzalez (95)d	175933066161800	175933	661618	82	170	na
Hacienda Vieja #2 (96)d	175709066145300	175709	661453	20	102	na
Magdalena #5 (97)d	175822066165400	175822	661654	23	na	na
Jauca 2b (98)d	175820066215000	175820	662150	13	100	na
U.S. Army #2A (99)d	175952066162400	175952	661624	89	170	na
U.S. Army #2 (C. Sant) (100)d	175924066171500	175924	661715	56	100	na
U.S. Army Test #1 (101)d	175942066170300	175942	661703	66	57	na
Isadora #3 (102)d	175909066185300	175909	661853	13	na	na
Pozas #2 (103)d	175917066194300	175917	661943	70	160	na
Castro #4 (104)d	175957066193400	1759570	661934	112	225	na
Pales #3 (105)d	175916066203300	175916	662033	49	na	na

Appendix 3. General information for wells in the South Coast aquifer between the Río Jueyes and Río Guamaní used in this study.—Continued

[Superscripts in left column represent the following: a, well used in fence diagram; b, well used in map of thickness of surficial clay and silt; c, well used in delineation of base of permeable material; d, well used to obtain hydrologic and hydraulic data such as water level, specific capacity data, and others; na, data not available; ddmmss, degrees minutes seconds]

Well name and reference number	USGS site identifier[1]	Latitude (ddmmss)	Longitude (ddmmss)	Land surface datum (feet above mean sea level)	Depth, (feet below land surface)	Open interval, (feet above mean sea level)
Díaz #2 (106)d	175937066203900	175937	662039	72	na	na
San José #1 (107)d	175957066200800	175957	662008	140	117	na
Santiago Batt #1 (108)d	175954066210500	175954	662105	102	53	na
Santiago #2 DW (109)d	175959066210200	175959	662102	105	200	na
Godreau #2 (110)d	175918066164100	175918	661641	69	na	na
Godreau 4 (111)d	175918066161900	175918	661619	73	na	na
Amadeo #1 (112)d	175925066165100	175925	661651	66	na	na
PREPA #4 (113)d	175835066145700	175835	661457	59	196	na
PREPA #6 (114)d	175825066142500	175825	661425	47	260	na
PREPA #7 (115)d	175845066142800	175845	661428	58	112	na
PREPA #9 (116)d	175810066151400	175810	661514	39	275	na
Phillips 11 (117)d	175715066084500	175715	660845	38	125	na
PRASA Fibers 2 (118)d	175738066084500	175737	660855	52	100	na
PRASA Reunión 2 (119)d	175721066085500	175721	660855	44	125	na
Fibers 2 (120)d	175755066085200	175755	660852	55	100	na
PRASA Pte Jobos (old) (121)d	175735066095900	175735	660959	7	148	na
Hormigonera Bruja (122)d	175755066105000	175755	661050	43	100	na
Central Guamani #2 (123)d	175752066105300	175752	661053	39	153	na
Cora #1 (124)d	175757066103900	175757	661039	44	155	32-152
Juana #4 (125)d	175853066101400	175853	661014	118		na
PRASA Villodas (126)d	175841066104500	175841	661045	82	143	na
PRASA Perpetuo (127)d	175822066134800	175822	661349	25	118	na
Aguirre #1 (128)d	175809066145300	175809	661453	41	na	na
Adela #2 (129)d	175848066145800	175848	661458	72	na	na
Adela #1 (130)d	175851066145700	175851	661457	72	26	na
Lannause 2 (131)d	175919066144400	175919	661444	87	na	na
González #2 (132)d	175959066141500	175959	661415	123	51	na

Appendix 3. General information for wells in the South Coast aquifer between the Río Jueyes and Río Guamaní used in this study.—Continued

[Superscripts in left column represent the following: a, well used in fence diagram; b, well used in map of thickness of surficial clay and silt; c, well used in delineation of base of permeable material; d, well used to obtain hydrologic and hydraulic data such as water level, specific capacity data, and others; na, data not available; ddmmss, degrees minutes seconds]

Well name and reference number	USGS site identifier[1]	Latitude (ddmmss)	Longitude (ddmmss)	Land surface datum (feet above mean sea level)	Depth, (feet below land surface)	Open interval, (feet above mean sea level)
PRWRA 5 (133)d	175924066142300	175924	661423	85	305	na
A-01 TW (134)d	175721066090200	175721	660902	33	101	na
Cautiño 7 (135)d	175908066081800	175908	660818	172	72	na
Aguirre Sugar 10 (136)d	175810066145100	175810	661451	43	55	na
Coquí 5 (137)d	175816066133100	175816	661331	16	150	na
Juana #2 (138)d	175823066101300	175823	661013	79	129	na
PRASA (139)d	175823066084500	175823	660845	na	58	na
PRASA (140)d	175742066082900	175742	660829	62	67	na
Reunión DW 1 (141)d	175756066082900	175756	660829	72	118	na
Salinas 4 (142)d	175922066171200	175922	661712	55	180	na
PRASA Campamento (143)d	175930066165600	175930	661656	66	140	na
Godreau 3A (144)d	175913066163500	175913	661635	66	102	na
Vélez (145)d	175922066174600	175922	661746	43	na	na
Isadora #4 (146)d	175853066182800	175853	661828	15	na	na
Hac. Teresa Dom (147)d	175754066162400	175754	661624	15	na	na
Godreau Solar #2 (148)d	175912066162500	175912	661625	64	na	na
USGS Piezo D (149)d	175910066155500	175910	661555	72	na	na
Colmado Cruz well (150)d	175845066164500	175845	661645	44	100	na
Magdalena #3 (151)4	175823066164600	175823	661646	26	30	na
Salinas Speedway (152)d	175814066154700	175814	6615477	43	na	na
Aguirre #1A (153)d	175811066151000	175811	661510	37	na	na
USGS Piezo C (154)d	175735066151800	175735	661518	15	na	na
Fortuna #3 (155)d	175858066151600	175858	661516	71	na	na
Fortuna #4 (156)d	175851066153000	175851	661530	59	na	na
Pioneer 1 (157)d	175815066153700	175815	661537	43	na	na
Piezo USGS Carmen (158)d	175826066173700	175826	661737	13	na	na

Appendix 3. General information for wells in the South Coast aquifer between the Río Jueyes and Río Guamaní used in this study.—Continued

[Superscripts in left column represent the following: a, well used in fence diagram; b, well used in map of thickness of surficial clay and silt; c, well used in delineation of base of permeable material; d, well used to obtain hydrologic and hydraulic data such as water level, specific capacity data, and others; na, data not available; ddmmss, degrees minutes seconds]

Well name and reference number	USGS site identifier[1]	Latitude (ddmmss)	Longitude (ddmmss)	Land surface datum (feet above mean sea level)	Depth, (feet below land surface)	Open interval, (feet above mean sea level)
PRASA Godreau 2 (159)d	175925066170600	175924	661704	59	na	na
PRASA Coco 3 (160)d	175908066172600	175908	175908	43	na	na
PRASA Las Margaritas (161)d	175826066181600	175826	661806	12	na	na
Deestano (162)d	175824066162500	175824	661625	36	na	na
AEE #5 (163)d	175833066151600	175833	661516	55	na	na
Abey (164)d	175821066144700	175821	661447	48	na	na
Hacienda Sabater #1 (165)d	175855066143100	175855	661431	62	na	na
PRWRA #4 (166)d	175909066142200	175909	661422	72	na	na
PRWRA #2 (167)d	175927066142000	175927	661420	90	na	na
PRWRA #3 (168)d	175944066142100	175943	661421	110	na	na
Luce& Co #21 (169)d	175855066141400	175855	661414	74	na	na
Magdalena # 4 (170)d	175915066143600	175915	661436	82	na	na
Pollera 2 (171)d	175916066131200	175916	661312	98	na	na
PRASA AEE (172)d	175828066142200	175827	661435	46	na	na
PRASA San Felipe (173)d	175822066125300	175822	661253	13	na	na
USGS Coquí 1 (174)d	175809066133200	175809	661332	16	na	na
Pozo Aguirre (175)d	175827066141100	175827	661411	175	na	na
PRASA Las Mareas (176)d	175739066156600	175739	661566	23	na	na
Ermitaño (177)d	175708066162900	175708	661629	2	na	na
Tumores (178)d	175856066123300	175856	661233	56	na	na
Amoros (179)d	175910066122400	175910	661224	98	na	na
USGS Piezo A (180)d	175925066145300	175925	661453	90	na	na
USGS Piezo G (181)d	175848066170700	175848	661707	40	167	na
Monsanto (182)d	175814066155900	175814	661559	42	na	na
Hac. Sabater 2 (183)d	175811066153600	175811	661536	72	na	na
JBNERR West (184)d	175722066151300	175722	661513	6.9	87, 20	na

Appendix 3. General information for wells in the South Coast aquifer between the Río Jueyes and Río Guamaní used in this study.—Continued

[Superscripts in left column represent the following: a, well used in fence diagram; b, well used in map of thickness of surficial clay and silt; c, well used in delineation of base of permeable material; d, well used to obtain hydrologic and hydraulic data such as water level, specific capacity data, and others; na, data not available; ddmmss, degrees minutes seconds]

Well name and reference number	USGS site identifier[1]	Latitude (ddmmss)	Longitude (ddmmss)	Land surface datum (feet above mean sea level)	Depth, (feet below land surface)	Open interval, (feet above mean sea level)
JBNERR East (185)d	175711066143500	175711	661435	4.9	74, 17	na
Las Mareas 3 (186)d	175633066084100	175633	660841	3	na	na
Phillips 4 (187)d	175640066085100	175640	660851	3	na	na
Phillips 3 (188)d	175648066083900	175648	660839	10	na	na
Josefa Sur (189)d	175710066092300	175710	660923	23	na	na
Reunión Sur (190)d	175721066083600	175721	660836	42	na	na
PRASA Jobos 1 (191)d	175735066100400	175735	661004	29	na	na
Adela 1 BTR (192)d	175754066102300	175754	661023	36	na	na
Central Guamani 1 (193)d	175754066104700	175754	661047	43	na	na
PRASA 2 (194)d	175757066094200	175757	660942	49	na	na
P. Morales Norte (195)d	175840066102100	175840	661021	97	na	na
Piezo J-24 (196)d	175823066182200	175823	661822	8	25	na
Benito (197)d	175842066113800	175842	661138	61	na	na
Chun Chin Irrigation (198)d	175805066105500	175805	661023	48	na	na
Juana (199)d	175815066102300	175815	661023	59	na	na
Chunchin (200)d	175805066120600	175805	661206	7	na	na
Fortuna 10 (201)d	175851066155100	175851	661551	59	na	na
Rosado 1 (202)d	175850066154000	175850	661540	59	na	na
USGS RASA B (203)d	175925066145400	175925	661454	89	109	na
Isadora new (204)d	175859066181200	175859	661812	26	na	na
Godreau #3 (205)d	175918066182800	175918	661828	44	na	na
PRASA Godreau 1 (206)d	175925066170601	175924	661704	59	na	na
Esperanza 2 (207)d	175801066154700	175801	661547	33	474-100	30-60
Godreau 1 (208)d	175926066155000	175927	661556	85	na	na
Santa Fe 1 (209)d	175911066155800	175911	661558	84	na	na
Santa Fe 2 (210)d	175859066155300	175859	661553	63	na	na

Appendix 3. General information for wells in the South Coast aquifer between the Río Jueyes and Río Guamaní used in this study.—Continued

[Superscripts in left column represent the following: a, well used in fence diagram; b, well used in map of thickness of surficial clay and silt; c, well used in delineation of base of permeable material; d, well used to obtain hydrologic and hydraulic data such as water level, specific capacity data, and others; na, data not available; ddmmss, degrees minutes seconds]

Well name and reference number	USGS site identifier[1]	Latitude (ddmmss)	Longitude (ddmmss)	Land surface datum (feet above mean sea level)	Depth, (feet below land surface)	Open interval, (feet above mean sea level)
Gonzalez 2 (211)d	175858066152800	175858	661527	69	na	na
Aguirre 6 (212)d	175812066134900	175812	661349	23	na	na
Ayerst (213)d	175740066090200	175740	660902	41	na	na
Fibers Superfund (214)d	175724066085500	175724	660855	39	na	na
Philips Petroleum 13 (215)	175719066085500	175720	660402	33	99	na
Juana 5 (216)	175814066102200	175858	661022	128	142	na
Jobos (217)	175814066102200	175814	661022	59	100	na

[1]Site identification number for each site based on the latitude and longitude of the site. First six digits are latitude, next six digits are longitude.

[2]Depth of shallow piezometer.

[3] Depth of deep piezometer.

[4]Depth range of well battery.

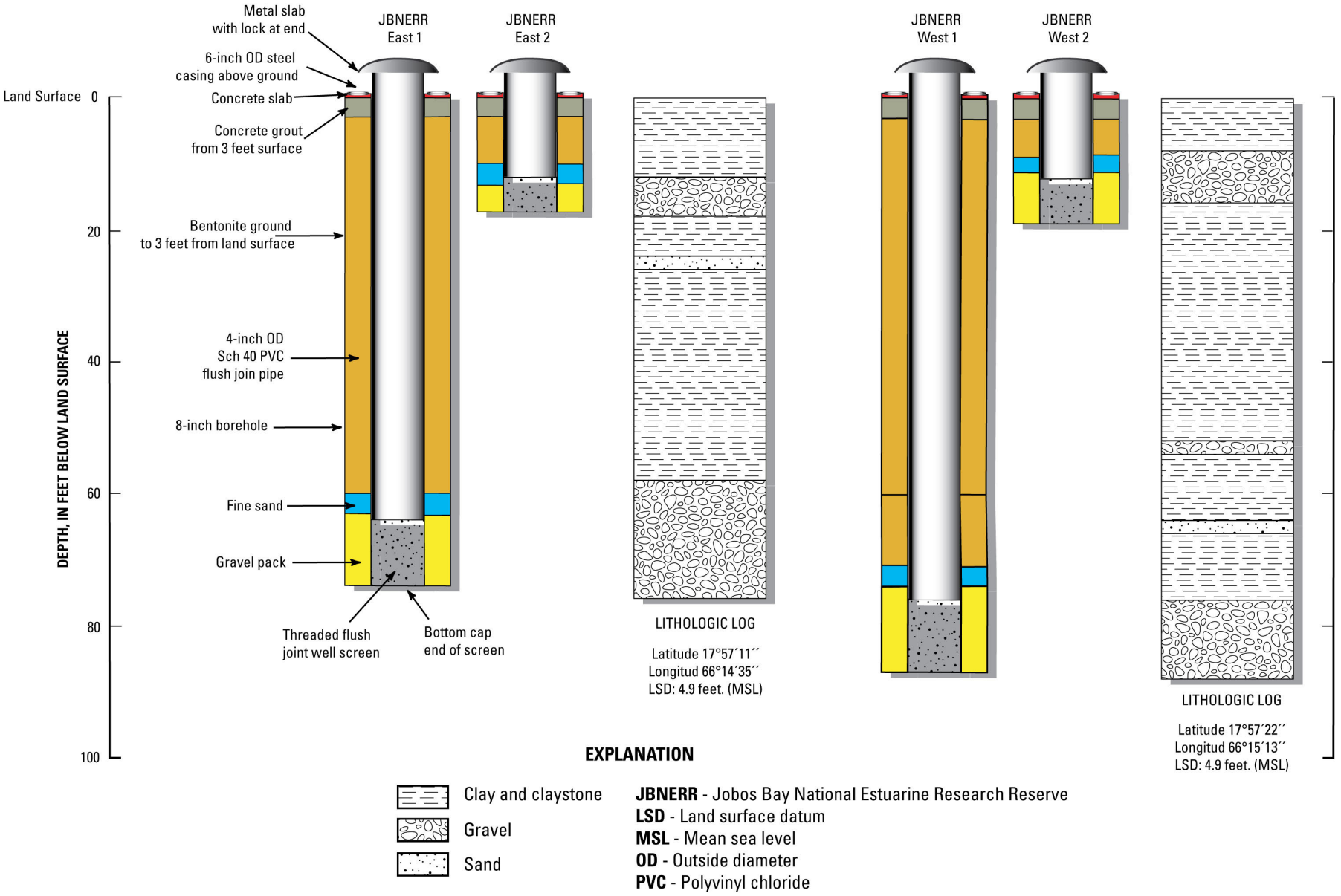

Appendix 4. Lithologic and construction data for the JBNERR East 1 and 2 and JBNERR West 1 and 2 piezometer nests installed near the northern boundary of the Jobos Bay National Estuarine Research Reserve. JBNERR 1 and JBNERR 2 reference nos. are 184 and 185, respectively, in appendix 3.

Appendix 5. Zoned recharge values used for transient calibration.

[Zone numbers shown within parenthesis, annual rainfall shown in figure 2]

Stress period number	Calendar year	Recharge per zone (feet per day)	Recharge per zone (inches per year)
1	1986	(1) 1.0×10^{-3}	4.4
		(2) 5.9×10^{-3}	25.8
		(3) 5.9×10^{-3}	25.8
		(4) 5.0×10^{-4}	2.2
		(5) 5.9×10^{-3}	25.8
2	1987	(1) 1.4×10^{-3}	6.1
		(2) 5.9×10^{-3}	25.8
		(3) 5.9×10^{-3}	25.8
		(4) 7.0×10^{-4}	3.1
		(5) 5.9×10^{-3}	25.8
3	1988	(1) 1.2×10^{-3}	5.3
		(2) 5.9×10^{-3}	25.8
		(3) 5.9×10^{-3}	25.8
		(4) 6.0×10^{-4}	2.6
		(5) 5.9×10^{-3}	25.8
4	1989	(1) 2.0×10^{-4}	8.8
		(2) 5.9×10^{-3}	25.8
		(3) 5.9×10^{-3}	25.8
		(4) 1.0×10^{-4}	0.4
		(5) 5.9×10^{-3}	25.8
5	1990	(1) 1.2×10^{-3}	5.3
		(2) 5.9×10^{-3}	25.8
		(3) 5.9×10^{-3}	25.8
		(4) 6.0×10^{-4}	2.6
		(5) 5.9×10^{-3}	25.8
6	1991	(1) 6.0×10^{-4}	2.6
		(2) 5.9×10^{-3}	25.8
		(3) 5.9×10^{-3}	25.8
		(4) 3.0×10^{-4}	1.3
		(5) 5.9×10^{-3}	25.8
7	1992	(1) 7.0×10^{-4}	3.1
		(2) 5.9×10^{-3}	25.8
		(3) 5.9×10^{-3}	25.8
		(4) 3.5×10^{-4}	1.5
		(5) 5.9×10^{-3}	25.8
8	1993	(1) 3.0×10^{-4}	1.3
		(2) 5.9×10^{-3}	25.8
		(3) 5.9×10^{-3}	25.8
		(4) 1.5×10^{-4}	0.7
		(5) 5.9×10^{-3}	25.8

Appendix 5. Zoned recharge values used for transient calibration.—Continued

[Zone numbers shown within parenthesis, annual rainfall shown in figure 2]

Stress period number	Calendar year	Recharge per zone (feet per day)	Recharge per zone (inches per year)
9	1994	(1) 6.0×10^{-4}	2.6
		(2) 6.0×10^{-4}	2.6
		(3) 6.0×10^{-4}	2.6
		(4) 3.0×10^{-4}	1.3
		(5) 6.0×10^{-4}	2.6
10	1995	(1) 2.0×10^{-4}	1.0
		(2) 2.0×10^{-4}	1.0
		(3) 2.0×10^{-4}	1.0
		(4) 1.0×10^{-4}	0.4
		(5) 2.0×10^{-4}	1.0
11	1996	(1) 1.4×10^{-3}	6.1
		(2)1.4×10^{-3}	6.1
		(3) 1.4×10^{-3}	6.1
		(4) 7.0×10^{-4}	3.1
		(5) 1.4×10^{-3}	6.1
12	1997	(1) 6.0×10^{-4}	2.6
		(2) 6.0×10^{-4}	2.6
		(3) 6.0×10^{-4}	2.6
		(4) 3.0×10^{-4}	1.3
		(5) 6.0×10^{-4}	2.6
13	1998	(1) 1.5×10^{-3}	6.6
		(2) 1.5×10^{-3}	6.6
		(3) 1.5×10^{-3}	6.6
		(4) 7.5×10^{-4}	3.3
		(5) 1.5×10^{-3}	6.6
14	1999	(1) 6.0×10^{-4}	2.6
		(2) 6.0×10^{-4}	2.6
		(3) 6.0×10^{-4}	2.6
		(4) 3.0×10^{-4}	1.3
		(5) 6.0×10^{-4}	2.6
15	2000	(1) 6.0×10^{-4}	2.6
		(2) 6.0×10^{-4}	2.6
		(3) 6.0×10^{-4}	2.6
		(4) 3.0×10^{-4}	1.3
		(5) 6.0×10^{-4}	2.6
16	2001	(1) 7.0×10^{-4}	3.1
		(2) 7.0×10^{-4}	3.1
		(3) 7.0×10^{-4}	3.1
		(4) 3.5×10^{-4}	1.5
		(5) 7.0×10^{-4}	3.1

Appendix 5. Zoned recharge values used for transient calibration.—Continued

[Zone numbers shown within parenthesis, annual rainfall shown in figure 2]

Stress period number	Calendar year	Recharge per zone (feet per day)	Recharge per zone (inches per year)
17	2002	(1) 6.0×10^{-4}	2.6
		(2) 6.0×10^{-4}	2.6
		(3) 6.0×10^{-4}	2.6
		(4) 3.0×10^{-4}	1.3
		(5) 6.0×10^{-4}	2.6
18	2003	(1) 1.6×10^{-3}	7.0
		(2) 1.6×10^{-3}	7.0
		(3) 1.6×10^{-3}	7.0
		(4) 8.0×10^{-4}	3.5
		(5) 1.6×10^{-3}	7.0
19	2004	(1) 6.0×10^{-4}	2.6
		(2) 6.0×10^{-4}	2.6
		(3) 6.0×10^{-4}	2.6
		(4) 3.0×10^{-4}	1.3
		(5) 6.0×10^{-4}	2.6

Appendix 6*a*. Observed water levels, simulated water levels, and calculated residuals for March, 1986, July 2002, and May 2004.

Observed ground-water levels for March 1986 used in steady-state calibration						
Report reference number	USGS site identifier	Well name	Observed water-level altitude (feet)	Layer	Simulated water level (feet)	Residual error (feet)
4	175830066135400	Templo Glove	16	3	20.75	-4.75
5	175813066133100	Coquí 2	-18	3	6.21	-24.21
9	175759066144400	Pozo Aguirre 2	10	3	24.12	-14.12
11	175822066104300	Cautiño 3	52	2	43.52	8.48
15	175757066131800	Coquí 4	6	3	5.85	0.15
16	175732066091900	Josefa Norte	21	3	44.57	-23.57
24	175646066082100	Luce & Co 4	1	3	0.16	0.84
27	175741066082100	Luce & Co 3	38	2	58.27	-20.27
31	175755066084800	Melania	47	3	58.80	-11.80
33	175718066083900	Phillips 7	19	3	28.25	-9.25
34	175754066084100	Fibers 1 (InterFibers 1)	54	2	60.72	-6.72
38	175735066090500	PRASA Fibers 3	30	3	47.64	-17.64
55	175850066174400	Salinas 2	13	3	13.76	-0.76
56	175821066182100	Antonneti #1	7	3	6.49	0.51
61	175928066174000	Vélez 1	23	3	25.37	-2.37
64	175908066180500	Isadora 2	12	3	16.22	-4.22
97	175822066165400	Magdalena 5	10	3	16.52	-6.52
103	175917066194300	Pozas 2	20	3	9.15	10.85
113	175835066145700	PREPA #4	47	3	36.56	10.44
116	175810066152700	PREPA #9	33	3	26.69	6.31
118	175738066084500	PRASA Fibers 2	32	2	53.19	-21.19
119	175721066085500	Reunión 2	32	2	36.23	-4.23
121	175735066095900	Puente Jobos	21	3	27.85	-6.85
123	175752066105300	Central Guamani 2	34	3	21.78	12.22
126	175841066104500	PRASA Villodas	58	1	64.75	-6.75
127	175822066134800	PRASA Perpetuo	7	3	12.95	-5.95

Appendix 6*a*. Observed water levels, simulated water levels, and calculated residuals for March, 1986, July 2002, and May 2004.—Continued

Observed ground-water levels for March 1986 used in steady-state calibration						
Report reference number	USGS site identifier	Well name	Observed water-level altitude (feet)	Layer	Simulated water level (feet)	Residual error (feet)
129	175848066145800	Adela 2	48	3	39.15	8.85
130	175851066145700	Adela 1	44	3	40.53	3.47
137	175816066133100	Coquí 5	-18	3	6.84	-24.84
138	175823066101300	Juana 2	64	2	50.63	13.37
141	175756066082900	Reunión DW 1	67	1	63.41	3.59
144	175913066163500	Godreau 3A	40	3	35.61	4.39
146	175853066182800	Isadora 4	8	3	10.66	-2.66
147	175754066162400	Hac. Teresa Dom	12	3	12.12	-0.12
149	175910066155500	USGS Piezo D	50	3	54.96	-4.96
151	175823066164600	Magdalena 3	12	3	18.16	-6.16
154	175735066151800	USGS Piezo C	8	3	16.92	-8.92
155	175858066151600	Fortuna 3	50	3	45.51	4.49
158	175826066173700	Piezo USGS Carmen	12	3	11.02	0.98
159	175924066170400	PRASA Godreau 2	32	2	31.27	0.73
162	175823066162400	Deestano	13	3	22.53	-9.53
164	175821066144600	Abey	43	3	31.96	11.04
168	175944066142100	PRWRA 3	88	1	70.71	17.29
170	175916066144000	Magdalena 4	46	3	51.79	-5.79
172	175828066142200	PRASA AEE	21	3	25.73	-4.73
173	175824066130900	PRASA San Felipe	8	2	12.83	-4.83
174	175809066133100	Coquí 1	2	3	5.38	-3.38
179	175910066122400	Amoros	87	1	78.41	8.59
180	175925066145400	USGS Piezo A	52	3	57.71	-5.71
182	175814066155900	Monsanto	14	3	25.86	-11.86

Appendix 6*a*. Observed water levels, simulated water levels, and calculated residuals for March, 1986, July 2002, and May 2004.—Continued

Observed ground-water levels for March 1986 used in steady-state calibration						
Report reference number	USGS site identifier	Well name	Observed water-level altitude (feet)	Layer	Simulated water level (feet)	Residual error (feet)
183	175906066143000	Hac. Sabater 2	49	3	46.48	2.52
186	175633066084100	Las Mareas 3	3	3	0.16	2.84
187	175640066085100	Phillips 4	3	3	0.90	2.10
188	175648066083900	Phillips 3	7	3	2.87	4.13
189	175710066092300	Josefa Sur	15	3	23.68	-8.68
190	175721066083600	Reunión Sur	22	2	34.09	-12.09
191	175735066100400	PRASA Jobos 1	23	3	26.36	-3.36
192	175754066102300	Adela 1 BTR	32	3	30.52	1.48
193	175754066104700	Central Guamani 1	33	3	23.85	9.15
194	175757066094200	PRASA 2	40	3	45.36	-5.36
195	175840066102100	P. Morales Norte	79	2	69.76	9.24
196	175823066182200	Piezo J-24	4	3	4.49	-0.49
197	175842066113800	Benito	54	2	63.57	-9.57
198	175805066105500	Benito Sur	37	2	25.61	11.39
199	175815066102300	Juana	50	3	41.42	8.58
200	175805066120600	Chunchin	17	3	8.31	8.69
Mean residual						-2.08
Standard deviation of residuals						9.53
Standard deviation of residuals divided by range in observations						0.090

Appendix 6*b*. Observed water levels, simulated water levels, and calculated residuals for March, 1986, July 2002, and May 2004.

Observed ground-water levels near Salinas, Puerto Rico, July 2002, compared with simulated water levels for 2002.						
Report reference number	USGS site identifier	Well name	Observed water-level altitude (feet)	Layer	Simulated water level (feet)	Residual error (feet)
3	175826066134400	PRASA Coqui #1	6.07	4	-6.28	12.35
40	175748066160600	Salich #1	-2.97	4	-8.99	6.02
41	175804066150700	Aguirre #3	-18.6	4	-8.23	-10.37
42	175810066155400	Fortuna #1	20.97	3	-1.29	22.26
52	175837066165400	Carmen 2	-0.32	4	3.78	-4.10
55	175850066174600	PRASA Salinas 2	0.83	4	0.01	0.82
64	175908066180400	Isadora #2	1.38	4	2.30	-0.92
72	175930066160300	Godreau 5	28.68	3	24.57	4.11
102	175909066185300	Isadora #3	-0.6	3	1.99	-2.59
110	175918066164100	Godreau #02	20.49	3	13.18	7.31
113	175835066145700	AEE #4	24.1	4	-3.57	27.67
114	175825066142500	AEE #6	23.62	4	-8.24	31.86
115	175845066142800	AEE #7	18.96	3	-2.23	21.19
116	175810066151400	AEE #9	-31.24	4	-7.09	-24.15
127	175822066134900	PRASA Perpetuo	0.81	4	-7.78	8.59
128	175809066145300	Aguirre #1	-11.37	4	-7.90	-3.47
130	175851066145700	Adela	20.9	4	-1.97	22.87
131	175919066144400	Lanausse #2	22.75	3	5.26	17.49
142	175922066171200	Salinas 4	17.26	2	4.35	12.91
145	175922066174600	Vélez	16.14	3	4.68	11.46
146	175853066182800	Isadora #4	2.32	4	1.31	1.01
147	175918066164100	Godreau #03	20.99	3	10.37	10.62
148	175912066155500	Godreau-Solar #2	23.8	3	9.91	13.89
149	175910066155500	USGS Piezo D	27.08	3	13.45	13.63
150	175845066164500	Colmado Cruz well	6.4	4	5.03	1.37
151	175823066164600	Magdalena #3	2.85	3	1.91	0.94
152	175814066154700	Salinas Speedway	-5.81	3	-4.41	-1.40

Appendix 6*b*. Observed water levels, simulated water levels, and calculated residuals for March, 1986, July 2002, and May 2004.—Continued

Observed ground-water levels near Salinas, Puerto Rico, July 2002, compared with simulated water levels for 2002.						
Report reference number	USGS site identifier	Well name	Observed water-level altitude (feet)	Layer	Simulated water level (feet)	Residual error (feet)
154	175735066151800	USGS Piezo C	1.65	4	-4.10	5.75
155	175858066151600	Fortuna #3	20.64	3	-0.06	20.70
156	175851066153000	Fortuna #4	20.2	3	1.20	19.00
157	175815066153700	Pioneer 1	1.03	3	-5.39	6.42
159	175924066170400	PRASA Godreau 2	-6.01	2	5.87	-11.88
160	175908661726000	PRASA Coco 3	14.05	3	4.05	10.00
161	175826066180600	PRASA Las Margaritas	-0.96	4	-0.30	-0.66
162	175824066162500	Deestano	-2.11	3	1.47	-3.58
163	175833066151600	AEE #5	22.75	4	-4.42	27.17
164	175821066144700	Abey	19.06	4	-5.32	24.38
165	175855066143100	Hacienda Sabater #1	20.14	3	-0.17	20.31
166	175909066142200	PRWRA #4	31.32	3	4.35	26.97
167	175927066142000	PRWRA #2	47.53	3	11.53	36.00
168	175943066142100	PRWRA #3	74.44	3	20.68	53.76
169	175855066141400	Luce & Co #21	22.32	3	-0.10	22.42
170	175915066143600	Magdalena #4	26.99	3	4.26	22.73
171	175916066131200	Pollera 2	69.08	1	17.09	51.99
173	175822066125300	PRASA San Felipe	1.97	4	-3.33	5.30
174	175809066133200	USGS Coqui	2.83	4	-6.15	8.98
175	175827066141100	Pozo Aguirre	7.68	4	-6.70	14.38
176	175739066156600	PRASA Las Mareas	-0.35	4	-5.35	5.00
177	175708066162900	Ermitaño	0.7	4	-0.58	1.28
178	175856066123300	Tumores	51.12	2	14.33	24.60
179	75910066122400	Amoros	91.75	1	39.99	51.76
Mean residual						12.63
Standard deviation of residuals						15.75
Standard deviation of residuals divided by range in observations						0.13

Appendix 6*c*. Observed water levels, simulated water levels, and calculated residuals for March, 1986, July 2002, and May 2004.

Observed ground-water levels near Salinas, Puerto Rico, May 2004, compared with simulated water levels for 2004.						
Report reference number	USGS site identifier	Well name	Observed water-level altitude (feet)	Layer	Simulated water level (feet)	Residual error (feet)
40	175748066160600	Salich #1	4.81	4	6.09	-1.28
42	175810066155400	Fortuna #1	33.10	3	23.56	9.54
64	175908066180400	Isadora #2	7.83	4	11.51	-3.68
72	175930066160300	Godreau #5	40.59	3	70.11	-29.52
94	175903066165000	USGS Godreau 7	14.54	4	17.33	-2.79
103	175917066194300	Pozas 2	27.66	3	6.08	21.58
110	175918066164100	Godreau #02	32.88	3	43.36	-10.48
113	175851066145700	Adela 1	32.61	4	22.11	10.50
113	175835066145700	AEE #4	30.03	4	18.47	11.56
114	175825066142500	AEE #6	18.78	4	11.14	7.64
115	175845066142800	AEE #7	29.02	3	20.86	8.16
116	175810066151400	AEE #9	17.54	4	11.35	6.19
127	175822066134900	PRASA Perpetuo	0.81	4	6.24	-5.42
128	175809066145300	Aguirre #1	19.02	4	11.99	7.03
131	175919066144400	Lanausse #2	34.98	3	34.83	0.16
140	175742066082900	PRASA Coqui	9.61	4	6.91	2.70
149	175910066155500	USGS Piezo D	37.29	3	45.61	-8.32
151	175823066164600	Magdalena #3	10.60	3	13.46	-2.86
154	175735066151800	USGS Piezo C	5.80	4	5.55	0.26
156	175851066153000	Fortuna #4	31.98	3	25.85	6.14
163	175833066151600	AEE #5	32.83	4	16.98	15.85
164	175821066144700	Abey	28.00	4	15.02	12.98
166	175909066142200	PRWRA #4	40.65	3	30.39	10.26
167	175927066142000	PRWRA #2	55.42	3	42.71	12.71
168	175943066142100	PRWRA #3	84.43	3	60.83	23.60
169	175855066141400	Luce & Co #21	32.41	3	24.43	7.98
170	175915066143600	Magdalena #4	39.18	3	32.96	6.22
173	175822066125300	PRASA San Felipe	5.72	4	6.83	-1.11
174	175809066133200	USGS Coqui	6.37	4	2.31	4.06
174	175739066156600	PRASA Las Mareas	5.58	4	4.90	0.68
175	175827066141100	Pozo Aguirre	12.57	4	11.15	1.42
180	175814066155900	Monsanto	8.98	3	13.35	-4.37
183	175811066155900	Burgos	18.16	3	11.12	7.04
201	175851066155100	Fortuna #10	34.81	3	32.51	2.30
202	175850066154000	Fortuna #5	32.87	3	29.19	3.68

Appendix 6*c*. Observed water levels, simulated water levels, and calculated residuals for March, 1986, July 2002, and May 2004.—Continued

Observed ground-water levels near Salinas, Puerto Rico, May 2004, compared with simulated water levels for 2004.						
Report reference number	USGS site identifier	Well name	Observed water-level altitude (feet)	Layer	Simulated water level (feet)	Residual error (feet)
203	175925066145400	USGS RASA B	38.05	3	41.22	-3.17
204	175859066181200	Isadora new	4.74	4	9.07	-4.33
205	175918066182800	Godreau #03	28.71	3	34.93	-6.22
Mean residual						3.07
Standard deviation of residuals						9.49
Standard deviation of residuals divided by range in observations						0.11